

11-2018

MATHEMATICAL MODELING OF CORONA VIRUS IN THE UNITED ARAB EMIRATES

Alya Saif Ahmad Alshehhi

Follow this and additional works at: https://scholarworks.uaeu.ac.ae/all_theses

 Part of the [Mathematics Commons](#)

United Arab Emirates University

College of Science

Department of Mathematical Sciences

MATHEMATICAL MODELING OF CORONA VIRUS IN THE
UNITED ARAB EMIRATES

Alya Saif Ahmad Alshehhi

This thesis is submitted in partial fulfillment of the requirements for the degree of
Master of Science in Mathematics

Under the Supervision of Dr. Abdessamad Tridane

November 2018

Declaration of Original Work

I, Alya Saif Ahmad Alshehhi, the undersigned, a graduate student at the United Arab Emirates University (UAEU), and the author of this thesis entitled "*Mathematical Modeling of Corona Virus in the United Arab Emirates*", hereby, solemnly declare that this thesis is my own original research work that has been done and prepared by me under the supervision of Dr. Abdessamad Tridane, in the College of Science at UAEU. This work has not previously been presented or published, or formed the basis for the award of any academic degree, diploma or a similar title at this or any other university. Any materials borrowed from other sources (whether published or unpublished) and relied upon or included in my thesis have been properly cited and acknowledged in accordance with appropriate academic conventions. I further declare that there is no potential conflict of interest with respect to the research, data collection, authorship, presentation and/or publication of this thesis.

Student's Signature _____ Date _____

Copyright © 2018 Alya Saif Ahmad Alshehhi
All Rights Reserved

Approval of the Master Thesis

This Master Thesis is approved by the following Examining Committee Members:

1) Advisor (Committee Chair): Abdessamad Tridane

Title: Associate Professor

Department of Mathematical Sciences

College of Science

Signature _____ Date _____

2) Co-Advisor: Sehjeong Kim

Title: Assistant Professor

Department of Mathematical Sciences

College of Science

Signature _____ Date _____

3) Member (External Examiner): Abdul Salam Jarrah

Title: Professor of Mathematics

Department of Mathematics and Statistics

American University of Sharjah

Signature _____ Date _____

4) Member : Muhammed Syam

Title: Professor

Department of Mathematical Sciences

College of Science

Signature _____ Date _____

This Master Thesis is accepted by:

Dean of the College of Science: Professor Ahmed Murad

Signature _____ Date _____

Acting Dean of the College of Graduate Studies: Professor Ali Al-Marzouqi

Signature _____ Date _____

Copy _____ of _____

Abstract

The Middle East Respiratory Syndrome Coronavirus (MERS-CoV) is a viral infectious disease that can be transmitted to humans through interaction with infected animals or humans. The Middle East respiratory syndrome (MERS) is still one of the main public health concerns in the Gulf region including United Arab Emirates. The fact that diseases have been imported into other parts of the world show the possibility of has a MERS pandemic. In this work, we are aiming to study a mathematical model of the MERS transmission among the UAE population and camels. The goal is to determine what are the paths of communication and find out the best way to control the disease spread. We will calculate the basic reproduction number \mathcal{R}_0 of the MERS model in the UAE, and we will compute disease-endemic equilibrium points. The sensitivity analysis of the basic reproduction number \mathcal{R}_0 will be performed. Also, we will perform computer simulations to investigate the MERS model.

Keywords: MERS-CoV infection in the UAE, basic reproduction number, numerical analysis, sensitivity analysis.

Title and Abstract (in Arabic)

النمذجة الرياضية لفيروس كورونا في دولة الإمارات

الملخص

متلازمة الشرق الأوسط التنفسية (كورونا فيروس) هو مرض فيروسي معدٍ يمكن أن ينتقل إلى البشر من خلال التفاعل مع الحيوانات المصابة أو البشر. لا تزال متلازمة الشرق الأوسط التنفسية واحدة من أهم اهتمامات الصحة العامة في منطقة الخليج بما في ذلك الإمارات العربية المتحدة. وتظهر الحقيقة أن هذا المرض قد تم توريده إلى أجزاء أخرى في العالم تزيد من إمكانية وجود وباء فيروس كورونا. في هذا العمل ، نحن نهدف إلى دراسة نموذج رياضي لانتقال فيروس كورونا بين سكان الإمارات والجمال. الهدف هو تحديد ما هي طرق التواصل ومعرفة أفضل طريقة للسيطرة على انتشار المرض. سنقوم بحساب رقم الاستنساخ الأساسي لنموذج كورونا في دولة الإمارات العربية المتحدة ، وسوف نحسب نقاط توازن المرض المستوطنة. وسيتم إجراء تحليل الحساسية لرقم الإنجاب الأساسي. أيضا ، سنقوم بتنفيذ عمليات المحاكاة الحاسوبية للتحقيق في نموذج كورونا.

مفاهيم البحث الرئيسية: عدوى فيروس كورونا في الإمارات العربية المتحدة ، رقم الاستنساخ الأساسي ، التحليل العددي ، تحليل الحساسية.

Acknowledgments

Firstly, I would like to express my sincere gratitude to my supervisor Dr. Abdessamad Tridane for the continuous support of my M.Sc study and related research, for his patience, motivation, and immense knowledge. His guidance helped me in all the time of research and writing of this thesis. Also his guidance helped me to be a better person, enhance my mathematical skills, and learn new practical programming. I would also like to acknowledge Dr. Sehjeong Kim of the Department of Mathematical Sciences at UAEU as Co-supervisor of this thesis, and I am gratefully indebted to her for her very valuable comments on this thesis.

Secondly, I would like to thank Prof Abdul salam Jarrah, from American University of Sharjah, Prof. Mohamed Syam for their guidance and for accepting to be part of this examination committee of my thesis.

Thirdly, I would like to send special thanks to Dr. Mohamed Salim, the chair of Department of Mathematical Sciences at the UAE University, for his continuous support and Dr. Nafaa Chbili, the coordinator of the Master program for his assistance and guidance through the master degree.

Fourthly, I would also like to thank the expert who was involved in the correction for this research project: Writing Center Supervisor in UAEU, Elizabeth Sarah Whitehouse of the experts who contributed in completing this work with her passionate participation, the correction could not have been successfully conducted without her.

I express my deepest thanks to my friends who were in different degree levels from different departments. Their advices and support helped me finish the journey of the masters degree. A spacial thanks to my friend Fatema Alawadhi for her advice's and tremendous assistance in the thesis formatting.

Last but not the least, I would like to thank my family: my parents and to my brothers and sister for supporting me spiritually throughout writing this thesis.

Dedication

To my beloved parents and teachers

Table of Contents

Title	i
Declaration of Original Work	ii
Copyright	iii
Approval of the Master Thesis	iv
Abstract	vi
Title and Abstract (in Arabic)	vii
Acknowledgments	viii
Dedication	ix
Table of Contents	x
List of Tables	xiii
List of Figures	xv
Chapter 1: Introduction of Thesis	1
Chapter 2: Zoonotic Diseases in the Middle East	4
2.1 Zoonotic Diseases	4
2.1.1 Definition	4
2.1.2 Factors Influencing the Emergence of Zoonotic Diseases	5
2.2 The List of Zoonotic Diseases	7
2.2.1 Etiological Factors	7
2.2.2 Method of Transmission	8
2.2.3 Reservoir Host	8
2.3 The Origin of Zoonotic Diseases in The Middle East	10

2.3.1	Emerging Zoonotic Viruses of Bat Origin	11
2.3.2	Emerging Zoonotic Viruses from other Sources	16
Chapter 3:	Zoonotic Diseases and their Math Models	29
3.1	Mathematical Models for SARS	29
3.2	Mathematical Models for Rift Valley Fever	30
3.3	Mathematical Models for Rabies	36
3.4	Mathematical Models for CHIKV	41
3.5	Mathematical Models for WNV	45
3.6	Mathematical Models for Brucellosis	47
3.7	Mathematical Models for Anthrax	49
3.8	Mathematical Models for Chikungunya Fever	50
3.9	Mathematical Models for Influenza	51
Chapter 4:	Mathematical Models of MERS-CoV	57
4.1	Models of Controlling MERS-CoV	57
4.2	Models of Transmission MERS-CoV	62
4.2.1	Deterministic Model	62
4.2.2	Stochastic Model	64
4.2.3	Spatiotemporal Heterogeneity Model	68
Chapter 5:	Mathematical Model of MERS in the UAE	72
5.1	Presentation of the Model	72
5.1.1	Variables	73
5.1.2	Human Transmission	74
5.1.3	Camels Transmission	74
5.2	Human and Camels Parameters Description	75
5.2.1	Human Parameters	75
5.2.2	Camels Parameters	75
Chapter 6:	Parameters Estimation	77
6.1	Parameters Estimation of Human	77

6.2	Parameters Estimation of Camels	79
Chapter 7: Mathematical Analysis		81
7.1	Boundedness and Positivity	81
7.1.1	Positivity	81
7.1.2	Boundedness	84
7.2	The Basic Reproduction Number	86
7.3	Endemic Equilibria	89
7.4	Jacobian Method-Routh-Hurwiz Criteria	97
7.4.1	Block Matrix	97
Chapter 8: Numerical Simulations		108
8.1	Time Series Simulation	108
8.2	Simulation of the Disease Equilibrium	110
8.2.1	Simulation of the Disease Free Equilibrium	110
8.2.2	Simulation of the Endemic Equilibrium	113
8.3	Sensitivity Analysis	118
8.3.1	For Infected Population (I_p)	118
8.3.2	For Hospitalized Population (H_p)	127
8.3.3	For Unaware Infected Camel Population (I_c^1)	135
8.3.4	For Aware Infected Camel Population (I_c^2)	139
8.4	Discussion	143
Chapter 9: Conclusion		144
References		148
Appendix		154

List of Tables

Table 2.1:	Zoonotic diseases caused by ecological factors	7
Table 2.2:	Zoonotic diseases caused by method of transmission	8
Table 2.3:	Zoonotic diseases caused by reservoir host	8
Table 2.4:	The number of SARS cases	12
Table 2.5:	The number of confirmed MERS-CoV cases	15
Table 2.6:	Influenza virus in avian species	24
Table 2.7:	Brucellosis cases in Abu Dhabi	25
Table 2.8:	Map of Zoonotic diseases in the Middle East	27
Table 4.1:	The most models of MERS-CoV	71
Table 6.1:	Description of the model parameters	77
Table 6.2:	Parameters of the human model	79
Table 6.3:	Parameters of the human model	80
Table 6.4:	Infected rate of camels per country	80
Table 8.1:	The parameters values and units	109
Table 8.2:	Initial conditions	110

List of Figures

Figure 2.1:	The significant type of zoonoses	9
Figure 2.2:	The Origin of Zoonotic Diseases	10
Figure 2.3:	The risk of Rabies in worldwide	17
Figure 2.4:	The distribution of Rift Valley fever outbreaks	18
Figure 2.5:	Total number of reported cases of CCHF	20
Figure 2.6:	The Geographic distribution of CHIK outbreaks	21
Figure 2.7:	The WNV in tested horses in the UAE	22
Figure 2.8:	The distribution of AHF in the KSA	23
Figure 2.9:	Brucellosis cases in the worldwide	26
Figure 2.10:	Global map of Anthrax distribution	28
Figure 3.1:	The compartmental model of RVFV	30
Figure 3.2:	A flow diagram of RVFV transmission	32
Figure 3.3:	A flow diagram of the RVF model	35
Figure 3.4:	The compartment of the Rabies model	36
Figure 3.5:	The diagram of the Rabies model	39
Figure 3.6:	Flowchart of rabies model	41
Figure 3.7:	The diagram of the CHIKV model	42
Figure 3.8:	The Compartment model of the CHIKV	44
Figure 3.9:	The compartment model of the WNV	45
Figure 3.10:	Flowchart of brucellosis model	47
Figure 3.11:	Flow chart of A/H1N1 influenza model	54
Figure 3.12:	Classification of infectious diseases	56
Figure 4.1:	The Compartmental structure MERS model	58
Figure 4.2:	Flow diagram of MERS model	60
Figure 4.3:	The model of MERS in the Republic of Korea	63
Figure 4.4:	The stochastic model of MERS	65

Figure 4.5:	The scheme of MERS with 2-step approach	69
Figure 5.1:	Flowchart of the MERS dynamics.	73
Figure 8.1:	Case 1: disease free equilibrium (when $\mathcal{R}_0 < 1$)	112
Figure 8.2:	Case 2: disease endemic equilibrium (when $\mathcal{R}_0 > 1$)	114
Figure 8.3:	Case 3: disease endemic equilibrium (when $\mathcal{R}_0 > 1$)	115
Figure 8.4:	Case 4: disease endemic equilibrium (when $\mathcal{R}_0 > 1$)	116
Figure 8.5:	Parameters sensitivity to I_p in case 1	119
Figure 8.6:	Parameters sensitivity to I_p in case 2	121
Figure 8.7:	Parameters sensitivity to I_p in case 3	123
Figure 8.8:	Parameters sensitivity to I_p in case 4	126
Figure 8.9:	Parameters sensitivity to H_p in case 1	128
Figure 8.10:	Parameters sensitivity to H_p in case 2	130
Figure 8.11:	Parameters sensitivity to H_p in case 3	132
Figure 8.12:	Parameters sensitivity to H_p in case 4	134
Figure 8.13:	Parameters sensitivity to I_c^1 in case 1	136
Figure 8.14:	Parameters sensitivity to I_c^1 in case 2	137
Figure 8.15:	Parameters sensitivity to I_c^1 in case 3	138
Figure 8.16:	Parameters sensitivity to I_c^1 in case 4	139
Figure 8.17:	Parameters sensitivity to I_c^2 in case 1	140
Figure 8.18:	Parameters sensitivity to I_c^2 in case 2	141
Figure 8.19:	Parameters sensitivity to I_c^2 in case 3	142
Figure 8.20:	Parameters sensitivity to I_c^2 in case 4	143
Figure 9.1:	Scenarios of MERS transmission among human	146

Chapter 1: Introduction

The Middle East Respiratory Syndrome (MERS) is a new infection that has emerged in humans which is related to lineage C Betacoronavirus (B CoV) and the sixth Coronavirus (CoV). It is a virus transmitted to humans [12]. MERS-CoV is a zoonotic virus [24]. A series of studies have shown that an animal origin and route of acquisition of MERS-CoV [39, 30]. Generally, there are many types of coronaviruses that naturally infect only one animal species or a small number of closely related species; MERS-CoV presence was known at the bats [43]. Furthermore, laboratory confirmed that from the testing sample of a nasal swab of the first cases of MERS, and they found that people infected by the same virus as bats and be enzootic in dromedary camels in Arabian peninsula and horn of Africa [39]. According to Mackay [39] there is animal-to-human transmission, and the camels are considered a major source of human infection with the Middle East Respiratory Syndrome, happening by close contact and consuming their product such as drinking raw camel milk, or camel urine and eating meat that has not been thoroughly cooked [39]. However, many people get MERS disease without contact with camels, which illustrates that infected humans can also carry the MERS-CoV and infect others through the air or close contact; that is called human-to-human transmission [30].

Once the virus infects a person, it takes an incubation period 2-14 days and the most common that the symptoms within the first five days to appear [73]. The symptoms of MERS could range from having no symptoms at all, to having severe illness leading to death. Early symptoms include fever, cough, chills, sore throat, breathing difficulties and quickly progresses to pneumonia that transforms to acute respiratory distress syndrome, mostly it leads to the organs failure [39, 7]. The people who are at the most risks of MERS are older men who have a weak immune system [39].

The First known case of the Middle East Respiratory Syndrome MERS was in 2012 in Jordon. At that time the most human cases of MERS appeared in the Arabian

Peninsula specifically in Saudi Arabia [39]. The UAE ranked second in the number of infected cases. MERS-CoV outbreaks have been increasing since 2012 in and around the Arabian Peninsula. According to the World Health Organization (WHO), 2079 cases have been reported globally, with 722 cases experiencing death as of September 6th, 2017 [24]. Since the first appearance of the cases of MERS until now, the past two years have seen outbreaks rapidly increase between humans through human-to-human transmission. The first cases that were reported outside the Middle East region mostly are carried a history for visiting the Middle East countries especially the United Arab Emirates and the Kingdom of Saudi Arabia(KSA) [1].

Recently in the Republic of Korea, there has been a healthcare-associated outbreak [1]. The lack of understanding of the dynamics of MERS-CoV transmission may lead to fatal dramatic outbreaks. Some factors also would assist in the spread of MERS, such as crowded gatherings of pilgrims in the holy places in the KSA and global events such as Expo 2020 which will be in the UAE [42]. These events also might be a factor of increasing the spread of MERS-CoV around the world. In 2015, there was an outbreak in health-care facilities in Republic of Korea [1]. After this incident, the study of Chowella et al. [14] showed that the MERS-CoV transmission among hospitalized was higher than its transmission in the community, so the hospitalized cases must receive more attention by epidemiologists. So far, there is no antiviral for MERS-CoV infection to prevent its spread. The only precaution taken to limit the spread of the disease is the isolation and hospitalization of the infected cases. The visitors coming from the Middle East area must be investigated and isolated if they are suspected of having any contact with MERS-CoV cases or having the disease symptoms in them [70].

This thesis is organized in the following way:

Firstly, Chapter 2 presents a definition of zoonotic diseases and factors that influence the emergence of zoonotic diseases then we introduce a group of diseases that have emerged in the Middle East region. Chapter 3 followed provides a range of zoonotic diseases that have appeared in this region with some of the mathematical models that are designed to study their dynamics.

As for the fourth chapter it concentrates on presenting the dynamics of MERS-CoV with various types of mathematical models to get the perfect understanding around the nature of transmission of this disease among humans and how we can control it.

Chapter 5, introduces a mathematical model of MERS infection with two patches: human population and camel population. The human population is modeled with an SEIHR model and the camels population is modeled with SIS model.

Chapter 6, uses a set of others papers to help us estimate the parameters of our model. Of course, not all the parameter are available since we have lack of camels data in the Middle East region.

The main result of this thesis is presented in Chapter 6, where a numerical analysis for our model is performed starting with presenting our well posed basic mathematical model by proving boundedness and positivity for two models. We next calculate the basic reproduction number \mathcal{R}_0 using the next generation method. Hence, we find the relationship between two thresholds(\mathcal{R}_{01} and \mathcal{R}_{02}). Next, we use very well-known results of the next generation method to give the stability results. Finally, we find the conditions of existence of possible endemic equilibria which concerning \mathcal{R}_0 .

To illustrate the outcomes of our analytical study, we give, in Chapter 7, time series simulations of the model using parameters estimation. The simulations confirm the mathematical finding by showing the results of a possible MERS epidemic in the UAE. These findings are discussed in this chapter in details. Moreover, we also introduce the sensitivity analysis of the parameters of the model and investigate in their impact on our variables; particularly on the burden of infection. All the simulations were done with R software with different open source packages [18, 60]. We finish this work by a conclusion in which we cover all aspects of our work. We are present some possible extension for this work. All the definitions which are used in the model are presented in Appendix 1. All the codes used in this thesis are presented for the reader in Appendix 2.

Chapter 2: Zoonotic Diseases in the Middle East

Recently, the world has seen outbreaks of several diseases that constituted a major health crisis resulting from zoonotic diseases. Due to the mortality and injuries caused by these diseases, public health institutions have been interested in studying these diseases to reduce the fear of rapid infections in different parts of the world.

2.1 Zoonotic Diseases

This section presents the definition of zoonotic diseases and the importance of highlighting them.

2.1.1 Definition

The World Health Organization (WHO) noted that zoonotic diseases are diseases that are transmitted from animals to humans in multiple conditions [49]. The possibility of transmitting diseases to humans are usually related to the human needs for animals as food or pets. The most way contributing to the invasion of zoonotic diseases around the world is mostly through animal importing especially the vertebrates [49] where 71.8% of them originates in wildlife [29]. Furthermore, these animals acquire the infection through different types of pathogen agents such as bacteria, parasites, fungi, viruses, and prions [66].

It is Important to point out that studies have found that animals and humans catch the same zoonotic diseases. However, the ecology of diseases in animals and humans are different. Therefore, the method of dealing with the two species is different.

Throughout the ages, zoonotic diseases have been considered a significant threat to human health, causing many human deaths. Therefore, we need measures to protect human health and fight infections in livestock and other animals, to avoid the spread of diseases among them and consequently in humans.

2.1.2 Factors Influencing the Emergence of Zoonotic Diseases

The zoonotic diseases weren't an example of contemporary diseases, but they have always existed for decades among a wide range of human diseases. The zoonotic diseases weren't an example of contemporary diseases, but they have always existed for decades among a wide range of human diseases. Recently, those diseases have increased through expansion in the geographical scope of the host or vector. As a result, the zoonotic diseases in humans have increased significantly over time and reached more than 70% of human diseases [69]. Global economies and public health have been affected to a large extent by emerging infectious diseases that pose a significant threat for human future [29].

Despite the development of medical technologies in health, which contributed to the diagnosis and detection a lot of pathogens but still, there are some of the problems that face them. For example, some of the pathogens do not cause only a massive outbreak among humans population but also they are high in lethality, where this dilemma has not been explained yet. There are some Known factors contributing to the emergence of zoonotic diseases such as human practices which lead to climate change and the destruction of the ecosystem. These excesses are an essential reason to understand the relationship between hosts and pathogens, including the wildlife, livestock, and humans. The crisis is continuing when these zoonotic diseases killing many animals and people, while many unknown factors are still emerging from wildlife reservoir.

1. Trade in Animals and Their Products

The risk of infections transmission increased when humans were interested in the bushmeat trade which in turn contributed to the transfer of live animals to central markets to became closely linked to human. Therefore that causing the transmission of zoonotic diseases between animals then humans [66, 49].

2. Human Movement

The movement of people around the world for tourism, education, commerce, or

the performance of Hajj and Umrah, has been revealed as a way of transmitting diseases in sizeable human populations [49].

3. Climate Variability and Ecological Change

Also, climate change has played a significant role in the distribution of vector and restricted pathogens into the geographical range [66]. As populations have expanded, people have been forced to deforestation, and the exploit natural land happens for agriculture, and building dams. The human intervention in the environment has led to the formation of potential pathogens and effects the vector born diseases [49].

4. Cultural Standards

In some of the Gulf countries such as the UAE, Saudi Arabia, and Oman people have the habit of dealing with camel products. For example, drinking unpasteurized milk directly without boiling, drinking camel urine as Arabian people think it has benefits, so if these cattle are infected may that contribute to the transmission of diseases to human [39]. In Kenya, their culture allows dogs and hyenas eat human bodies infected with worms. This habit leads to a continuous cycle of disease transmission in nature [49].

5. Transportation of Virus Infected Mosquitoes

All transportation such as aircraft, ship, train, motor, and other vehicles may contribute to the transport of infected mosquitoes with viruses into new areas, for example Yellow Fever, Chikungunya Fever, Dengue Fever, etc [49].

2.2 The List of Zoonotic Diseases

There is a wide range of zoonotic diseases identified through modern laboratory techniques. These techniques have found more than 300 of these zoonoses where each of them have a classification that distinguishes them [49].

2.2.1 Etiological Factors

The Table 2.1 shows the list of zoonoses that based on etiological factors[49].

Bacterial zoonoses	e.g. anthrax, brucellosis, plague, leptospirosis, salmonellosis, lyme disease.
Viral zoonoses	e.g. rabies, arbovirus infections, KFD, yellow fever, influenza.
Rickettsial zoonoses	e.g. murine typhus, tick typhus, scrub typhus, Q-fever.
Protozoal zoonoses	e.g. toxoplasmosis, trypanosomiasis, leishmaniasis.
Helminthic zoonoses	e.g. echinococcosis (hydatid disease), taeniasis, schistosomiasis, dracunculiasis.
Fungal zoonoses	e.g. deep mycosis - histoplasmosis, cryptococcosis, superficial dermatophytes.
Ectoparasites	e.g. scabies, myiasis.

Table 2.1: Zoonotic diseases caused by ecological factors

2.2.2 Method of Transmission

The Table 2.2 shows the list of zoonoses that based on transmission method [49].

Direct zoonoses	It needs a direct connection to transfer it from the infected vertebrate host to the sensitive host as (man). During that time the agent may be remain it self or undergo to changes and developing in time of transmission e.g. rabies, anthrax, brucellosis, leptospirosis, toxoplasmosis.
Cyclozoonoses	It needs more than one vertebrate host species but at that time there are no invertebrate host to complete the agent life cycle e.g. echinococcosis, taeniasis.
Metazoonoses	In biological methods transmitted by invertebrates, at that time the agent multiplies or develops, and has an external incubation period before birth and moving to another vertebrate host. e.g. plague, arbovirus infections, schistosomiasis, leishmaniasis.
Saprozoonoses	It needs to vertebrates in addition a non-animal development site such as soil, plant material and dove Projectione. e.g. aspergillosis, coccidioidomycosis, cryptococcosis, histoplasmosis, zygomycosis.

Table 2.2: Zoonotic diseases caused by method of transmission

2.2.3 Reservoir Host

The Table 2.3 shows the list of zoonoses that based on reservoir host [49].

Anthropozoonoses	Infections is in lower vertebrate animals and was transmitted to man from it, e.g. rabies, leptospirosis, plague, arboviral infections, brucellosis and Q-fever.
Zooanthroponoses	Infections is in man and was transmitted to lower vertebrate animals from it, e.g. streptococci, staphylococci, diphtheria, enterobacteriaceae, human tuberculosis in cattle and parrots.
Amphixenoses	Infections is in both man and lower vertebrate animals and was transmitted between them, e.g. salmonellosis, staphylococcosis.

Table 2.3: Zoonotic diseases caused by reservoir host

The flowchart in Figure 2.1 represents the most significant type of zoonoses, where zoonoses that appeared in the Middle East are colored red.

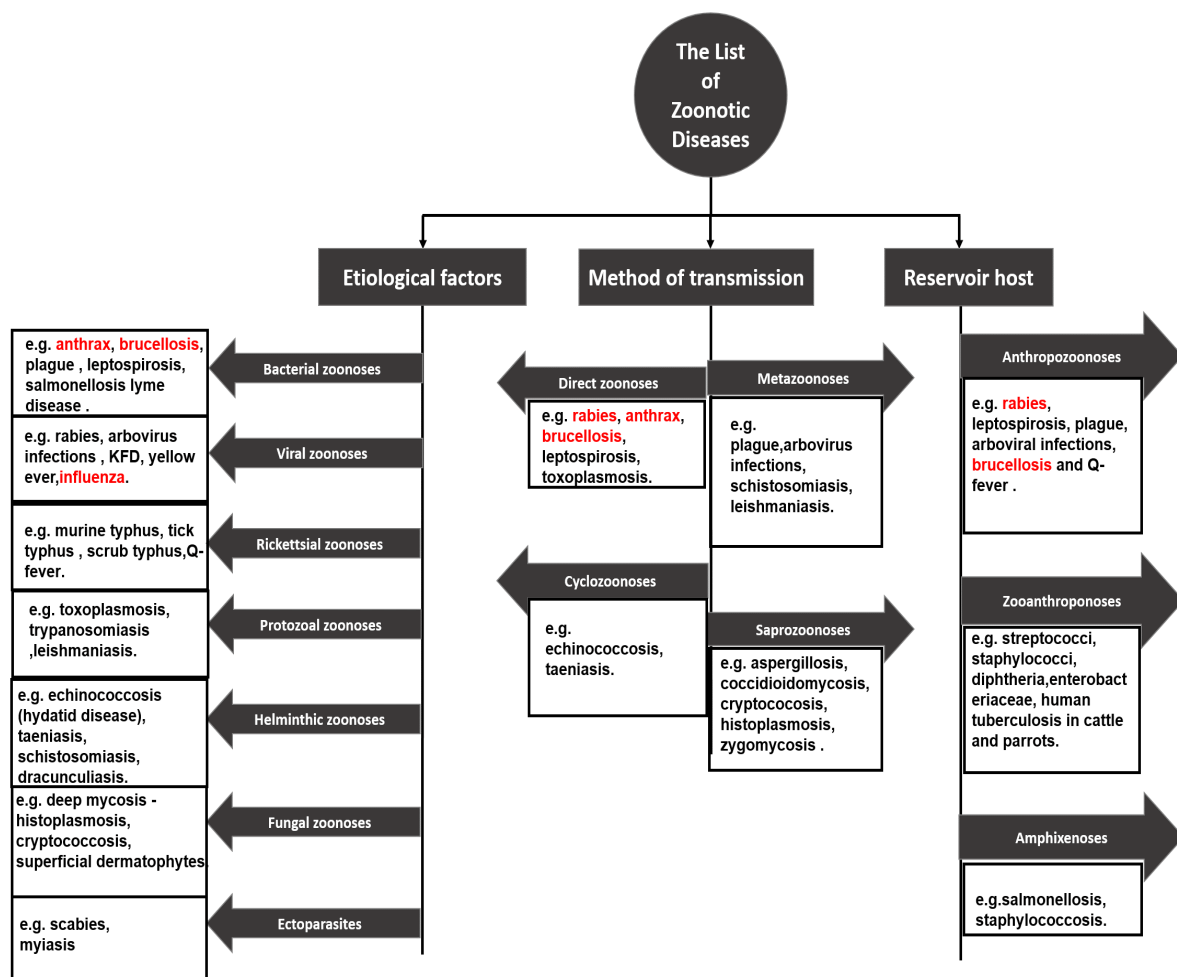


Figure 2.1: The significant type of zoonoses

2.3 The Origin of Zoonotic Diseases in The Middle East

The zoonotic diseases in the middle east have two type of origin, one of them by bat and the other by vector, wildlife and livestock.

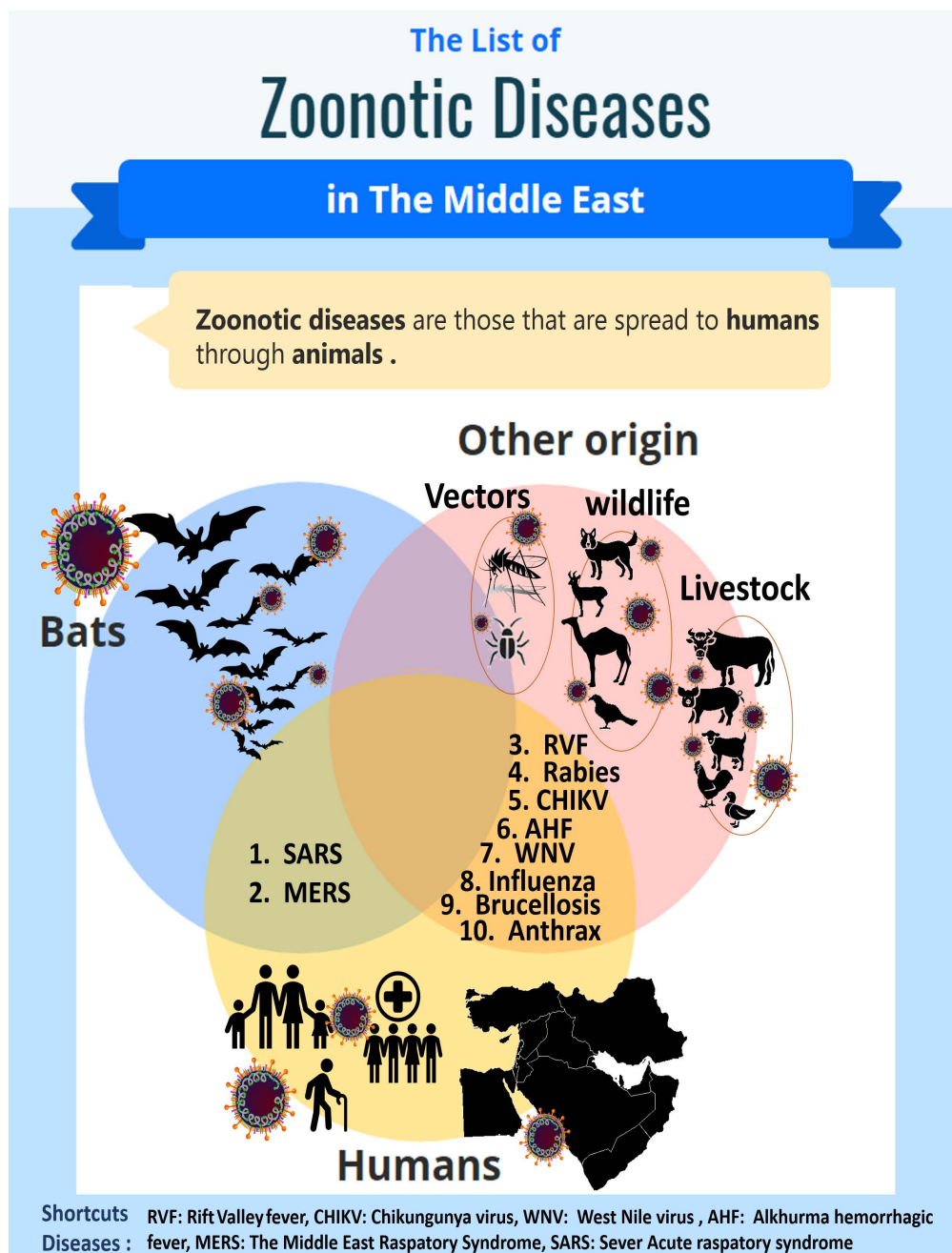


Figure 2.2: The Origin of Zoonotic Diseases

2.3.1 Emerging Zoonotic Viruses of Bat Origin

Bats have been discovered as a vast reservoir host for viruses that infect animals and then transmit to humans causing severe diseases. Bats are considered as the best reservoir of zoonotic infection due to their ability to live for many years. Also, they can get flies on a large scale which allow them to acquire and distribute the pathogens through this range. In addition, bats are mammalian and contain many species, approximately more than 1,200 species spread around the world. The vast colonies and caves inhabited by bats for many years constitute the largest gathering of viral pathogens [66]. It is noteworthy that, bats are not affected by these viruses that due to their immune system, which is characterized by the interaction with viral pathogens compared to other animals [53].

According to Ranjan study in the past two decades, the viruses that are present in the bat are multiple and contribute to the enormous numbers of diseases around the world. So the risk of zoonotic infections led to alert health institutions to intensifying studies around them since the studies in this field was scarce [53].

1. Severe Acute Respiratory Syndrome Virus

In late 2002, severe acute respiratory syndrome appeared in southern China caused by the SARS virus found in bats of the genus *Renolovus* as a reservoir host. Also, the palm civets have been infected with the SARS virus. The Chinese government exterminated these bats to prevent more SARS outbreaks. At the end of 2003, the cases of infection reached 8,000 casualties by SARS where approximately killed 800 people [66, 33]. As reported by WHO, Kuwait is the only Arabic country that have received an instance of SARS. The Table 2.4 summarizes the cumulative number of SARS cases reported for the period from 16 November 2002 until 7 August 2003 [15]. The Table 2.4 summarizes the cumulative number of SARS cases.

Areas	Cumulative number of cases			Status							Date onset first probable case	Date onset last probable case
	Female	Male	Total	Median age (range)	Number of cases Currently hospitalized	Number of cases recovered	Number of deaths	Number of CFR (%) ¹	Number of Imported cases (%)	Number of CW affected (%)		
Australia	4	2	6	15 (1-45)	0	6	0	0	6 (100)	0 (0)	24-Mar-03	1-Apr-03
Brazil	1	1	2	4	0	1	0	0	1 (100)	0 (0)	3-Apr-03	3-Apr-03
Canada	151	100	251	49 (1-98)	10	200	41	17	5 (2)	108 (43)	23-Feb-03	12-Jun-03
China	Pending	Pending	5327	Pending	29	4949	349	7	NA	1002 (19)	16-Nov-02	25-Jun-03
China, Hong Kong Special Administrative Region	977	778	1755	40 (0-100)	7	1448	300	17	NA	386 (22)	15-Feb-03	31-May-03
China, Macao Special Administrative Region	0	1	1	28	0	1	0	0	1 (100)	0 (0)	5-May-03	5-May-03
China, Taiwan	349	319	665	46 (2-79)	10	475	180	27	50 (8)	86 (13)	25-Feb-03	15-Jun-03
Colombia	1	0	1	28	0	1	0	0	1 (100)	0 (0)	2-Apr-03	2-Apr-03
Finland	0	1	1	24	0	1	0	0	1 (100)	0 (0)	30-Apr-03	30-Apr-03
France	1	6	7	49 (26 - 61)	0	6	1	14	7 (100)	2 2 (29)	21-Mar-03	3-May-03
Germany	4	5	9	44 (4-73)	0	9	0	0	9 (100)	1 (11)	9-Mar-03	6-May-03
India	0	3	3	25 (25-30)	0	3	0	0	3 (100)	0 (0)	25-Apr-03	6-May-03
Indonesia	0	2	2	56 (47-65)	0	2	0	0	2 (100)	0 (0)	6-Apr-03	17-Apr-03
Italy	1	3	4	30.5 (25-54)	0	4	0	0	4 (100)	0 (0)	12-Mar-03	20-Apr-03

Table 2.4: The number of SARS cases

Areas	Cumulative number of cases			Status					Date onset first probable case	Date onset last probable case	
	Female	Male	Total	Median age (range)	Number of cases currently hospitalized	Number of cases recovered	Number of deaths	CFR (%)			Number of imported cases (%)
Kuwait	1	0	1	50	0	1	0	0	1 (100)	0 (0)	9-Apr-03
Malaysia	1	4	5	30 (26-84)	0	3	2	40	5 (100)	0 (0)	22-Apr-03
Mongolia	8	1	9	32 (17-63)	0	9	0	0	8 (89)	1 (11)	6-May-03
New Zealand	1	0	1	67	0	1	0	0	1 (100)	0 (0)	20-Apr-03
Philippines	8	6	14	41 (29-73)	0	12	2	14	7 (50)	4 (29)	5-May-03
Republic of Ireland	0	1	1	56	0	1	0	0	1 (100)	0 (0)	27-Feb-03
Republic of Korea	0	3	3	40 (20-80)	0	3	0	0	3 (100)	0 (0)	10-May-03
Romania	0	1	1	52	0	1	0	0	1 (100)	0 (0)	19-Mar-03
Russian Federation	0	1	1	25	1	0	0	0	NA	0 (0)	5-May-03
Singapore	161	77	238	35 (1-90)	0	205	33	14	8 (3)	97 (41)	5-May-03
South Africa	0	1	1	62	0	0	1	100	1 (100)	0 (0)	3-Apr-03
Spain	0	1	1	33	0	1	0	0	1 (100)	0 (0)	26-Mar-03
Sweden	1	2	3	33	0	3	0	0	3 (100)	0 (0)	
Switzerland	0	1	1	35	0	1	0	0	1 (100)	0 (0)	9-Mar-03
Thailand	5	4	9	42 (2-79)	0	7	2	22	9 (100)	12 (11)	11-Mar-03
United Kingdom	2	2	4	59 (28-74)	0	4	0	0	4 (100)	0 (0)	1-Mar-03
United States	16	17	33	36 (0-83)	7	26	0	0	31 (94)	1 (3)	9-Jan-03
Viet Nam	39	24	63	43 (20-76)	0	58	5	8	1 (2)	36 (57)	23-Feb-01
Kuwait	1	0	1	50	0	1	0	0	1 (100)	0 (0)	9-Apr-03

Table 2.4: The number of SARS cases (Continued)

2. The Middle East Respiratory Syndrome Virus

The Arabian Peninsula has seen some of the zoonotic diseases, such as the Coronavirus, which causes the Middle East respiratory syndrome(MERS). Usually, the MERS infection is caused by the direct or indirect contact with the camels that carry the same coronavirus present in the bat [10]. This is especially because some of these camels are imported from the Horn of Africa, and usually their health history is often unknown [39]. The most people who infected by MERS are farmers, herders, fishermen, veterinarians, and wildlife workers. The spread of the disease was not confined to the local population but also spread around the world as a result of human movement and the contact with camels and human who are carrying the disease. For example, Hajj in Saudi Arabia and the habit of the sacrifice of animals with unknown health history is a threat to the Arabian Peninsula and will be a major challenge to control the spread of MERS in this region. Moreover, 1,700 people have been infected with MERS where third of them have died, the infections by MERS-CoV are still continuous. The Table 2.5 shows the number of laboratory-confirmed MERS-CoV cases reported by Middle East countries by year since 2012 [67]. The Table 2.5 shows the number of laboratory-confirmed MERS-CoV cases.

Country reporting	Number of laboratory Confirmed MERS-CoV Cases reported
Algeria	2
Austria	2
Bahrain	1
China	1
Egypt	1
France	2
Germany	3
Greece	1
Iran	6
Italy	1
Jordan	28
Kuwait	4
Lebanon	1
Malaysia	1
Netherlands	2
Oman	7
Philippines	2
Qatar	16
Republic of Korea	185
Saudi Arabia	1482
Thailand	3
Tunisia	3
Turkey	1
United Kingdom	4
United Arab Emirates	79
United States of America	2
Yemen	1
Total	1841
*Data as of 2 December 2016	

Table 2.5: The number of confirmed MERS-CoV cases

Because SARS and MERS are two diseases from the same family of the coronavirus, we need to compare these diseases to determine the nature of the Coronavirus. The last studies indicate that both diseases transfer to humans through the intermediate animals that received the virus from the bats. Furthermore, MERS-CoV targets the older patients, and they are mostly male, while SARS-CoV focused on younger patients who were healthy. With regard to SARS outbreak in 2002 which originated from Southern China and it took eight months to spread SARS with 8,273 cases. In late 2003, there have been no more cases of SARS disease. On the other hand, MERS Continued to spread from 2012 until the present day, while the number of infections is still lower than SARS [38]. However, SARS has been spread very quickly between human in the world com-

pared to MERS [38]. According to recent researches, the MERS is more fatality than SARS but appears to be less infectious. Thus The mortality rate in MERS and SARS was 41%, 10% respectively [20]. Besides that, the incubation period between SARS and MERS were approximately similar which is 5.5 days and 4.6 days respectively.

The primary cases of infection by MERS reach approximately 61% of all reported cases. This cases of the MERS-CoV, are documented with infected camel [23]. Humans always have been associated with animals to meet their needs for animal protein and other things but as the population continues to grow, the human needs for will be greater, as will the risk associated with zoonotic diseases. The Middle East countries import camels that may be carrying the corona-virus, we need a lot of attention on this issue. It's assumed that there are laws governing animals from other environments that should be subjected to medical tests before they are sent. However, the secondary cases of MERS which result from contact between infected human with healthy human are a significant problem that needs consideration.

2.3.2 Emerging Zoonotic Viruses from other Sources

Bats are one of the most common sources of zoonotic diseases. Although, there are also many zoonotic diseases that threaten health institutions by viruses with other reservoir hosts.

1. Rabies

Rabies is a severe viral disease caused by the rabies virus (RABV) [63]. The disease usually spreads due to bites of rabid animal [55]. Dogs are the main reservoirs of rabies in developing countries, while foxes, raccoons, and coyotes are the main reservoirs of this disease in developed countries [56]. The infected animals and human with RABV show encephalitis as a result of infecting the central nervous system which historically leads to death [63, 55]. In 1992, the first cases of rabies were reported in the United Arab Emirates specifically in Al Ain [67]. The disease was reported to have been transmitted from Oman to UAE through red fox bites which considered as a reservoir host of rabies in these countries, where around 12 dromedaries, five sheep, and four goats

were infected in Al Ain. After four months, the disease moved to Abu Dhabi and Dubai and killed 44 animal from four different species. The last rabies case appeared in the UAE in 2014 [67]. The disease also appeared in Saudi Arabia in 2007, where 48 camel herders reported infection more than 4,000 animals through bites of wild dogs which is also considered as a reservoir host of the disease in the KSA and Yemen [67]. The map in Figure 2.3 shows the risk of Rabies around the world [44].

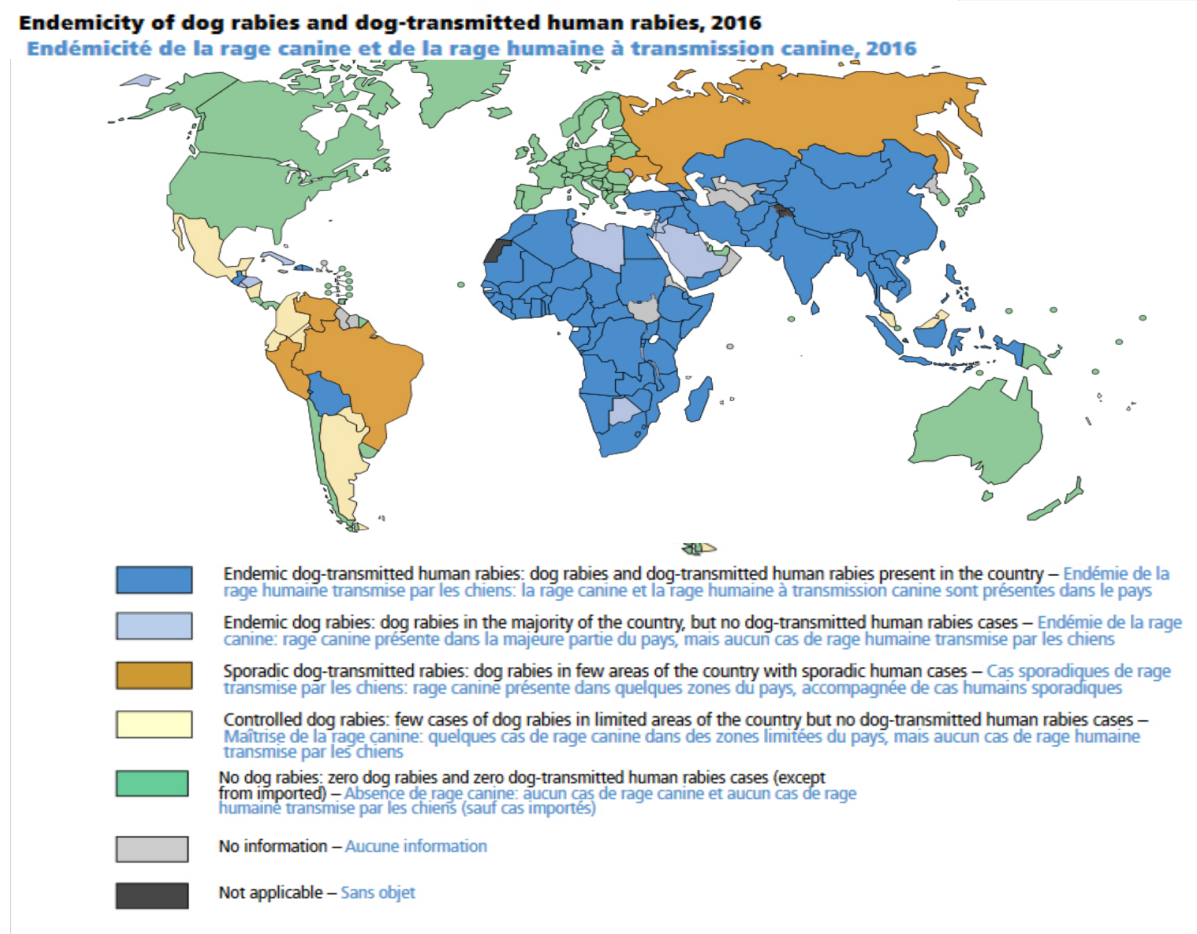


Figure 2.3: The risk of Rabies in worldwide

2. Rift Valley Fever

Rift Valley Fever (RVF) is a viral zoonosis that has had a major impact on livestock production, food security and human health over the years in the African continent. Later, in the Arabian Peninsula, specifically in Saudi Arabia and Yemen, as a result of the import of infected animals from the African continent [65]. RVF is found in humans and animals through mosquito bites, which is considered the viral carrier of the fever. Also, the diseases transmitted to human through blood exposure that carry the disease and the other body fluids, in addition to drinks the humans to unpasteurized milk of cattle [8]. In 2001, the Saudi Ministry of Health reported that 882 people were infected by RVF, including 124 people who died. Studies indicate that the RVF epidemiology remain unclear. However, it seem that the spread of the disease was associated with the conditions of the wetlands after heavy rainfall, because of the breeding of mosquitoes and the suitability of these conditions for sheep gatherings in the pastures. So there are periods of intensive activity of virus and animal behavior during epidemics that we should know more about it [8, 65].

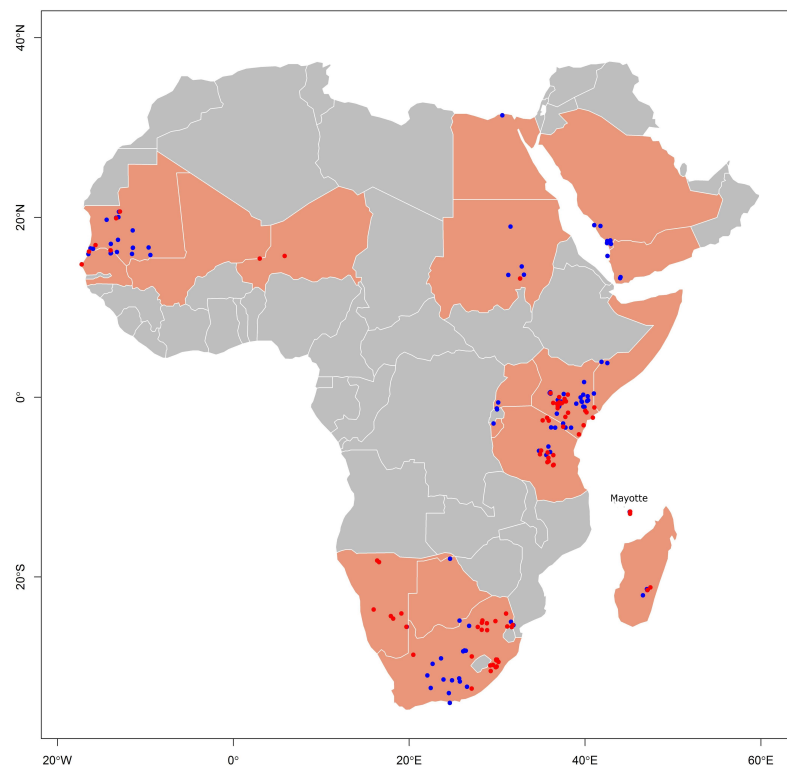


Figure 2.4: The distribution of Rift Valley fever outbreaks

The map that shown in Figure 2.4 display the distribution of Rift Valley fever outbreaks across the African continent and the Arabian Peninsula between 1998 and 2016 as reported by ProMED-mail (blue) and between 2005 and 2016 as reported by the World Organization for Animal Health (red). Countries affected are highlighted in salmon and include: Botswana, Burundi, Egypt, Kenya, Madagascar, Mali, Mauritania, Mayotte (France), Namibia, Niger, Saudi Arabia, Senegal, Somalia, South Africa, Sudan, Tanzania, Uganda, Yemen [65].

3. Crimean-Congo Haemorrhagic Fever Virus

Crimean-Congo Haemorrhagic Fever(CCHF) is a severe disease carried by ticks [67]. Ticks are considered as the main vector, and natural reservoir of infection in mammals and they show the symptoms of the disease on them, but it doesn't appear in the ticks. The primary method of transmission to humans is through tick bites, also through human contact with tissues or blood of infected animals [66]. The infection has spread around 30 countries in Asia, the Middle East, Southeast Europe and Africa since 1944. The disease causes unspecified mild fever and sometimes becomes severe [66]. There are a lot of regions that affected with CCHF in Arabian Peninsula such as the United Arab Emirates, Oman, and Saudi Arabia. Hyalomma ticks formed the main cause of the CCHF outbreak in these areas with high fatalities [67]. The first appearance of CCHF was in 1979 in Dubai, which is known as a hospital outbreak. No other cases were reported in the United Arab Emirates until 1994 when the epidemic occurred between abattoir workers [9]. Additionally, in the mid of 1990s, the human infection also identified in Oman, and there was study confirmed that the cattle and ticks are spreading the virus locally. Besides, some cases of CCHF have recently been reported in Iraq [9]. The Figure 2.5 shows the total number of reported cases of CCHF by countries in 2013 [9].

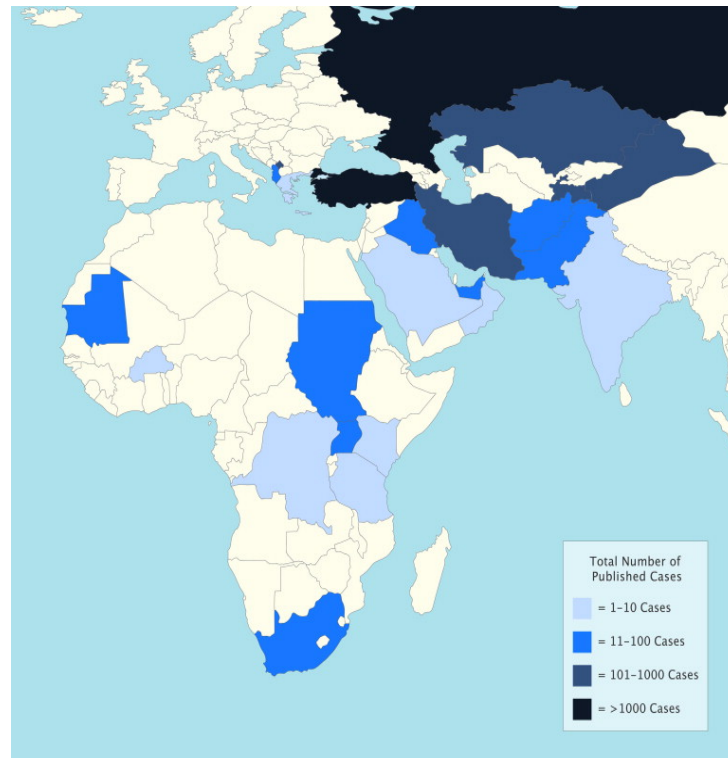


Figure 2.5: Total number of reported cases of CCHF

4. Chikungunya Virus

Chikungunya(CHIK) is an infection carried by the Aedes mosquitoes which are considered as the primary vector. The CHIKV has appeared in the subtropical regions of Africa, the Indian Ocean islands, and some parts of Asia [66]. In 1658, the first possible clinical description of the infection was identified in Cairo, Egypt. Previously, the incidence of the disease at that time was low in the Middle East region until 2011 where CHIK cases are confirmed in the Middle East and North Africa. Also, more than 15,000 cases are suspected outbreaks in Yemen [28]. Recently, the spread of CHIK disease has appeared in the Arabian Peninsula, where the outbreaks have reported Kuwait and Saudi Arabia [28]. The Figure 2.6 shows the geographic distribution of human prevalence studies and reported outbreaks and cases for Chikungunya virus in the Middle East and North Africa [28].

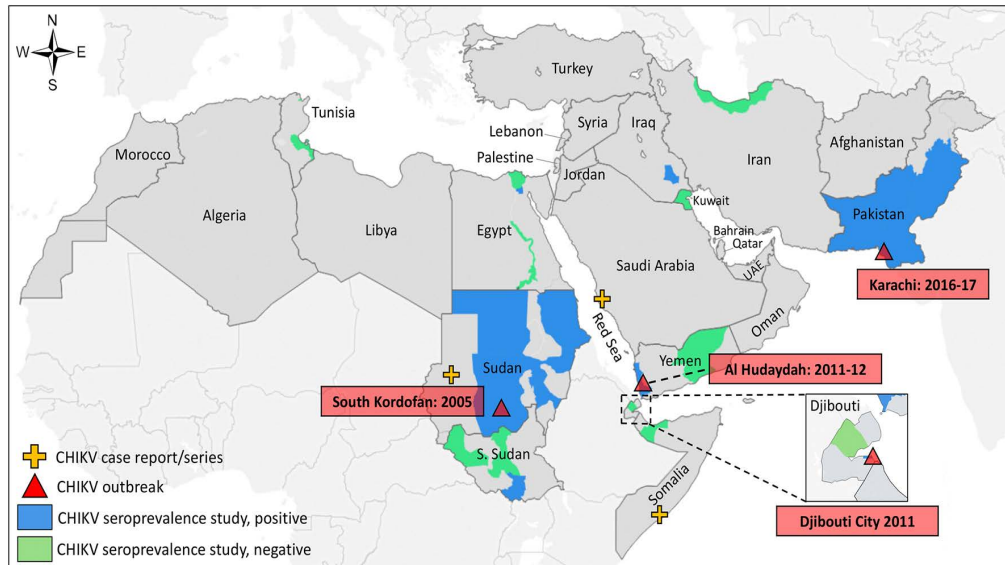


Figure 2.6: The Geographic distribution of CHIK outbreaks

5. West Nile virus

West Nile virus (WNV) is a deadly neurological disease vector born disease. WNV has emerged by the cycles of infection between mosquitoes and birds [17]. Birds and more than 100 species of mammals are considered a natural reservoir host to the WNV [17, 58]. Bats have also been found to be susceptible to infections, and they are becoming increasingly dangerous because of their closeness to animals and humans [58]. The WNV disease attacks the central nervous system of infected animals and humans which often causes death [13]. Its symptoms range from mild fever to severe neurological illness [66]. The WNV has a history of spreading in the countries in Africa, the Middle East, Europe and parts of southern Europe [58]. Between 1951 and 1954, Egypt witnessed many significant outbreaks, which contributed to the understanding epidemiology of WNV. It was observed that about 75% of human infections with West Nile Fever (WNF) are mostly asymptomatic and less than 1% of infections developed to severe stages varying from flu-like to severe neurological symptoms [58]. The WNV also appears in the UAE. In 2007, a serological survey conducted by all the emirates of the country except Umm Al Quwain revealed the existence of 144 horses carrying WNV's antibodies [68]. The Figure 2.7 shows the serological prevalence of WNV antibodies in horses tested in the UAE[68].

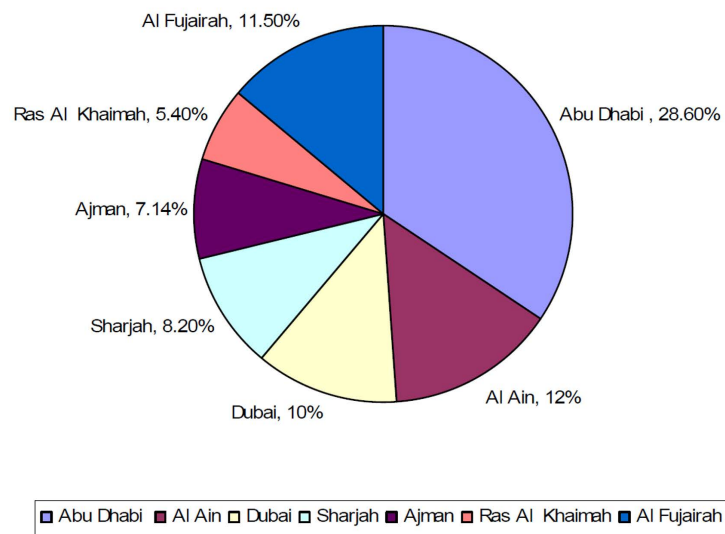


Figure 2.7: The WNV in tested horses in the UAE

6. Alkhurma Hemorrhagic Virus

Alkhurma hemorrhagic fever (AHF) is the zoonotic disease caused by Alkhurma Hemorrhagic virus (AHV), ticks are considered as the main vector for infection. Humans get the infection through sheep and camels that carry the virus. The ticks were founded separated from the camels in some countries such as Saudi Arabia, Kuwait, and Yemen [67]. Alkhurma Hemorrhagic fever (AHF) first appeared in Saudi Arabia in the mid-1990s. AHF was found specifically in Jeddah in the blood of some butchers aged 24 to 39 years [6]. Later, the infection was seen in many patients in Saudi Arabia, and there are also rare cases of infection occurred in Egypt [4]. The Figure 2.8 shows the locations of Alkhurma hemorrhagic fever virus in the Kingdom of Saudi Arabia. Red: confirmed cases, blue: positive serology [4].

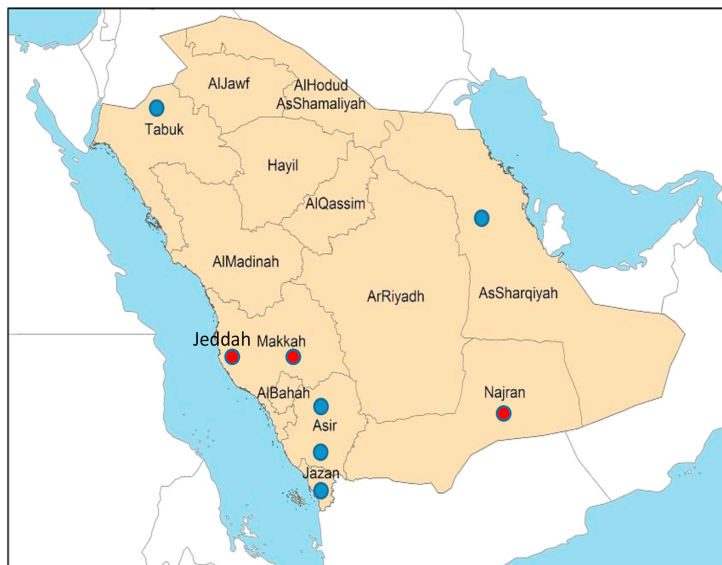


Figure 2.8: The distribution of AHF in the KSA

7. Influenza

The Arabian Peninsula has seen many types of influenza viruses that have emerged as a result of mutations of influenza virus circulating in birds population. A devastating outbreak of H5N1 avian flu occurred in Saudi Arabia in 2005 when an infected falcon returned from a hunting trip in Mongolia [67]. Also, H9N2 influenza viruses were isolated in the UAE over the last decade from infected avians such as chicken and bustards. The number of isolates was (8, 10), respectively. Moreover, there are human cases of the H1N1 in the UAE [67]. The Table 2.6 shows Influenza virus strains isolated from different avian species over the last 10 years in the United Arab Emirates.

Species	Avian influenza virus	Number of isolates
Chicken	H9N2	8
Falcon	H5N1	3
	H7N3	2
	H9N2	1
	H7N1	1
Bustard	H9N2	10
	H7N1	7
	H1	1
	H10	1
Quail	H9N2	8
Stone curlew	H9N2	3
Plover	H9N2	1
Dove	H11	1
Pheasant	H9N2	2

Table 2.6: Influenza virus in avian species

8. Brucellosis

Brucellosis is a profound health problem, with more than 500,000 new cases a year [67]. Brucellosis has several types; however, the most two common types are *Brucella melitensis* and *Brucella abortus*. Brucellosis is one of the most critical animal bacterial diseases that has been observed in the Arabian Peninsula in recent years. The transmission of the virus to humans is referred to as lousy fever or Malta fever. In the Middle East, 15 countries reported *Brucella Melitensis* cases and another 9 reported *Brucella Abortus*. Most dangerous type is the first type which can cause orchitis and epididymitis in men and pregnancy loss in women. And most human cases are caused by the consumption of unpasteurized milk.

Saudi Arabia is also a significant reservoir for human Brucellosis due to two reasons. First, climate change has contributed to the multiplicity of regional endemic disease, the effects of the grazing activities that followed rainy seasons caused a high incidence of Brucellosis. Second is the uncontrolled massive importation of wild animals [51]. Saudi Arabia reported around 4,534 human cases in 2003. Brucellosis's cases were also detected in the United Arab Emirates. The Brucellosis cases are often reported in Dubai because it is a popular international travel destination. However, Abu Dhabi is the biggest emirate where the families in rural areas are interested in the pastoral life in

"Al-Ezba." Pastoral life includes mixed herds of Goats, sheep, and camels with people consume animal products in traditional ways, and that led to contribute the spread of Brucellosis [3]. A total of 480 cases of brucellosis were reported in UAE. The Table 2.7 display the notifications of human brucellosis cases in Abu Dhabi by year and status.

Also, some countries in the Middle East such as Syria, Turkey, Oman, and Saudi Arabia recorded the highest rate of infection. According to OIE data, the Brucellosis cases Syria has estimated around 1603 cases per year per million people. In 2004, Turkey reported approximately 15,000 cases of Brucellosis concentrated in the poor eastern areas. The southern region of Oman also has an estimated 1,000 cases per year [51].

year	Brucellosis Cases				
	N	Confirmed		Probable	
		n	percentage (%)	n	percentage (%)
2010	47	37	78.7	10	21.3
2011	75	61	81.3	14	18.7
2012	135	96	71.1	39	28.9
2013	99	69	69.7	30	30.3
2014	49	26	53.1	23	46.9
2015	75	39	52.0	36	48.0
Total	480	328	68.3	152	31.7

Table 2.7: Brucellosis cases in Abu Dhabi

In Kuwait, the yearly incidence was almost 500 cases per million people. The Iraqi war thus contributed to a significant reduction in the prevalence of Brucellosis caused by the loss of many animals during the invasion, but Kuwait is still an endemic region. The annual rate in Jordan exceeded 300 cases per million, but the Ministry of Health in an ongoing attempt to control the disease. In Palestine, the yearly rate showed that the number of reported cases was increasing. In recent years, The State of Lebanon suffers from an increase in the number of brucellosis cases, which is especially endemic in the Bekaa region. The Ministry of Health said that most cases of infection observed among females compared to all international cases which recorded among men [51]. The Figure 2.9 shows the brucellosis cases around the world.

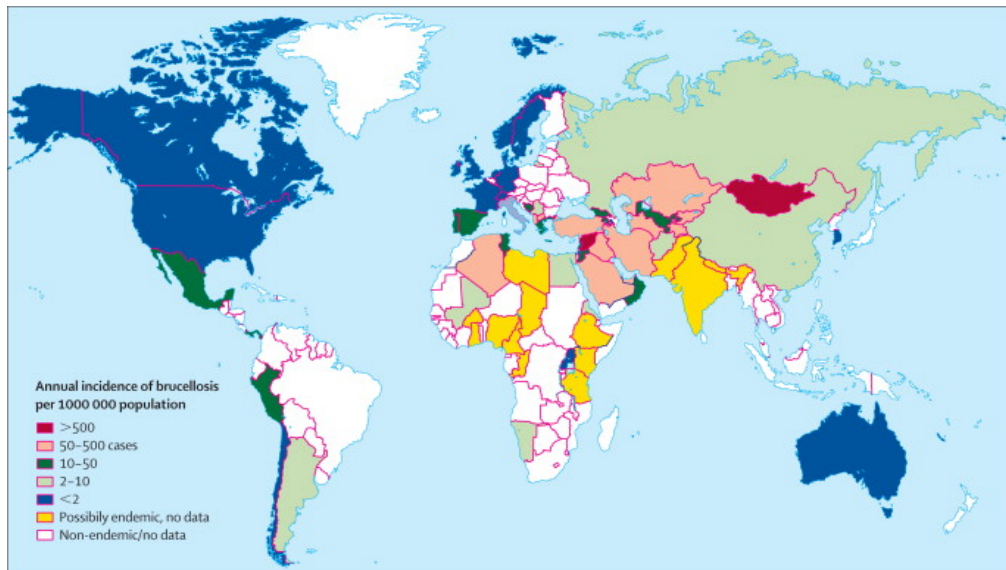


Figure 2.9: Brucellosis cases in the worldwide

9. Anthrax

Anthrax is a threat to livestock in many African and Asian countries. Rare cases had been identified in the Arabian Peninsula in ruminants, which get infected by contact with decomposed animals. The only way to control the disease is through vaccination and by disposing of rid of the animal's carcasses. Polluted dust can also lead to Anthrax. Human infections often result by contact with sick animals [67]. The Figure 2.10 shows the map of the global Anthrax Distribution as defined by the World Health Organization [26].

In Brief, we introduced the definition of zoonotic diseases, also we distributed the diseases according to pathogens. We also discussed some of the factors that are considered the main reasons for having this type of diseases and they pose a major threat to human health. Even though there are maybe a vaccine, a treatment, for some of this diseases but still, there are many fears around this diseases.

The Table 2.8 briefly presents the list of zoonotic diseases and countries of the Middle East region that have been appeared in it.

Middle East Country	Egypt	Iran	Turkey	Iraq	Saudi Arabia	Yemen	Syria	United Arab Emirates	Jordan	Palestine	Lebanon	Oman	Kuwait	Qatar	Bahrain	Armenia
Diseases																
The Middle East respiratory syndrome virus(MERS)	✓	✓	✓	✓	✓	✓	✓	✓	✓	✓	✓	✓	✓	✓	✓	✓
Severe acute respiratory syndrome virus(SARS)													✓			
Rift Valley Fever (RVF)	✓				✓	✓										
Rabies	✓	✓	✓	✓	✓	✓	✓	✓	✓	✓	✓	✓	✓	✓	✓	✓
Crimean-Congo Haemorrhagic Fever Virus (CCHF)				✓	✓			✓				✓				
Chikungunya Virus (CHIKV)	✓				✓	✓		✓					✓			
West Nile virus (WNV)	✓							✓								
Alkhurma Hemorrhagic Fever (AHF)	✓					✓	✓								✓	
Influenza																
H5N1																
H9N2																
H1N1																
Anthrax																
Brucellosis																

Table 2.8: Map of Zoonotic diseases in the Middle East

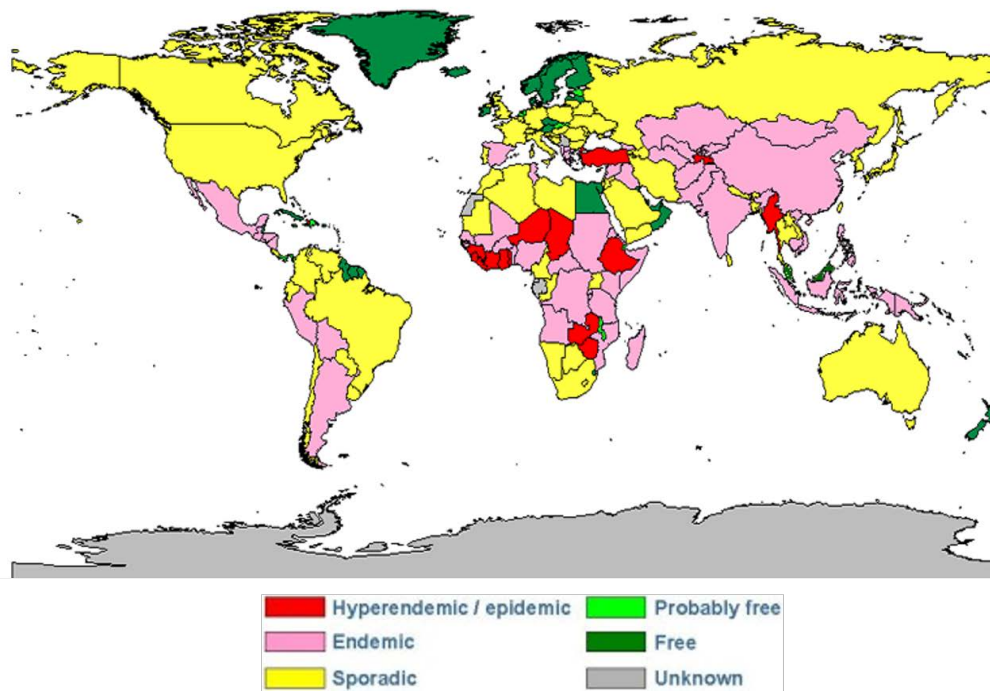


Figure 2.10: Global map of Anthrax distribution

Chapter 3: Zoonotic Diseases and their Math Models

Zoonotic diseases are a global concern for public health, accounting for approximately 75% of human infectious diseases. For decades the Middle East region was adversely impressed by zoonoses where it was threatening wildlife and therefore humans. Mathematical models played an important role in guiding the development of the control policies for these diseases. This chapter will review some of these models that have been developed to study zoonoses, especially those that appeared in the Middle East region. These models describe the dynamics of these diseases by interpreting the various assumptions around these diseases and by using the available data of each disease to gain a better understanding and get better control strategies.

3.1 Mathematical Models for SARS

After the outbreak of Severe Acute Respiratory Syndrome (SARS) in 2003, many studies focused on an understanding of a mathematical model which is related to the SARS [25]. So, Han's [25] study provided an overview of some mathematical models of SARS which was published during the epidemic.

First, a compartmental model was designed to simulate the transition of SARS in Beijing. As well as, the study used the time series and Bayes method to predict the number of potential SARS cases and deaths at the Beijing hospital. The data of SARS was only used for simulation. Also, the study was interested in predicting the SARS epidemic in the short term. The population of the study was classified into only two groups: infected or suspected of being infected humans. The study concluded that the description of transmission of SARS model was better in the deployment period compared to the control period [25]. A second study of Han's [25] also used the previous technique, but to simulate and evaluate the effects of prevention and control measures in SARS transmission. The study concluded that the model contains an anti-epidemic parameter factor to measure the effects of isolation measures. Also, a theoretical method

was created to calculate its value from 0-1 using fuzzy mathematics.

Third, a stochastic compartmental model was used for SARS model to define the relationship between control methods and their effectiveness [25]. The study found that the factors that determine the effectiveness of SARS control have been identified through intervention intensity and timing [25]. Fourth, this type of models was also used for the population of Vietnam, where the study focused on mimicking the SARS epidemic by Monte Carlo simulation. The simulation showed that super-spreading events played an essential role in the spread of SARS [25].

3.2 Mathematical Models for Rift Valley Fever

Many modeling tools have been used to determine the risk of Rift Valley fever (RVF) and the severity of the epidemic. There is a study [11] that examines the dynamic model of transmission of RVF among ruminants and takes into consideration that sick ruminants may expose to abortion due to RVF. The model also was based on a system for vector-borne diseases, by considering ruminants as hosts and mosquitoes as vectors [11]. The SIR model was divided into the human compartments are the susceptible (S), infectious (I), and recovered (R) individual, while mosquitoes compartments represent SIS model which is divided into the susceptible (U) and infectious mosquitoes (V). A diagram in Figure 3.1 shows the transmission of RVF between ruminants and mosquitoes [11].

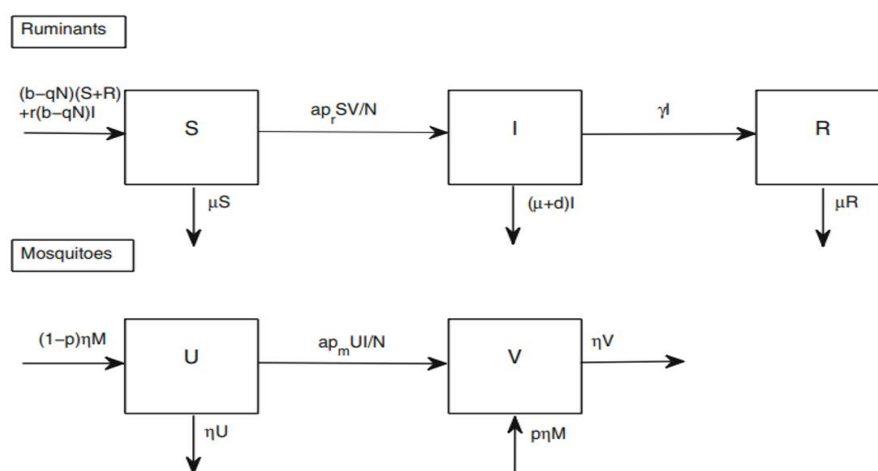


Figure 3.1: The compartmental model of RVFV

The following mathematical model shows the dynamics of RVF.

$$\begin{aligned}
\frac{dS}{dt} &= (p - qN)(S + R) + r(p - qN)I - ap_r \frac{SV}{N} - \mu S, \\
\frac{dI}{dt} &= \frac{SV}{N} - (\mu + d + \gamma)I, \\
\frac{dR}{dt} &= \gamma I - \mu R, \\
\frac{dU}{dt} &= (1 - p)vM - ap_m \frac{UI}{N} - vU, \\
\frac{dV}{dt} &= pvM + ap_m \frac{UI}{N} - vV.
\end{aligned} \tag{3.1}$$

The results of this study shows that a virus exists at low levels amongst ruminant after outbreaks in endemic areas. There is also a possibility of subsequent outbreaks when new ruminants come into these areas. The study also indicates that the severity of RVF outbreaks is due to several factors, including high mortality due to infected ruminant prevalence, a high ratio of mosquitoes, and short lifespan of ruminant which can contribute to amplification of outbreaks. According to the study the best solution to reduce the RVF outbreaks is to use the effective vaccination for animals before the onset of the disease and attention to treatment after the outbreak [11].

The study of *Mpeshe et al.* [11], depended on a deterministic model with hosts of mosquitoes, livestock, and humans to obtain some quantitative ideas about the mosquitoes dynamics. The model is a system of nonlinear ordinary differential equations.

A flow diagram in Figure 3.2 shows the transmission of RVF virus from vector to host, host to host, and host to vector [46].

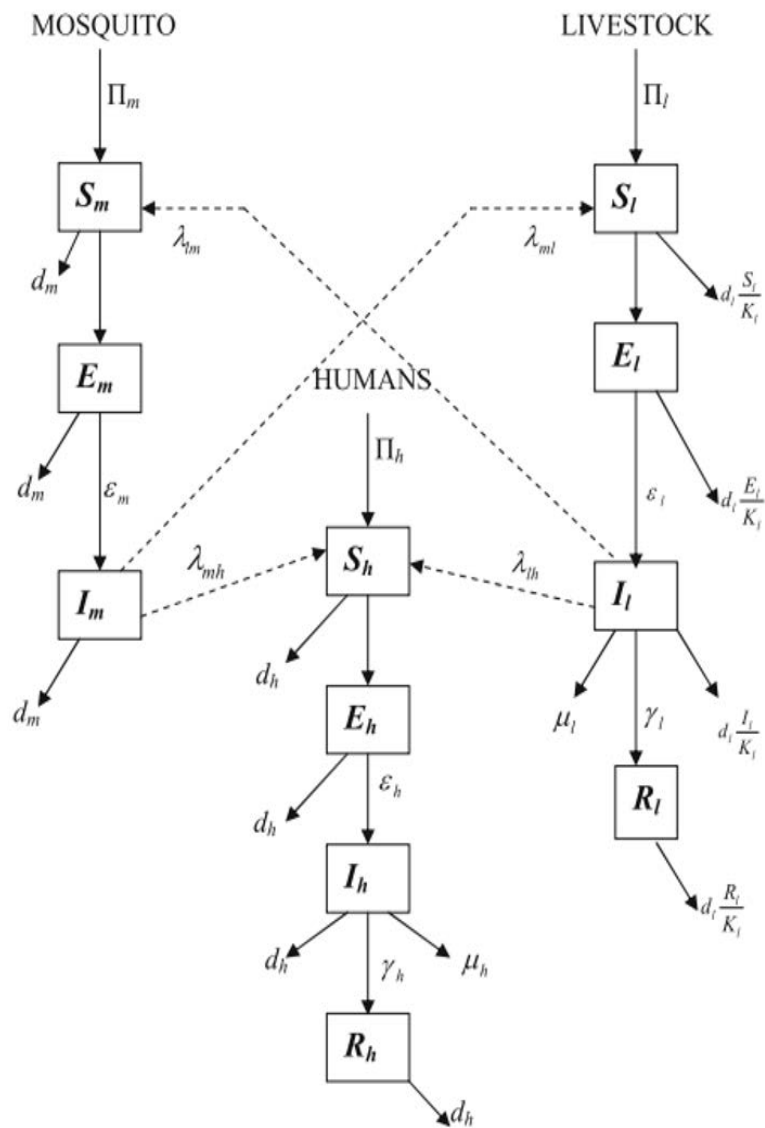


Figure 3.2: A flow diagram of RVFV transmission

The following mathematical model shows the transmission dynamics of RVF between three populations.

- MOSQUITOES

$$\begin{aligned}
 \frac{dS_m}{dt} &= \Pi_m - (d_m + \lambda_{lm} \frac{I_l}{L}) S_m, \\
 \frac{dI_m}{dt} &= \lambda_{lm} \frac{I_l}{L} S_m - (\varepsilon_m + d_m) E_m, \\
 \frac{dR_m}{dt} &= \varepsilon_m E_m - d_m I_m, \\
 \frac{dM_m}{dt} &= \Pi_m - d_m M,
 \end{aligned} \tag{3.2}$$

- LIVESTOCK

$$\begin{aligned}
 \frac{dS_l}{dt} &= \Pi_l - (d_l + \frac{L}{K_l} + \lambda_{ml} \frac{I_m}{M}) S_l, \\
 \frac{dE_l}{dt} &= \lambda_{ml} \frac{I_m}{M} S_l - (d_l + \frac{L}{K_l} + \varepsilon_l) E_l, \\
 \frac{dI_l}{dt} &= \varepsilon_l E_l - (d_l + \frac{L}{K_l} + \mu_l + \gamma) I_l, \\
 \frac{dR_l}{dt} &= \gamma I_l - d_l + \frac{R_l}{K_l} L, \\
 \frac{dL}{dt} &= \Pi_l - d_l + \frac{L^2}{K_l} - \mu_l I_l,
 \end{aligned} \tag{3.3}$$

- HUMANS

$$\begin{aligned}
\frac{dS_h}{dt} &= \Pi_h - (d_h + \lambda_{lh} \frac{I_l}{L} + \lambda_{mh} \frac{I_m}{M}) S_h, \\
\frac{dE_h}{dt} &= \lambda_{lh} \frac{I_l}{L} + \lambda_{mh} \frac{I_m}{M} S_h - (\epsilon_h + d_h) E_h, \\
\frac{dI_h}{dt} &= \epsilon_h E_h - (d_h + \mu_h + \gamma_h) I_h, \\
\frac{dR_h}{dt} &= \gamma_h I_h - d_h R_h, \\
\frac{dH}{dt} &= \Pi_h - d_h H - \mu_h I_h,
\end{aligned} \tag{3.4}$$

The threshold \mathcal{R}_0 of the study [46] was used in the model to reaches the local stability of the equilibrium. The study refers to the importance of arriving a specific measure of the initial transmission of disease. Also, the research acknowledges the significance of the endogenous balance which was determined by conducting sensitivity analysis and finding the most sensitive model parameters [46]. The results of this study show that the natural mosquito death rate d_m is considered as most sensitive parameters for both \mathcal{R}_0 and the disease prevalence in mosquitoes. The study also found that the spread of the disease was more sensitive between cattle and humans. So, the study suggested that the best preventive strategy for human life from outbreaks is through the isolation of livestock from humans [46].

Since RVF was a significant threat to the USA with massive economic damage to livestock and food supplies, there was a model that study the dynamics of the spread of the pathogen of which depended on the movement of humans, cattle, and mosquitoes [47]. A schema in in Figure 3.3 shows the spatial and epidemiological structure of RVF [47].

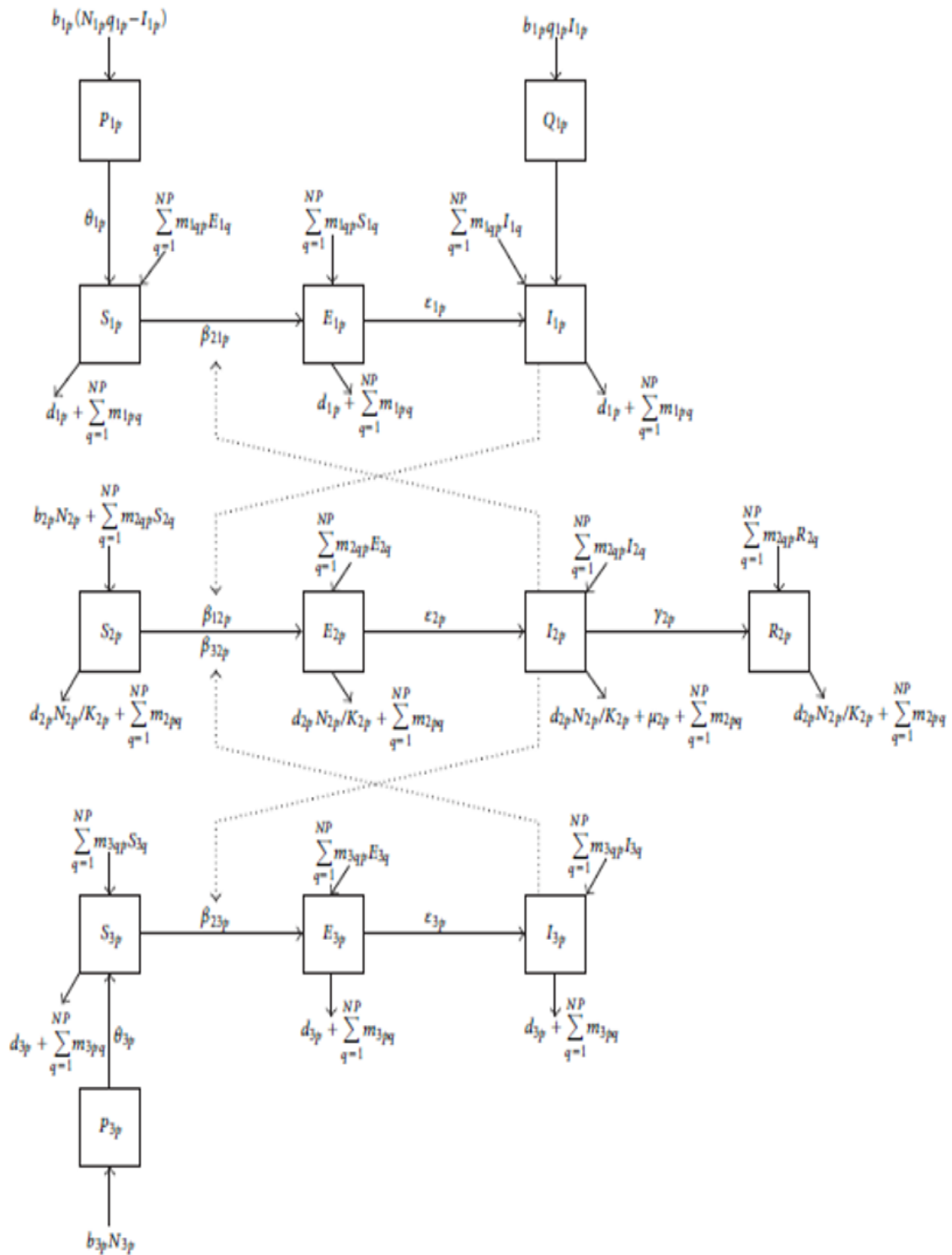


Figure 3.3: A flow diagram of the RVF model

This study used a system of ODEs to describe the transmission of RVFV among the three generic species traveling between patches with includes the effects of space. The populations of each patch is divided into susceptible, incubating, infectious, or immune to RVF, see reference [47]. The transition of RVFV was horizontal between two species

of mosquitoes and one species of livestock and transmission of the virus from mother-to-offspring in one of the mosquito species. The model is based on the division of geographical regions into small patches with adding the influence of space. Hence the model focuses on the movement of these species between patch-to-patch. The benefits of this study lie in understanding the methodology of RVF between patches and analyzing the probability of entering a pathogen on others region that free from pathogens [47].

3.3 Mathematical Models for Rabies

The rabies disease has been a prominent example of the development of mathematical modeling of the emergence and spread of infectious diseases. The dynamical models of rabies has taken the fundamental "SEIR" system where the populations is divided into particular classes of a susceptible (S), exposed (E), infectious (I), and recovered/removed individual (R) [50]. The rabies structures range from systems of ordinary differential equations (ODEs) to based computational simulations to the stochastic agent. The early construction of rabies model illustrates that the R class of "SEIR" compartmental model was transfered to the removed category due to no cases of natural recovery at that time and the vaccinations also weren't available [50]. The Figure 3.4 shows the compartment diagram of basic SEIR framework used in early ODE formulations for rabies [50].

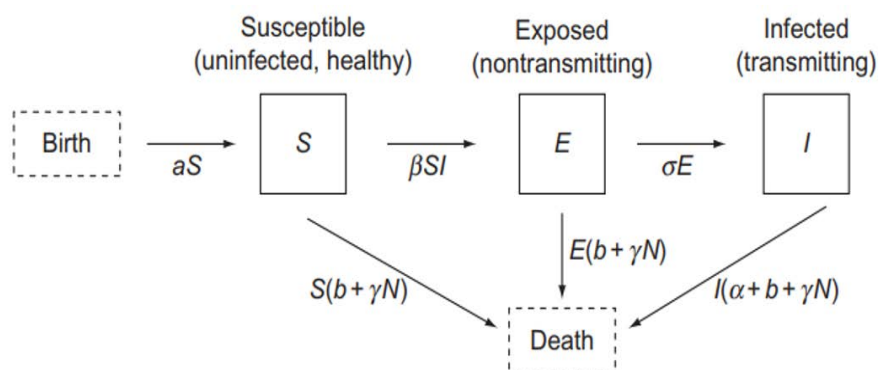


Figure 3.4: The compartment of the Rabies model

The following compartment model shows the transmission dynamics of Rabies.

$$\begin{aligned}
\frac{dS}{dt} &= rS - \gamma SN - \beta SI, \\
\frac{dE}{dt} &= \beta SI - (\sigma + b + \gamma N)E, \\
\frac{dI}{dt} &= \sigma E - (\nu + b + \gamma N)I, \\
N &= S + E + I,
\end{aligned} \tag{3.5}$$

There have been some descriptive studies that investigated the environmental factors such as habitats and foxes density that can affect the spatial spread of the virus, when rabies continued to progress towards neighboring areas [50]. These studies establish the modeling approach that use reaction-diffusion methods to describe the wave of the propagation behavior of rabies. The studies also contributed to providing a predictive model on how to implement a barrier in front of the transmissions wave to stop the epizootic expansion. The system relied on a framework of the reaction-diffusion formulation with the following coupled partial differential equations (PDEs) [50].

$$\begin{aligned}
\frac{\partial S(x,t)}{\partial t} &= r\left(1 - \frac{N}{K}\right)S - \beta SI, \\
\frac{\partial E(x,t)}{\partial t} &= \beta SI - \left(\sigma + b + \frac{N}{K}\right)E, \\
\frac{\partial I(x,t)}{\partial t} &= \sigma E - \left(\nu + b + \frac{N}{K}\right)I + D\frac{\partial^2 I}{\partial x^2}, \\
N &= S + E + I,
\end{aligned} \tag{3.6}$$

Models formed by *Anderson et al.* (1981) and *Murray et al.* (1986), which used the deterministic ODE and PDE frameworks, to understand the essential ideas about the dynamics of rabies virus in wildlife [50]. These models relied on ideal conditions to understand the behavior of dynamic systems. Also, these early deterministic models looked

at the homogeneous landscape with constant rates and the events were continual during the time. That model led to ask significant questions about the nature of environmental interactions. Landscape heterogeneity is likely to be an essential factor to understand the ecological interactions it wasn't taken consideration in deterministic models [50]. For example, data have indicated that fox rabies movement throughout Europe, has been characterized by rapid movement in valleys, and the transmission of the virus was slow in the areas near to these valleys. Later, it was concluded that rivers were practical barriers to the transmission of the disease and contributed to delaying the progress of the epidemic. Recently, most studies resorted to applying network models to study the environmental heterogeneity [50]. The diagram in Figure 3.5 shows the network model that used for rabies. The landscape is subdivided into N populations. The parameters μ_i and $\lambda_{i,j}$ are rates for processes that connect populations; here μ_i describes the rate at which long distance trans-location occurs in a particular population i , and $\lambda_{i,j}$ describes local movement of the virus from population i to j . The flowchart ($a \rightarrow f$) illustrates the sequence followed for iterating and updating the model over time. [50].

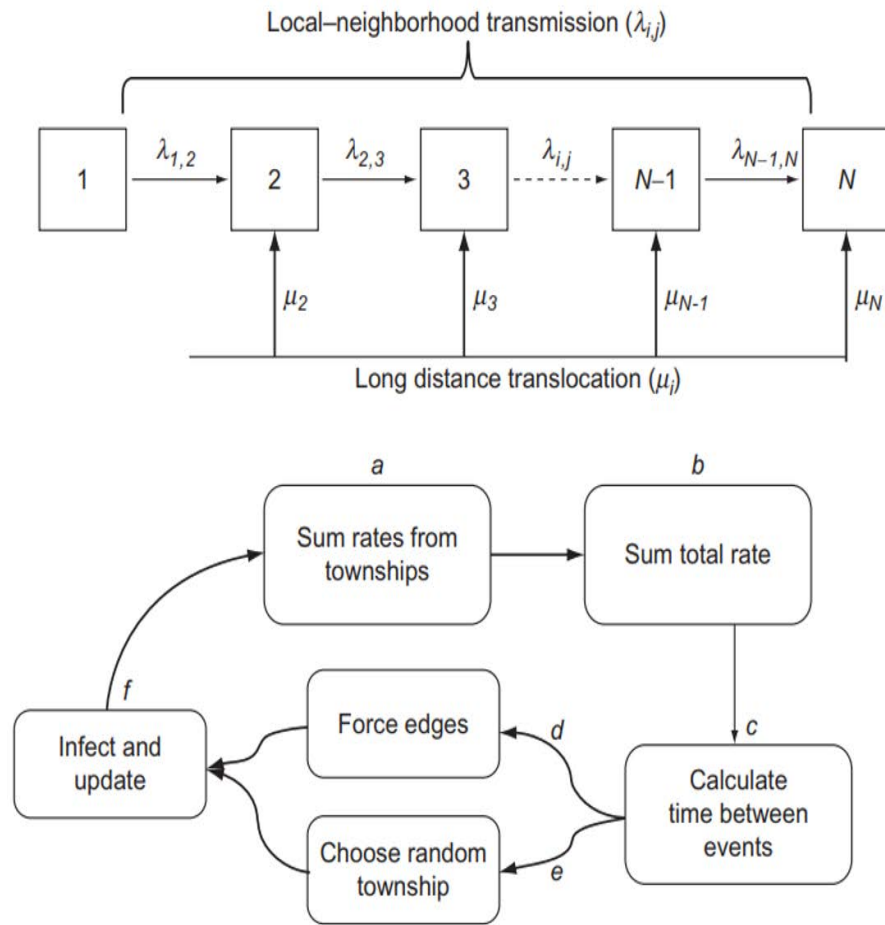


Figure 3.5: The diagram of the Rabies model

The stochastic impacts were explored in the model behavior by using a variety of techniques with some of the distributions to describe the process rate in an ODE and PDE approach. The approach was executed algorithmically with processes rates as birth (a) or death (d). For example, the first equation of model (3.5) the expected number of new susceptible individual in the interval dt could be implemented using a Poisson distribution with parameter rate $[rS(t)]dt$ [50].

Panjeti et al. [50], have introduced a system of stochastic SEIR model which contribute in the approach of simulation of discrete changes in the number of susceptible, exposed, infectious, and vaccinated individuals produced by births, deaths, infections, and movement within all subpopulations [50]. This model is more detailed than previous models, providing a high degree of biological realism depend on current knowledge about rabies virus infection. In this model, the spatial component is integrated, consider-

ing that the index i is present in all classes. This compartmental model consists of, S_i , E_i , I_i , and R_i are the number of susceptible, exposed, infectious, and vaccinated individuals at location i , respectively. And A_i is the total number of non-infectious individuals, N_i is the local population size [50]. The flowchart in Figure 3.6 illustrating the interactions in model of rabies.

The following Compartment model shows the transmission dynamics of Rabies.

$$\begin{aligned}
\frac{dS}{dt} &= aA_i - bN_iS_i - \beta I_iS_i - \nu S_i - (\Phi + \Phi_{LDT})S_i + \Sigma(\Phi K_{ij} + \Phi_{LDT}\hat{K}_{ij})S_j, \\
\frac{dE}{dt} &= \beta I_iS_i - bN_iE_i - \sigma E_i - (\Phi + \Phi_{LDT})E_j, \\
\frac{dI}{dt} &= \sigma E_i - \aleph I_i - (\Psi + \Psi_{LDT})I_i + \Sigma(\Psi K_{ij} + \Psi_{LDT}\hat{K}_{ij})I_j, \\
\frac{dR}{dt} &= \nu S_i - bN_iR_i - (\Phi + \Phi_{LDT})R_i + \Sigma(\Phi K_{ij} + \Phi_{LDT}\hat{K}_{ij})R_j, \\
A_i &= S_i + E_i + R_i, \\
N_i &= S_i + E_i + I_i + R_i,
\end{aligned} \tag{3.7}$$

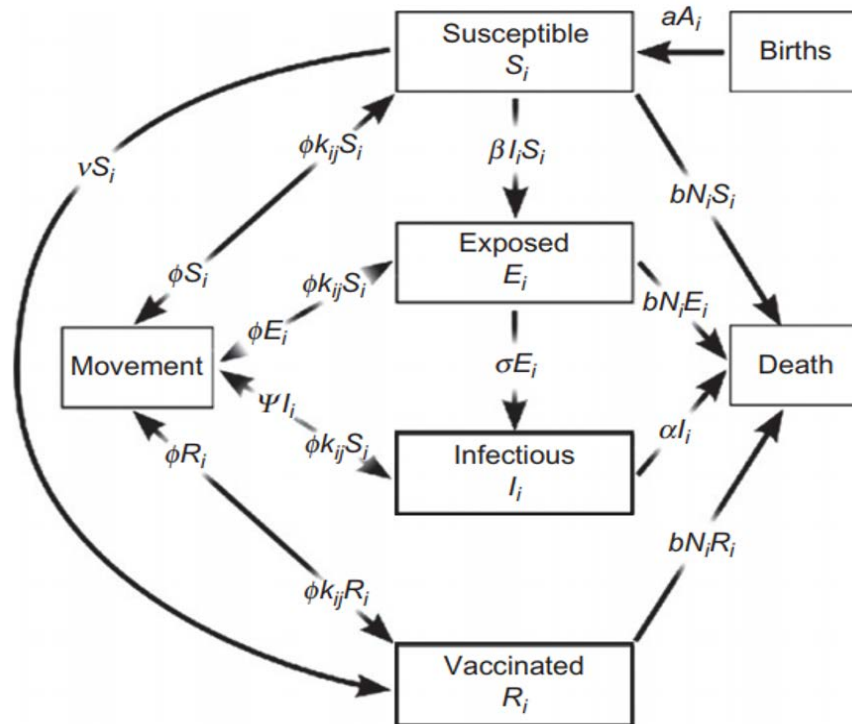


Figure 3.6: Flowchart of rabies model

The flowchart in Figure 3.6 illustrating interactions in the model. A "Movement" is represented as a class, but simply indicates how the process allows for the rearrangement of individuals spatially [50].

3.4 Mathematical Models for CHIKV

Mathematical modeling has contributed to the understanding of the biological history of Chikungunya infection [71]. Therefore, the study of *Yakob et al.* [71] used the data of the Chikungunya outbreak in 2006 in Reunion Island were used to construct a simple and deterministic mathematical model for virus transmission between humans and mosquitoes [71]. The compartmental model showed the fundamental "SEIR" system where the populations were subdivided into particular classes of susceptible humans (S), exposed to infection (E) before becoming infectious (Ia asymptotically) or (I symptomatically) and then recover (R). The populations of mosquitoes subdivided to Susceptible mosquitoes (X) exposed to infection (Y) before becoming infectious (Z) [71]. The figure 3.7 shows the compartmental construction of the epidemiological model for Chikungunya transmission.

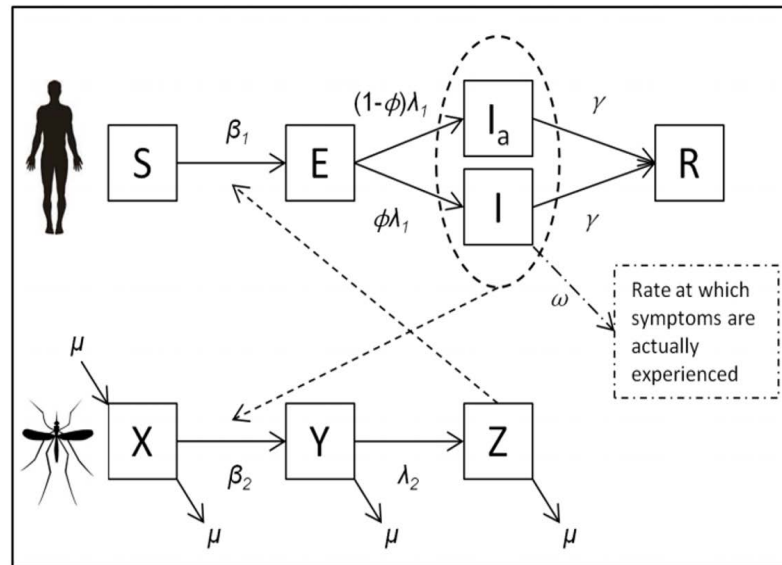


Figure 3.7: The diagram of the CHIKV model

The following Compartment model shows the transmission dynamics of Chikungunya among human and mosquitoes.

$$\frac{dS}{dt} = \beta_1 SZ,$$

$$\frac{dE}{dt} = \beta_1 SZ - \lambda_1 E,$$

$$\frac{dI}{dt} = \phi \lambda_1 E - \gamma I, \quad (3.8)$$

$$\frac{dI_a}{dt} = (1 - \phi) \lambda_1 E - \gamma I_a,$$

$$\frac{dR}{dt} = \gamma(I + I_a),$$

$$\begin{aligned}
\frac{dX}{dt} &= \mu - \beta_2 X(I + I_a) - \mu X, \\
\frac{dY}{dt} &= \beta_2 X(I + I_a) - \lambda_2 Y - \mu Y, \\
\frac{dZ}{dt} &= \lambda_2 Y - \mu Z,
\end{aligned} \tag{3.9}$$

The model has contributed to providing an approximation for peaks of the prevalence of an epidemic and final epidemic size. The study applied the model with Monte Carlo simulation for sensitivity analysis which in turn demonstrated the strong influence of both the latent period of infection in humans and the pre-patent period. The study also explained the importance of separating variables to obtain a precise and appropriate model as well as its importance in reporting control [71].

Another study focused on the formation of a dynamic stochastic model of climate-based mosquitoes population to determine the time periods that may pose epidemiological risks and to plan different intervention measures [57]. The Figure 3.8 provide a graphical representation of the Chikungunya model.

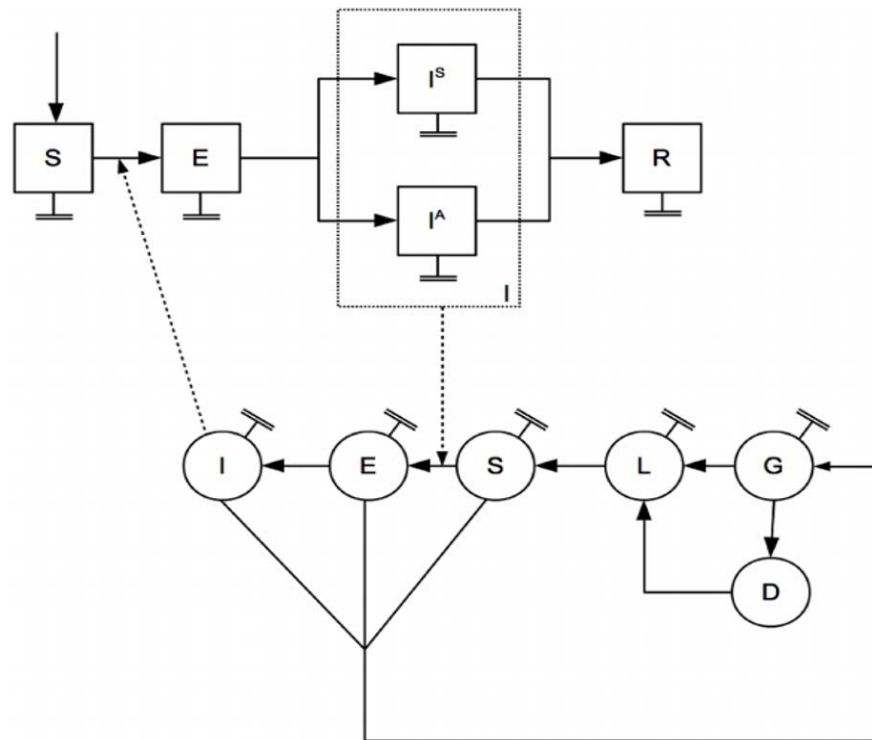


Figure 3.8: The Compartment model of the CHIKV

The diagram 3.5 shows the graphical representation of the Chikungunya model. Squares and circles represent the dynamic model for humans and mosquitoes, respectively. Human population is divided into susceptible (S), exposed (E), symptomatic (IS) and asymptomatic (IA) infective, and recovered (R) individuals. The mosquito population is divided into immature eggs (G), larvae (L) and eggs under a diapause (D) state, and mature susceptible (S), exposed (E) and infected (I) states. Full arrows represent the transition from one state to the other. Lines with parallel end represent natural mortality. Dotted lines represent infection dynamics. for more information around the model see [57].

This model was based on temperature data from different locations of Chikungunya cases in the United States to study the geographical sensitivity of the epidemic potential [57]. The study noted that the season's changes followed with the risk of the epidemic sites. This risk was shown in temperature changes and its periods also during the period when the population of mosquitoes was growing. The way of identifying those periods contributes to the effectiveness of resorting to a strategy to control the size of the population of mosquitoes. For other sites that show a yearly change in temper-

ature where that leads to develop the population size of mosquitoes and pose an active epidemiological threat. Human proportions had been reduced the likelihood and magnitude of outbreaks of sites that experience different temperatures throughout the year. This model can apply to other vector-borne diseases [57].

3.5 Mathematical Models for WNV

The study of *malik et al.* [40], provide a deterministic model which was developed for studying the dynamics of West Nile virus transmission through mosquitoes between two groups of domestic and wild birds. During this time, multiple effective communication rates were established between vectors and the two populations of birds [40]. The Figure 3.9 shows the compartmental construction of the epidemiological model for WNV transmission [40]. The digram in Figure 3.9 shows the compartment model of WNV among mosquitoes, domestic birds and wild birds.

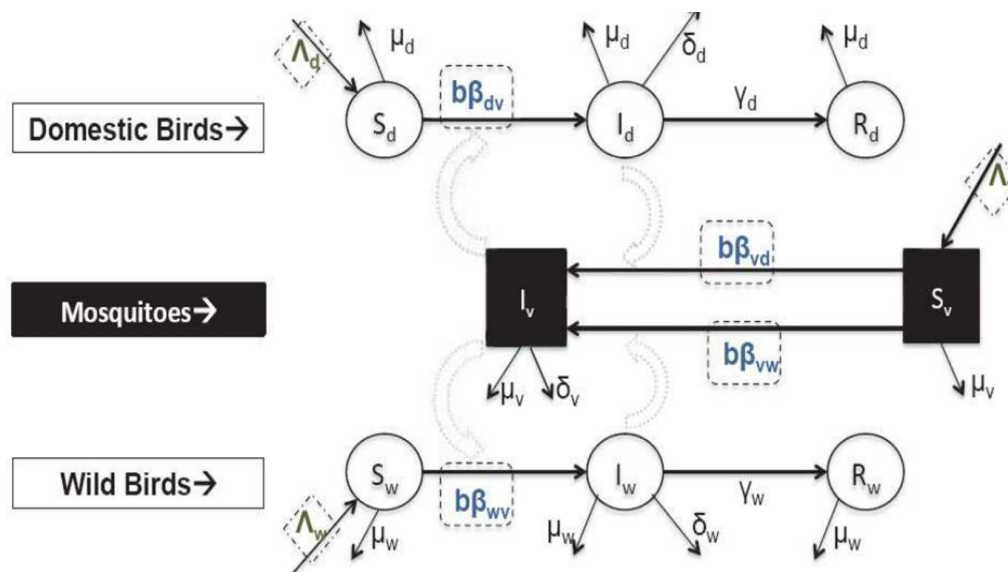


Figure 3.9: The compartment model of the WNV

The following Compartment model shows the transmission dynamics of WNV.

$$\begin{aligned}
\frac{dS_v}{dt} &= \lambda_v - b\beta_{vw}S_vI_w, \\
\frac{dI_v}{dt} &= b\beta_{vw}S_vI_w + b\beta_{vd}S_vI_d - (\mu_v + \delta_v)I_v, \\
\frac{dS_w}{dt} &= \lambda_w - b\beta_{wv}S_wI_v - \mu_wS_w, \\
\frac{dI_w}{dt} &= b\beta_{wv}S_wI_v - (\mu_w + \gamma_w + \delta_w)I_w, \\
\frac{dR_w}{dt} &= \gamma_wI_w - \mu_wR_w,
\end{aligned} \tag{3.10}$$

$$\begin{aligned}
\frac{dS_d}{dt} &= \lambda_d - b\beta_{dv}S_dI_v - \mu_dS_d, \\
\frac{dI_d}{dt} &= b\beta_{dv}S_dI_v - (\mu_d + \gamma_d + \delta_d)I_d, \\
\frac{dR_d}{dt} &= \gamma_dI_d - \mu_dR_d,
\end{aligned} \tag{3.11}$$

The analysis of this model was based on the system of ordinary differential equations. The system indicates that the epidemiological threshold which is known as the reproduction number was less than one that means the disease is free and stable globally [40]. Also, the disease uniformly persists and was associated with small variations in the parameters of the model when the reproduction number was higher than one. Under certain conditions, the model shows that the equilibrium was endemic and unique as the numerical simulation indicates that this equilibrium was asymmetrically stable. The study found that the optimal way to control the WNV in the two populations of birds is to reduce the density of mosquitoes [40].

3.6 Mathematical Models for Brucellosis

Recently, great efforts have been made to control the Brucellosis disease and reduce its transmission among pets and then to human [37]. However, the infection persists in some countries, including in the Middle East. Therefore, a mathematical model was developed for the dynamics of brucellosis transmission, which includes seasonal effects. The Figure 3.10 shows the flowchart of brucellosis model [37].

The following system of ordinary differential equations present the model of transmission dynamics of brucellosis:

$$\frac{dS}{dt} = A - \beta_1[E(t) + I(t)]S(t) - \beta_2B(t)S(t) - (\mu + \tau)S(t) + kH(t),$$

$$\frac{dH}{dt} = \tau S(t) - \gamma\beta_1[E(t) + I(t)]H(t) - \gamma\beta_2H(t)B(t) - (\mu + k)H(t),$$

$$\frac{dE}{dt} = \beta_1[S(t) + \gamma H(t)][E(t) + I(t)] + \beta_2[S(t) + \gamma H(t)]B(t) - (\sigma + \mu)E(t), \quad (3.12)$$

$$\frac{dI}{dt} = \sigma E(t) - (\mu + c)I(t),$$

$$\frac{dB}{dt} = \beta_3(E + I) - (d + \delta)B,$$

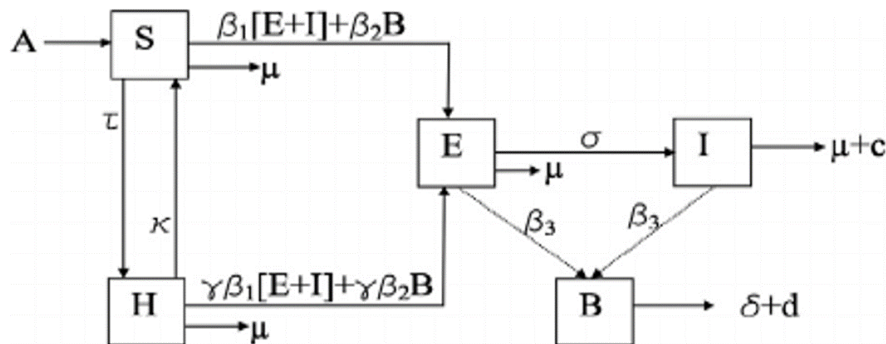


Figure 3.10: Flowchart of brucellosis model

The model in Figure 3.10 provides a clear picture of the transmission of the underlying disease and searches for the strengths and weaknesses of previous prevention and control strategies. So, the basic reproduction number associated with the time-periodic for this model was analyzed, and the results were determined from the threshold dynamics. The system of ODEs shows the dynamics of brucellosis in a time-periodic environment [37].

$$\begin{aligned}
\frac{dS}{dt} &= A - \beta_1[E(t) + I(t)]S(t) - \beta_2B(t)S(t) - (\mu + \tau)S(t) + kH(t), \\
\frac{dH}{dt} &= \tau S(t) - \gamma\beta_1[E(t) + I(t)]H(t) - \gamma\beta_2H(t)B(t) - (\mu + k)H(t), \\
\frac{dE}{dt} &= \beta_1[S(t) + \gamma H(t)][E(t) + I(t)] + \beta_2[S(t) + \gamma H(t)]B(t) - (\sigma + \mu)E(t), \quad (3.13) \\
\frac{dI}{dt} &= \sigma E(t) - (\mu + c)I(t), \\
\frac{dB}{dt} &= \beta_3(E + I) - d(t) + \delta B(t),
\end{aligned}$$

Also, the study conducted an optimal control on the use of animal vaccination and environmental disinfection as measures to control diseases against brucellosis infection [37].

Depending on both spatial and seasonal variations, a nonlinear model was constructed to investigate the dynamics of brucellosis transmission. The spatial model of that system was adopted to the structure patches and for the seasonal effects which were based on the use of time-periodic model parameters [72]. This framework was achieved by a two-patch model, as well as a detailed analysis of cases with and without seasonal fluctuations, respectively. The following system of ordinary differential equations (ODEs) describe the brucellosis transmission dynamics [72].

$$\begin{aligned}
\frac{dS}{dt} &= A_1 - (\mathfrak{K}_1 I_1 + \beta_1 B_1) S_1 - (\theta S + \mu_1) S_1, \\
\frac{dH}{dt} &= (\mathfrak{K}_1 I_1 + \beta_1 B_1) S_1 - (\theta I + c_1 + \mu_1) I_1, \\
\frac{dE}{dt} &= \phi_1 I_1 - d_1 B_1, \\
\frac{dI}{dt} &= A_2 - (\alpha_2 I_2 + \beta_2 B_2) S_2 - \mu_2 S_2 + \theta_S S_1, \\
\frac{dB}{dt} &= (\alpha_2 I_2 + \beta_2 B_2) S_2 - (\mu_2 + c_2) I_2 + \theta_I I_1,
\end{aligned} \tag{3.14}$$

The basic reproductive numbers contributed to the results of the threshold dynamics through different constructed scenarios. The results indicate the importance of integrating spatial and seasonal heterogeneity in the development of strategies to control brucellosis [72].

3.7 Mathematical Models for Anthrax

This study presents a deterministic mathematical model that includes migrations, births, and death from other diseases to trying to study the effects of anthrax transmission. The study focuses on the consequences of ingestion of carcasses, environmental pollution resulting from it and the role of migration rates in the persistence and extinction of animal populations [22]. The epizootic siac anthrax model with animal migration is described by the following system of four partial differential equations in $(x,t) \in \omega \times [0,\infty]$:

$$\begin{aligned}
\frac{\partial s}{\partial t} &= d \nabla^2 S + rn(1 - \frac{n}{K}) - as - \eta_c sc - \eta_i \frac{si}{n} - \mu s, \\
\frac{\partial i}{\partial t} &= d \nabla^2 i + as + \eta_c sc + \eta_i \frac{si}{n} - \gamma i - \mu i, \\
\frac{\partial a}{\partial t} &= -\alpha a + \beta c, \\
\frac{\partial c}{\partial t} &= (\gamma + \mu)i - \delta(s + i)c,
\end{aligned}
\tag{3.15}$$

The study also was concerned with the calculation of the basic reproduction number R_0 of the anthrax model taking into account the concentration on the animal migration $R_0(d)$ and without inclusion it R_0 , respectively. The study found that when $R_0 < 1$ that lead to the extinction of epizootic anthrax then the animal population persists without the disease. In contrast when $R_0 > 1$ it is possible to have a catastrophic extinction for both susceptible animals and infected animals with anthrax [22]. When $R_0(d) > 1$, that means the estimation for anthrax region was obtained and some special conditions of existence of diseases have been found in this region. The study shows that the process of reducing levels of ingestion of carcasses by removing carcasses from reserves doesn't always leads to a reduction in the proportion of infected animals with anthrax. As a result, the high levels of environmental carcasses caused by anthrax often result in the catastrophic extinction of animal populations [22].

3.8 Mathematical Models for Chikungunya Fever

The Chikungunya virus, which transmitted to humans by mosquitoes, is a severe tropical disease that first appeared in 1953. The mathematical models based on differential equations for the transmission of the Chikungunya virus developed for mosquito populations and virus transmission to the human population. The first model uses SI and SIR models while the second model depends on a stage structure model [45]. These models are an essential tool for studying vector-borne infections. The model also takes

into account the dynamics of the vector when the size of the population not constant as well as contact rate, which depends on the size of the vector population. Furthermore, the global analysis of the equilibrium is founded by uses the Lyapunov functions also by providing results on the theory of competitive systems and periodic stability [45].

In another study, a new model of Chikungunya was developed focusing on time-varying parameters with three types of control. The conditions for ensuring eradication or continuation of the disease have been provided in this model either for periodic model parameters or for changing general parameters. By switched systems theory the study focuses on using multiple Lyapunov functions in order to demonstrate sufficient results for removal and destruction of breeding sites and reduced contact rate schemes. The analytic results found for disease removal by pulse vaccination utilized methods from Floquet theory. Numerical simulation was used to obtain effective analysis of control schemes [36].

3.9 Mathematical Models for Influenza

Since its first outbreak in Hong Kong, avian influenza has caused numerous human infections to spread all over the world. The disease, caused by the transmission of avian influenza A to humans, is a zoonotic disease such as H5N1 and H7N9. Avian influenza A H5N1 infected more than 500 people, where the mortality rate reached about 60% of reported cases. Also, the mortality rate from avian influenza A H7N9 reached about 35% of confirmed cases in China [35]. To understand and analyze the dynamic behavior of the transmission of avian influenza to humans, a mathematical model of SI-SIR was constructed with some assumptions. The Model was based on the logistic growth for the avian population; also another model was built on the Allee effect. Moreover, a study obtained a threshold value for the spread of avian influenza by finding the equilibrium points of the two systems to examine the local or global asymptotical stability for each point. The asymptotical stability examination was done by resorting to use some of the techniques like linear analysis technique, combining Liapunov function method and Lasalle's invariance principle [35].

$$\begin{aligned}
\frac{dS_a}{dt} &= g(S_a) - \beta_a S_a I_a, \\
\frac{dI_a}{dt} &= \beta_a S_a I_a - (\mu_a + \delta_a) I_a, \\
\frac{dS_h}{dt} &= \pi_h - \beta_h S_h I_a - \mu_h S_h, \\
\frac{dI_h}{dt} &= \beta_h S_h I_a - (\mu_h + \delta_h + \gamma) I_h, \\
\frac{dR_h}{dt} &= \gamma I_h - \mu_h R_h,
\end{aligned} \tag{3.16}$$

In 2009, the influenza A / H1N1 virus swept across the world, spreading to more than 214 countries. The majority of cases were confirmed by 2010, with 18,449 deaths [31]. During that period, the Republic of Korea was interested in developing a mathematical model for the dynamics of transmission of influenza A / H1N1. Based on government strategies, the simulation period was divided into three periods [31]. The first period was using the non-pharmaceutical strategy. In the second period, non-pharmaceutical and antiviral strategies were implemented. During the third period, the vaccine strategy is added. Period 1 indicated a significant reduction in the transmission rate due to government policies applied, such as the difference between the fitted data and the uncontrolled transmission rate obtained from the \mathcal{R}_0 basic reproduction number of the model without intervention [31]. Thus, the rate of decline in transmission is used as an upper bound in non-pharmaceutical control which is interested in the study of optimal control strategies, as the new approach contributes to the creation of a realistic upper bound of control. The study also obtained a real-time prediction for injury by referring to the mathematical modeling of early stages of the epidemic as well as, investigating the impact of vaccination coverage and timing associated with cumulative events. The conclusion refers to the importance of early vaccination and its useful role in the prevention of the epidemic [31]. The Figure 3.11 shows the flowchart of the 2009 A / H1N1

influenza model. Note that the antiviral factor is not included in Period 1 and vaccination is not considered in Period 1 and Period 2 [31].

The transmission model of the 2009 A/H1N1 influenza is then governed by non-linear differential equations as follows:

$$\begin{aligned}
 \frac{dS}{dt} &= -\beta \frac{S}{N} \Lambda - \nu S, \\
 \frac{dE}{dt} &= \beta \left(\frac{S}{N} + \frac{U}{N} + \frac{V}{N} \right) \Lambda - kE, \\
 \frac{dI}{dt} &= pkE - \alpha I - aI, \\
 \frac{dA}{dt} &= (1-p)kE - \eta A, \\
 \frac{dR}{dt} &= \alpha I + aI + \eta A, \\
 \frac{dA}{dt} &= -\beta \frac{U}{N} \Lambda + (1-e)\nu s, \\
 \frac{dR}{dt} &= -\beta \frac{U}{N} \Lambda + e\nu S - \omega V, \\
 \frac{dR}{dt} &= \omega V
 \end{aligned} \tag{3.17}$$

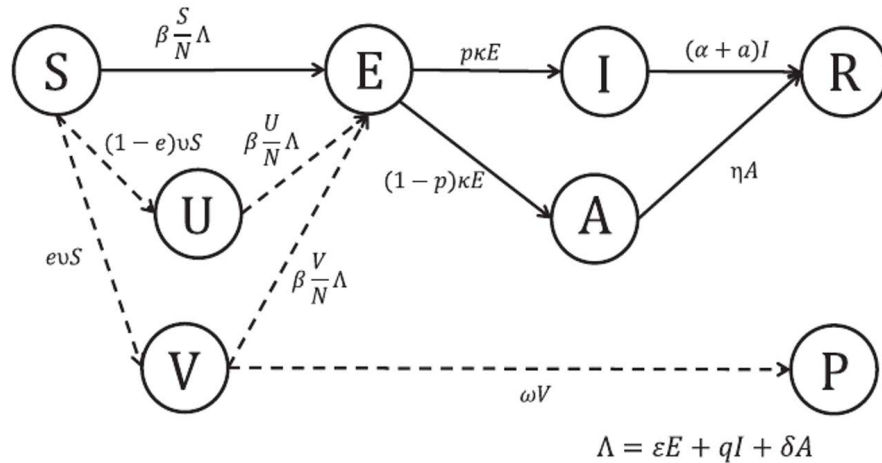


Figure 3.11: Flow chart of A/H1N1 influenza model

This study introduces the SEIR epidemic model with time delay system. By considering (DDEs) which is a model of delay differential equations to find a more realistic description of the dynamics of influenza A (H1N1) [32]. The study starts with investigating the positivity and boundedness of the model solution. Depending on the Lyapunov LaSalle invariance principle of the system to provide sufficient conditions to show the global stability of both equilibria (disease-free equilibrium and endemic disease equilibrium). Also, to maintain stability behavior, they estimate the length of delay beside conducting the bifurcation analysis. The threshold dynamics is founded in detail by the basic reproduction number, where $\mathcal{R}_0 < 1$ shows that the infectious population will disappear, which mean the disease will die out, but if $\mathcal{R}_0 > 1$ the infectious populations will persist [32]. Finding the importance of sensitivity analysis by showing which parameter values have a significant impact on the model dynamics of the influenza A (H1N1) model. Also, numerical simulations with application to H1N1 infection are given to verify the analytical results [32].

$$\begin{aligned}
\frac{dS}{dt} &= A - \beta(I(t) + \eta E(t))S(t) - (\phi + \mu)S(t), \\
\frac{dV}{dt} &= \phi S(t) - (1 - \sigma)\beta(I(t) + \eta E(t))V(t) - \mu V(t), \\
\frac{dE}{dt} &= \beta(I(t) + \eta E(t))S(t) + (1 - \sigma)\beta(I(t) + \eta E(t))V(t) - k_1 E(t) - \mu E(t), \\
\frac{dI}{dt} &= k_1 E(t) - dI(t) - \delta I(t) - \mu I(t), \\
\frac{dR}{dt} &= \delta I(t) - \mu R(t),
\end{aligned} \tag{3.18}$$

$$\begin{aligned}
\frac{dS}{dt} &= A - \beta I(t)S(t) - \mu_1 S(t), \\
\frac{dV}{dt} &= \beta I(t)S(t) - k_1 E(t - \tau) - \mu_2 E(t), \\
\frac{dE}{dt} &= k_1 E(t - \tau) - dI(t) - \delta I(t) - \mu_3 I(t), \\
\frac{dI}{dt} &= \delta I(t) - \mu_4 R(t),
\end{aligned} \tag{3.19}$$

In conclusion, we have discussed different types of mathematical models for each disease to monitor and predict outbreaks of zoonotic diseases. In general, epidemiological models can be classified into three categories: statistical, mechanical, and automated. Public health organizations around the world use such models to assess the development of disease outbreaks and emerging epidemic policies. The Figure 3.12 presents an overview of mathematical models for infectious diseases [59].

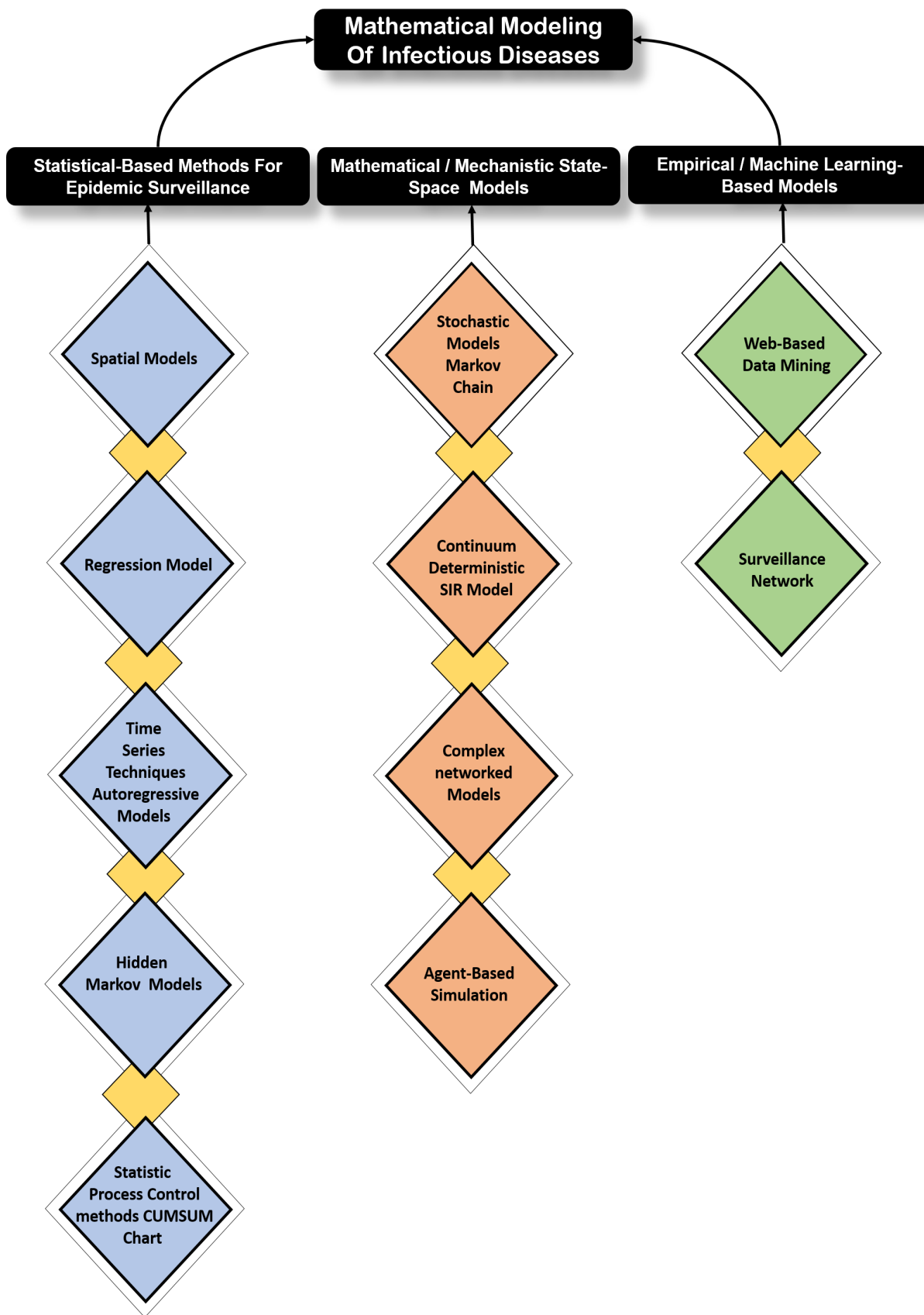


Figure 3.12: Classification of infectious diseases

Chapter 4: Mathematical models of MERS-CoV

Between 2012 and 30 June 2018, 2229 laboratory-confirmed cases of MERS-CoV infection were reported to WHO [48]. The disease takes two methods in transmission among human either by animal-to-human or human-to-human. The second method constitutes the majority of cases of infection in the worldwide [39]. So we need to study different types of mathematical models which is essential to reach the outcomes that contribute to MERS control. In this chapter, we present various types of mathematical models that explain the dynamic of transmission of MERS-CoV and optimal control strategies.

4.1 Models of Controlling MERS-CoV

Since the onset appeared of MERS cases in 2012, researchers have been interested in designing mathematical models to explain the nature of the disease. According to Al Asuoad study [2], the MERS model was provided a compartmental structure similar to SARS model. Both models consist of combined systems, of nonlinear ordinary differential equations (ODEs). The model forecasts were equipped with data from Saudi Arabia outbreaks during 2013-2016 [2].

The study also dealt with a model of the population of one city while neglecting their spatial spread. They assumed that the populations is large enough to justify the use of a continuous description based on ordinary differential equations. The study also indicated that the presence of the geographical distribution of the disease in one city requires models with partial differential equations, which may complicate the model and thus making it more difficult to understand the disease [2]. As shown in Figure 4.1, the study demonstrate the model dynamics by five sub-population groups: susceptible (S), exposed or asymptomatic (E) (individuals who carry the virus and can infect others but have no symptoms), infected (I), isolated (J), and recovered (R) individuals. The flow diagram of the model is depicted [2].

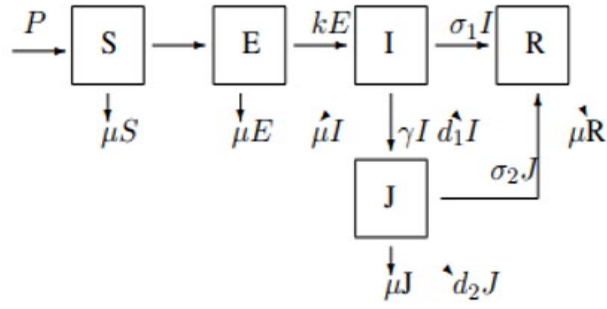


Figure 4.1: The Compartmental structure MERS model

The following mathematical model shows the dynamics of MERS.

$$\begin{aligned}
 \frac{dS}{dt} &= P - \frac{S(\beta I + \varepsilon_E \beta E + \varepsilon_J \beta J)}{N} - \mu S, \\
 \frac{dE}{dt} &= \frac{S(\beta I + \varepsilon_E \beta E + \varepsilon_J \beta J)}{N} - (k + \mu)E, \\
 \frac{dI}{dt} &= kE - (\gamma + v_1 + d_1 + \mu)I, \\
 \frac{dJ}{dt} &= \gamma I - (v_2 + d_2 + \mu)J, \\
 \frac{dR}{dt} &= v_1 I + v_2 J - (\mu)R.
 \end{aligned} \tag{4.1}$$

Where the initial conditions are $S(0) = S_0, E(0) = E_0, I(0) = I_0, J(0) = J_0, R(0) = R_0$.

The predictions of the MERS model are fitted to data from the outbreaks in Riyadh (Saudi Arabia) during 2013-2016. The model simulation results indicated that the MERS disease would finally be contained in the city [2]. The study also shows that the outbreak risk and the containment time depend entirely on first-hand contact coefficients and the constant rate of the isolation. The previous result was observed through

simulations after adding the randomness to the coefficients of the model, which is sensitive to the scaled contact rate between people and isolation rate. The analysis of the model refers that the usage of the stability theory for the ODEs showed that the isolation was the only way to control the disease [2]. Also, the stability theory illustrates the endemic steady state which was locally stable. The study highlighted the importance of the analytical results and the typical behavior demonstrated by the numerical simulation with the estimated parameters in the city of Riyadh. The estimated parameters indicated significant implications for the subsequent containment of the disease in the city. Also, the study points out that the mathematical model emphasizes the importance of isolation of infected individuals to avoid future MERS outbreaks. Besides that, the model was generic which can be used to analyze epidemics in different parts of the Middle East and other countries [2].

The model has been designed to study the dynamics of transmission of two groups of (MERS-CoV) patients, where the first group consist the residents of Mecca while the another group pilgrims who are visiting Mecca. Additionally, the model was used to assess the effect of quarantine on susceptible individuals, as well as to know the impact of a possible anti-MERS-CoV vaccine during the dynamics of transmission it among individuals [41]. This study considers quarantine as the temporary removal of susceptible individuals (those who fear infect with the MERS) from the general population. The study suggested two hypothesis that the quarantine-exposed individuals are presumed to have no infection during quarantine and the second is that don't detect infected cases without the appearance of symptoms during quarantine [41].

The study divided the population into two groups: where the group 1 Include the total population $N_1(t)$ at time t , it's divided to seven mutually-exclusive compartments of un-vaccinated non-quarantined susceptible ($S_1(t)$), un-vaccinated quarantined susceptible ($S_{1Q}(t)$), vaccinated susceptible ($S_{1V}(t)$), non-quarantined exposed (i.e., latently-infected, and showing no clinical symptoms of MERS-CoV) ($E_1(t)$), non-quarantined symptomatic (i.e., infected with clinical symptoms of MERS-CoV) ($I_1(t)$), non-quarantined hospitalized (isolated) ($H_1(t)$) and recovered ($R_1(t)$) individuals [41].

Similar to group 2, the total population $N_2(t)$ at time t it is divided into unvaccinated non-quarantined susceptible ($S_2(t)$), unvaccinated quarantined susceptible ($S_{2Q}(t)$), vaccinated susceptible ($S_{2V}(t)$), exposed ($E_2(t)$), symptomatic ($I_2(t)$), hospitalized ($H_2(t)$) and recovered ($R_2(t)$) individuals. Thus, the total population at time t , $N(t)$, is given by $N(t) = N_1(t) + N_2(t)$, [41].

A flow diagram in Figure 4.2 display the model for the transmission dynamics of MERS-CoV during a mass gathering, in the presence of quarantine and mass vaccination [41].

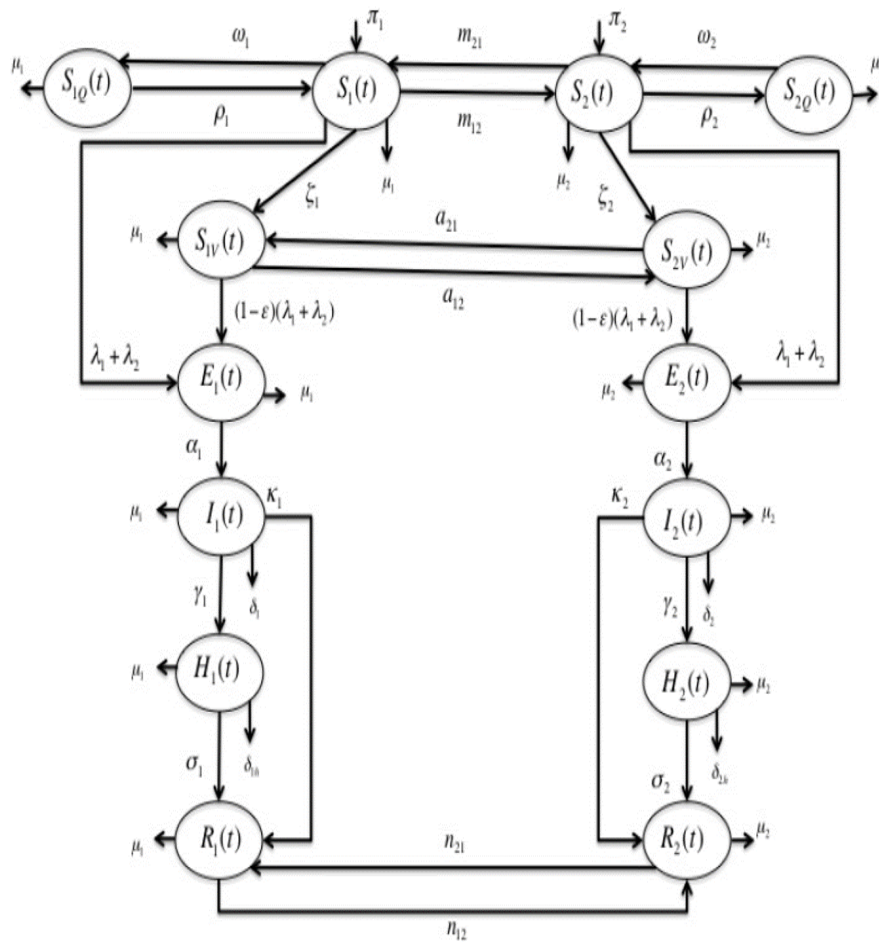


Figure 4.2: Flow diagram of MERS model

The following mathematical model shows the dynamics of MERS.

$$\begin{aligned}
\frac{dS_1}{dt} &= \pi_1 + \rho_1 S_{1Q} + m_{21} S_2 - (\lambda_1 + \lambda_2) S_1 - \xi_1 S_1 - \omega_1 S_1 - m_{12} S_1 - \mu_1 S_1, \\
\frac{dS_{1Q}}{dt} &= \omega_1 S - 1 - \rho_1 S - 1Q - \mu_1 S_{1Q}, \\
\frac{dS_{1V}}{dt} &= \xi_1 S_1 + a_{21} S_{2V} - (1 - \varepsilon)(\lambda_1 - \lambda_2) S_{1v} - a_{12} S_{1V} - \mu_1 S_{1V}, \\
\frac{E_1}{dt} &= (\lambda_1 - \lambda_2) S_1 + (1 - \varepsilon)(\lambda_1 - \lambda_2) S_{1v} - \alpha_1 E_1 - \mu_1 E_1, \\
\frac{dI_1}{dt} &= \alpha_1 E_1 - \gamma_1 I_1 - \kappa_1 I_1 c - \mu_1 I_1 - \delta_1 I_1, \\
\frac{dH_1}{dt} &= \gamma_1 I_1 - \sigma_1 H_1 - \mu_1 H_1 - \delta_{1h} H_1, \\
\frac{dR_1}{dt} &= \kappa_1 I_1 + \sigma_1 H_1 - n_{21} R_2 n_{12} R_1 - \mu_1 R_1, \\
\frac{dS_2}{dt} &= \pi_2 + \rho_2 S_{2Q} + m_{12} S_1 - (\lambda_1 + \lambda_2) S_2 - \xi_2 S_2 - \omega_2 S_2 - m_{21} S_2 - \mu_2 S_2, \\
\frac{dS_{2Q}}{dt} &= \omega_2 S - 2 - \rho_2 S - 2Q - \mu_2 S_{2Q}, \\
\frac{dS_{2V}}{dt} &= \xi_2 S_2 + a_{12} S_{1V} - (1 - \varepsilon)(\lambda_1 - \lambda_2) S_{2v} - a_{21} S_{2V} - \mu_2 S_{2V}, \\
\frac{E_2}{dt} &= (\lambda_1 - \lambda_2) S_2 + (1 - \varepsilon)(\lambda_1 - \lambda_2) S_{2v} - \alpha_2 E_2 - \mu_2 E_2, \\
\frac{dI_2}{dt} &= \alpha_2 E_2 - \gamma_2 I_2 - \kappa_2 I_2 - \mu_2 I_1 - \delta_1 I_1, \\
\frac{dH_2}{dt} &= \gamma_2 I_2 - \sigma_2 H_2 - \mu_2 H_2 - \delta_{2h} H_2, \\
\frac{dR_2}{dt} &= \kappa_2 I_2 + \sigma_2 H_2 - n_{12} R_2 n_{21} R_2 - \mu_2 R_2
\end{aligned} \tag{4.2}$$

The model is subject to a backward bifurcation, which appears to arise because of the assumption that the vaccine provides incomplete infection protection. The model can contain one or more endemic equilibria when the number of reproduction associated with it exceeds the unity [41]. Uncertainty and sensitivity analyzes are performed to determine the impact of uncertainty in parameter estimates of the model, as well as to identify critical milestones that drive the transmission of the disease. The study of malik el at. [41], reformulated the model and it used as an optimal control problem, also the resulting model is used to assess the impact of different control strategies [41]. Numerical simulations of the optimal control model indicate that if the cost of implementing quarantine and vaccination strategies are high, then both strategies can be managed by using their maximum possible levels for a relatively shorter period (i.e. "hit-hard and hit-early"), then reduce the coverage gradually in the next few days afterward. Moreover, the global strategy, based on the joint use of quarantine and vaccination strategies, has proved to be more efficient than applying each of them individually [41].

4.2 Models of Transmission MERS-CoV

4.2.1 Deterministic Model

The year 2015 saw the first and most massive epidemically outbreak of the MERS outside the Middle East particularly in the Republic of Korea [70]. Subsequently, the Republic of Korea described the deterministic SEAIHR model among humans population only because there are no zoonotic infections of MERS-CoV. The model was divided into compartments the susceptible (S), exposed (E), asymptomatic(A), symptomatic infected(I), hospitalized (H), and removed (R) individual, the total number of human population in the Republic of Korea (N) [70].

A flow diagram in Figure 4.3 shows the compartmental model of MERS in the Republic of Korea [70].

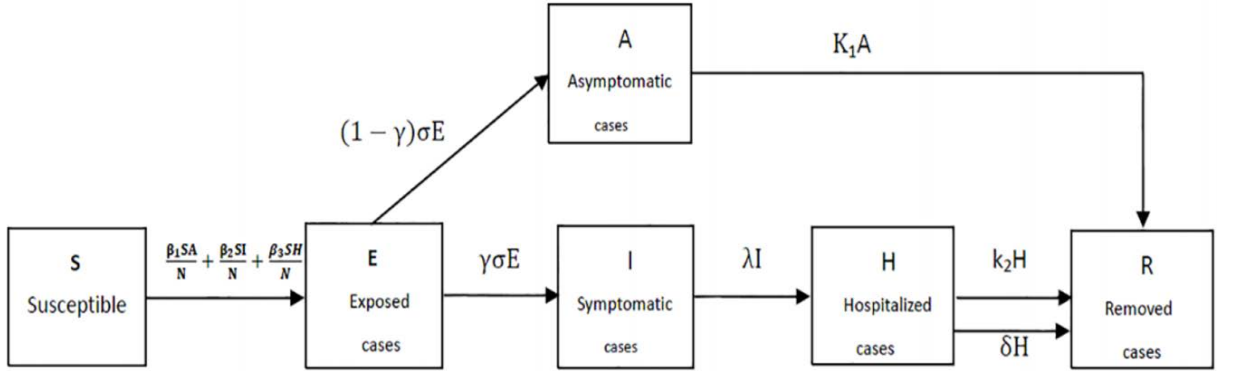


Figure 4.3: The model of MERS in the Republic of Korea

The following mathematical model shows the dynamics of MERS.

$$\frac{dS}{dt} = -\beta_1 \frac{SA}{N} - \beta_2 \frac{SI}{N} - \beta_3 \frac{SH}{N}$$

$$\frac{dE}{dt} = -\beta_1 \frac{SA}{N} - \beta_2 \frac{SI}{N} - \beta_3 \frac{SH}{N} - \nu E$$

$$\frac{dA}{dt} = (1 - \gamma)\nu E - k_1 A$$

$$\frac{dI}{dt} = \gamma\nu E - \lambda I$$

$$\frac{dH}{dt} = \lambda I - k_2 H - \delta H$$

$$\frac{dR}{dt} = k_1 A + k_2 H + \delta H$$

(4.3)

Based on detailed patient data, two dynamic models were designed to simulate deployments from May 20 to June 8 and from June 9 to July 10, respectively. The model of Republic of Korea indicates that the basic reproduction number \mathcal{R}_0 was 4.422 [70].

The rapid spread of MERS cases mostly due to the lack of targeted protection and control measures as was shown by the numerical analysis. The partial correction also determined by the fact that the parameters β_1 and γ have strong links with \mathcal{R}_0 , which means that the infection and the proportion of symptomless cases have a significant role in the spread of the disease [70]. By sensitivity analysis, the study concluded that the most effective measures to control the disease are strengthening the ability of self-protection against the risk of infection and the rapid isolation of confirmed cases. In addition, monitoring the close contacts of a human with infected cases is important as well [70].

4.2.2 Stochastic Model

Most studies have provided a dynamic transmission of the MERS outbreak with a deterministic model, although it is unrealistic. In order to arrive at a more realistic model, the stochastic model was used in the study of Chowell et al [14]. This type of model also contributes to the provision of information that could help evaluate the real progression of MERS-CoV during the 2013 year, and response to changes in disease surveillance, control interventions, or viral adaptation. Also, the importance of the stochastic model lies in helpfully correcting the decisions and strategies of health institutions and explains policies more than deterministic models [14].

The study was directed by the stochastic model, which contains a transmission model of SEIR compartmental that includes the main epidemiological characteristics of the outbreak of MERS-CoV. The model consists of the transition settings between three stages (first, the transmission of the virus to animals from another unspecified animal reservoir, as well as the transition from human to human in the community and the hospital). According to Chowell et al. [14], the importance of the stochastic models is evident especially when the rate of infection is low.

Schematic representation in Figure 4.4 shows the transition of MERS cases (indicated by arrows) among the different epidemiological states in model [14].

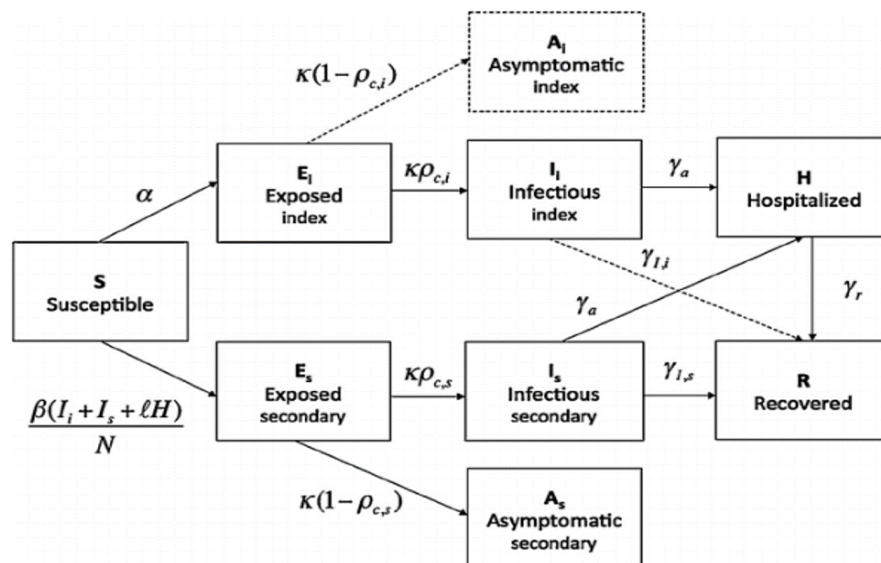


Figure 4.4: The stochastic model of MERS

The following mathematical model shows the dynamics of MERS.

$$\begin{aligned}
\frac{dS}{dt} &= -\beta S \frac{(I_i + I_s + I_H)}{N} - \alpha \\
\frac{dE_i}{dt} &= -\alpha - \kappa E_i \\
\frac{dE_s}{dt} &= \beta S \frac{(I_i + I_s + I_H)}{N} - \kappa E_s \\
\frac{dI_i}{dt} &= \kappa \rho_{c,i} E_i - \gamma_a I_i - \gamma_{i,i} I_i \\
\frac{dA_i}{dt} &= \kappa (1 - \rho_{c,i}) E_i \\
\frac{dI_s}{dt} &= \kappa \rho_{c,s} E_s \\
\frac{dA_s}{dt} &= \kappa (1 - \rho_{c,s}) E_s \\
\frac{dH}{dt} &= \gamma_a I_i + \gamma_a I_s - \gamma_r H \\
\frac{dR}{dt} &= \gamma_r H + \gamma_{i,i} I_i - \gamma_{i,s} I_s \\
\frac{dC_i}{dt} &= \kappa \rho_{I,i} E_i \\
\frac{dC_s}{dt} &= \kappa \rho_{I,s} E_s \\
\frac{dC_{EH}}{dt} &= \beta S \frac{I_H}{N} - \kappa C_{EH} \\
\frac{dIH}{dt} &= \kappa \rho_{c,s} C_{EH}
\end{aligned} \tag{4.4}$$

The study also seeks to understand the difference in values derived from $R_{overall}$ and R_i . This difference is sometimes due to secondary cases being less transmissible than index cases or due to biological differences during the disease transition, and control measures for index cases may be less efficient than secondary cases [14]. To obtain a clear result on the disorders caused by the outbreak of the MERS-CoV, the study developed a stochastic transition model that identifies the transmission of both index and secondary cases. The model also includes different case reporting scenarios where case-control has consistently linked disease, with both severe illness conditions being hospitalized from those who treated in the community. Using the Markov-Shin-Monte-Carlo estimation technique to match the MERS data in 2013 with the model, and providing new estimates for reproduction number with considering previous estimations. There is also a need to review other gaps in the data, which in turn contributes to the clarification of the disease transition process for 2014 and beyond [14].

As a result of the significant uncertainty about the nature of the virus and the severity of human-to-human transmission, the study developed a stochastic transition model that understands the transmission of disease among index cases (who get infect from camels) and secondary cases (who get infect from infected human) [14]. In 2013, from April to October, the secondary cases of the infected human with MERS in KSA received strong support from the control authorities compared to primary cases [14]. The model shows that the percentage of infection in the secondary cases was less than of the cases of infection on the primary case which didn't receive such support. Besides, the study also shows the importance of monitoring viral adaptations that may have portability to crossing the border as all zoonotic diseases. The study also showed the role of bias in observation (especially the difficulty of observing asymmetric and less severe index cases) which leads to distortion of the reasoning and interpretation of the parameters of transmission [14].

4.2.3 Spatiotemporal Heterogeneity Model

The cases of the Coronavirus, which causes the respiratory syndrome in the Middle East, indicate that there have been discrepancies in time and geography since their inception in the Middle East. So, a range of models was used to estimate case generation rates along animal and human transport routes and spatiotemporal heterogeneity. And by using the stochastic model along with the time series of incidence in the region to estimate the zoonotic and human to human transmission parameters associated with time [52]. The model also shows that secondary transmission cannot be determined between the reported cases. Besides, this approach was linked to the analysis of cases imported from the region to assess the rate of underreporting. Among all these potential models with different parameters and scenarios, the most appropriate model is characterized by significant heterogeneity in time and space and is referred to both the transmission of animals and humans-humans [52]. By the spring of 2014, the time variance contributed to an increase the spreading disease 17 times and three times among both humans and camels, respectively, that made the reproductive rate higher than 1 in all areas under study. The model shows that the cases of the MERS, which represents the secondary cases (human to human), reach a high rate around 75% while the cases associated with an epidemiological link with another case are 34% [52]. Overall, the estimated reporting rate was 0.26. The importance of the environmental component and the substantial impact on the epidemic are evident, with high levels of spatial heterogeneity in the transmission of zoonoses compared to humans. Expectations indicate that the proportion of interrupted formed a small percentage of reported cases and is responsible for the secondary transfer. Thus, the ideal solution to reduce the spread of the epidemic requires a more comprehensive understanding of the source of animal origin and their transmission path [52].

In this study, the researchers worked on two-step to estimate the porting rate ρ , the sporadic generation rate for non-human cases $p_s^r p(t)$ and the reproduction ratio $R^r(t)$ as a function of time t in each region r . The first step depended on modeling the time series of incidence in the Middle East, where this step has been used to import the cases

and the stochastic data-driven model of the spatial diffusion of the epidemic around the world [52].

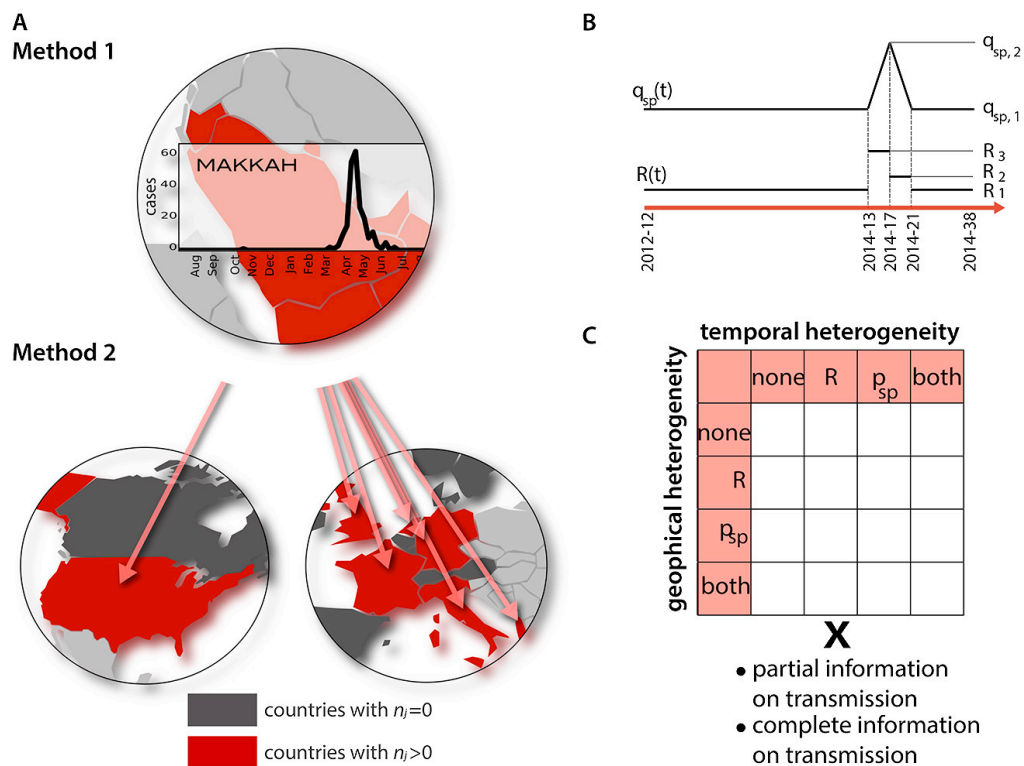


Figure 4.5: The scheme of MERS with 2-step approach

The scheme in Figure 4.5 contains a 2-step approach which is illustrated by model A B and C. Model A which is Step 1 depends on the t of 20 imputed epidemic curves for 17 regions in the Middle East (there is one curve shown for the sake of visualization corresponding to the region experiencing with the largest number of cases). It allows model selection and estimation of $R^r(t)$ and $q_{sp}^r(t) = \rho p_{sp}^r(t)$. Model B which is Step 2 shows the t of imported cases from Western Europe and North America and allows estimating ρ . The scheme (Model B) of the functional forms assumed for $R(t)$ and $q_{sp}(t)$ when temporal heterogeneity (either for one of the parameters or both) is considered in the model. Parameters $q_{sp,1}$, $q_{sp,2}$, R_1 , R_2 , R_3 are estimated. Model C: which shows the combination of parameters yielding the 32 models for exploration.

According to the transmission scenario, the study was concerned with the calculation of transmissions between each region in view of the possibility of notification

cases, including those involving $s^r(t)$ the transmission from human-to-human:

$$P(d_s^r p(t) = D^r(t) s^r(t) \& d_s(t) = s^r(t))$$

The $d_s p(t)$ are reported cases of intermittent generation. By requiring that $D^r(t)$, assuming the same reporting rate ρ for both secondary and primary cases, the $d_s^r(t)$ was binomial with the probability of $\frac{\beta_r R(t-1) D^r(t-1)}{E(D^r(t))}$, whereas

$$(d_s^r p(t) = D^r(t) - s^r(t) \& d_s(t) = s^r(t))$$

(4.5)

$$= e^{E(D_r(t))} \frac{(\beta_r R(t-1) D^r(t-1))^{s^r(t)} (N^r \alpha_r q_s p(t))^{D^r(t) - s^r(t)}}{s^r(t)! (D^r(t) - s^r(t))!}$$

For the partial information on transmissions scenario, we computed

$$(d_s^r(t) = D(t) - s^r(t) \text{ and } d_s p(t) s^r(t))$$

(4.6)

$$= e^{E(D^r(t))} \frac{(\pi \beta_r R(t-1) D^r(t-1))^{s^r(t)}}{s^r(t)!} \times \frac{(1-\pi) \beta_r R(t-1) D^r(t-1) + N^r \alpha_r q_s p(t)}{(D^r(t) - s^r(t))!}^{D^r(t) - s^r(t)}$$

In the end, this chapter shows that all studies of the MERS-CoV models concentrate their effort in studying the disease transmission only among the human population see Table (4.1). We know that MERS-CoV is coming from an animal source where it includes bats and camels. Later, the humans got the infection. We don't know for certain how is the cycles of the virus in these animals. MERS-CoV has been found in camels in several countries. It appears that some people became infected after contact with camels, so more information is needed to figure out the possible role that camels and other animals may play in the transmission of MERS-CoV. However, we should consider the model of the camel population in those countries that showcase infection by camel-to-human.

#	Author	Type of model	Human population	Camel population
1	Al-Asuoad et al. 2016	The system of nonlinear ordinary differential equations (ODEs)	✓	✗
2	Malik et al. 2015	The two-group model for the transmission dynamics of MERS-CoV.	✓	✗
3	Xia et al. 2015	A deterministic SEAIHR model	✓	✗
4	Chowell et al. 2014	A stochastic SEIR-type compartmental transmission model	✓	✗
5	Poletto et al. 2016	A spatial heterogeneity model	✓	✗

Table 4.1: The most models of MERS-CoV

Chapter 5: Mathematical Model of MERS in the UAE

In this chapter, we study two population model of the MERS-CoV. It is clear that the cases of infection in the UAE resulted by contact with infected camels or human, so we investigate on the model contain two patches camels and human. The two patches will explain the dynamic of MERS-CoV among camel population and human population.

5.1 Presentation of the Model

In this section we develop and investigate a mathematical model of MERS infection with two patches: human population and camels population. The human population is modeled with an SEIHR model which is similar approach to the SARS. The camels population is modeled with SIS model, where the I compartments in the camels population model will be divided into two sub-compartments of the unaware I_c^1 and the aware infected camels I_c^2 . The reason we consider SIS model for the camels because there is no clear definition of the diagnosis process for the camels and we don't know if the camel can have chance to recover but what we know that the camels have tolerant to the virus.

The flowchart (5.1) represents the compartments of my model where the human population is divided into susceptible S_p , the E_p represents the population of the infected, and possibly infectious but with no symptoms, the infected and infectious that show symptoms represented by I_p , the infected hospitalized is H_p , and the recovered R_p . The total human population is $N_p = S_p + E_p + I_p + H_p + R_p$.

The camels population is divided into susceptible S_c , unaware infected camels I_c^1 and aware infected camels I_c^2 , with $N_c = S_c + I_c^1 + I_c^2$.

The time frame of the infection starting with infected camels getting in contact with healthy (susceptible) people and also with health camels (susceptible). There are several evidence that show that the same strain MERS-CoV exist in bats. For this rea-

son virus, we assume that the susceptible camels population becomes infected after the bats transfer the MERS-CoV to them. Then the unaware infected camels became aware infected camels after symptom appears.

The direct contact between camels and humans lead to infection with some probability. Moreover, we assume that a portion of the infected people are possible infectious but does not show symptoms until after an incubation period. Furthermore, we assume that hospitalized people are also a source of infection, since several cases of the infection happen in hospitable setting.

Recently, mathematical models have been developed to analyze MERS outbreaks in an effort to better understand the disease transmission and determine the strength and weakness of current prevention and control strategies. In particular, we proposed the following system of differential equations to model the transmission dynamics of MERS:

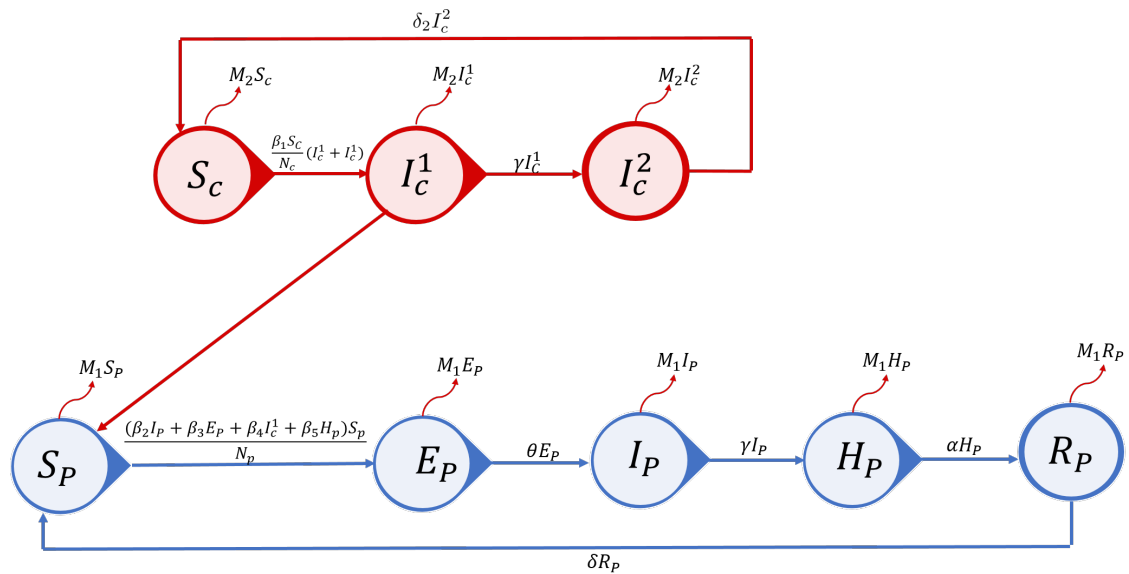


Figure 5.1: Flowchart of the MERS dynamics.

5.1.1 Variables

We define first the variables that describe the dynamic of the Corona-MERS virus, which are as follows:

S_c/S_p : Camels/Human susceptible populations

$I_c^1/I_c^2/I_p^1$: Unaware infected vector/aware infected vector /infected Human, respictively

E_p : Infected populations and possible infectious but does not show symptoms

H_p : Hospitalized populations

R_p : Recovered populations

5.1.2 Human Transmission

The equations of human population are given by

$$\begin{aligned}
 \frac{dS_p}{dt} &= \Lambda_p - \mu_1 S_p - \frac{(\beta_2 I_p + \beta_3 E_p + \beta_4 I_c^1 + \beta_5 H_p) S_p}{N_p} + \delta_p R \\
 \frac{dE_p}{dt} &= \frac{(\beta_2 I_p + \beta_3 E_p + \beta_4 I_c^1 + \beta_5 H_p) S_p}{N_p} - (\mu_1 + \theta_p) E_p \\
 \frac{dI_p}{dt} &= \theta_p E_p - (\mu_1 + \gamma_p + \xi_p^1) I_p \\
 \frac{dH_p}{dt} &= \gamma_p I_p - (\alpha_p + \mu_1 + \xi_p^2) H_p \\
 \frac{dR_p}{dt} &= \alpha_p H_p - (\delta_p + \mu_1) R_p
 \end{aligned} \tag{5.1}$$

5.1.3 Camels Transmission

The equations of the transmission of the disease among the camel are given below

$$\begin{aligned}
\frac{dS_c}{dt} &= \Lambda_c - \mu_2 S_c - \frac{\beta_1 S_c}{N_c} (I_c^1 + I_c^2) + (\delta_1 I_c^1 + \delta_2 I_c^2) \\
\frac{dI_c^1}{dt} &= \frac{\beta_1 S_c}{N_c} (I_c^1 + I_c^2) - (\xi_1 + \gamma + \mu_2 + \delta_1) I_c^1 \\
\frac{dI_c^2}{dt} &= \gamma I_c^1 - (\xi_2 + \mu_2 + \delta_2) I_c^2
\end{aligned} \tag{5.2}$$

5.2 Human and Camels Parameters Description

We explain in this section the parameters of the human models and the camels model.

5.2.1 Human Parameters

Λ_p is the human population increase by immigration or new born, μ_1 is the death rate human, β_2 is the infection rate of infected people, β_3 the infection rate of exposed people camel, β_4 the infection rate of infected unaware camels, β_5 the infection rate of hospitalized people. δ_p represent the recovery rate of the human. The detection rate of infected people is represented by θ_p . ξ_p^1 represents the death rate due to the infection. ξ_p^2 represents the death rate due to the hospital. The rate of hospitalization of the infected human is represented by γ_p . Finally, this population have also recovery rate given by α_p .

5.2.2 Camels Parameters

Λ_c is the population increase by immigration or new born, μ_2 is the death rate camel, β_1 is the infection rate by camel to camel, δ_1 and δ_2 represent the recovery rate of the unaware and the aware infected camels, assuming that some camel can recover from the infection. ξ_1 and ξ_2 represent the death rate due to the infection of the unaware and the aware infected camels. Finally γ represents the rate of detecting a sick camel.

we conclude that all parameters of the camel population and human population

reflects natural of disease in this region. So, the model takes into consideration the lifestyle of people in the UAE by considering the contact between camels and human. Each parameter has a particular definition in this model contribute to explain the nature of the disease among human population and camels population and between the two communities.

Chapter 6: Parameters Estimation

In this chapter, we will use a set of papers [41, 70, 14, 34, 5] to estimate the parameters of our model. Of course, not all the parameter are available since there is a lack of camels data in the Middle East. For examples, it is very difficult to estimate the parameters of the death related to the infection, the infection rate among the camels, and the recovery rate of the camels. However, the best way to have reasonable estimates of camels parameters is by approximating them and setting their ranges with other zoonatic diseases.

Table 6.1: Description of the model parameters

Parameters Description	Dimension for the Core Model
Λ_p Birth Rate of human and New Immigration Rate	$Human \times Days^{-1}$
Λ_c Birth Rate of camels and New Immigration Rate	$Camel \times Days^{-1}$
μ_1 Death rate of human	$Human \times Days^{-1}$
μ_2 Death rate of camel	$Camel \times Days^{-1}$
β_1 Infection rate by camel to camel	$Days^{-1}$
β_2 Infection rate of infected people	$Days^{-1}$
β_3 Infection rate of exposed people	$Days^{-1}$
β_4 Infection rate of infected unaware camels	$Days^{-1}$
β_5 Infection rate of hospitalized people	$Days^{-1}$
δ_p Recovery rate of the human	$Days^{-1}$
δ_1 Recovery rate of the unaware infected camels	$Days^{-1}$
δ_2 Recovery rate of the aware infected camels	$Days^{-1}$
α_p Recovery rate of hospitalized human	$Days^{-1}$
θ_p Detection rate of infected people	$Days^{-1}$
γ_p rate of hospitalization of the infected human	$Days^{-1}$
γ rate of detecting a sick camel	$Days^{-1}$
ξ_p^1 Death rate due to the infection	$Days^{-1}$
ξ_p^2 Death rate due to the hospital	$Days^{-1}$
ξ_1 Death rate due to the infection of the unaware infected camels	$Days^{-1}$
ξ_2 Death rate due to the infection of the aware infected camels	$Days^{-1}$

6.1 Parameters Estimation of Human

My work concerns the MERS-CoV situation in the UAE, and since the collected data on the disease was insufficient. To estimate the parameters for the human population

we used studies that contain data focused on patients reported in The Kingdom of Saudi Arabia done in South Korea and Saudi Arabia. The unit in Model is taken as $days^{-1}$.

To estimate the birth rate and immigration rate of the UAE, we need to find the total population which was estimated in 2018 to be about 9,790,857 persons. According to country matter website, the births and deaths for this year are approximately 83,675 and 11,430, respectively [16]. By using birth rate formula [61], and other equations to find the desired birth rate (see Appendix). Hence the birth rate Λ_p is 47.97 per day. Also, the normal death rate of human is $\mu_1 = 3.198399 \times 10^{-6}$ per day (see Appendix).

The infection rate of infected people β_2 , exposed people β_3 , hospitalized people β_5 are unknown. According to a study be conducted in South Korea by Xia and others, and by depending on the data of MERS-CoV reported cases. The researchers used the method of least-squares to estimate the values of these parameters where they found that $\beta_2 = 0.7833$, $\beta_3 = 0.8756$ and $\beta_5 = 0.4568$ [70]. Also, the incubation period which is the time until exposed people showed the symptoms and became infected, and that refer to the rate of exposed people to become infected $\theta_p = 0.2$. Referred to the rate of hospitalization of the infected human $\gamma_p = 0.2$ [70].

As for the rate of recovery of the infected human showed by $\delta_p = 0.125$ and the recovery rate of hospitalized human $\alpha_p = 0.2$, where this values of parameters refer to confirmed cases of Saudi Arabia which done by the study of Malik and others [41]. In addition, The number of death cases due to the infection was 12 from 134 case [15]. Then by using the death rate formula (6.1) I estimated that the death for both infected and hospitalized individuals would be $\xi_p^1 = 3.36 \times 10^{-6}$, $\xi_p^2 = 3.36 \times 10^{-6}$ respectively. The Table 6.2 provide the values and ranges of the parameters of the human model (5.1).

$$\text{Birth/Death rate} = \frac{(\text{number of birth/death})}{(\text{total population})} \quad (6.1)$$

Parameters	Baseline value(per day)	Range (per day)	Reference
Λ_p	47.97	[7500/365, 4000/365]	calculated
μ_1	3.198399×10^{-6}	[3.198399×10^{-3} , $1/3.198399 \times 10^{-11}$]	calculated
β_2	0.7833	[0.5925, 0.8592]	[70]
β_3	0.8756	[0.853, 0.9324]	[70]
β_5	0.4568	[0.3839, 0.6751]	[70]
δ_p	0.125	[1/9, 1/7]	[41]
α_p	0.2	[1/6, 1/4]	[41]
θ_p	0.2	[1/6, 1/4]	[70]
γ_p	0.708	[0.4, 0.8]	[14]
ξ_p^1	3.36×10^{-6}	[6×10^{-7} , 5×10^{-3}]	calculated
ξ_p^2	3.36×10^{-6}	[6×10^{-7} , 5×10^{-3}]	calculated

Table 6.2: Parameters of the human model

6.2 Parameters Estimation of Camels

Almost all the studies on the MERS-CoV focused on the transmission of the disease among humans. Fewer studies focused on the disease aspect on the camels. To my knowledge, there is no study on the camel population which makes estimating of the parameters of the camel model very challenging.

According to FAO data, the birth rate of camels in the United Arab Emirates has been increasing during the current period compared to previous years. Indeed, the statistical year book in Abu Dhabi in 2015 and 2016 shows that the total camel population was 383887, 394224, respectively. And the death rate of camel population in these two year was 28269, 34963, respectively [19]. We calculated the birth rate of camels per day, and found to be $\Lambda_c = 97.1925$, and the death rate is $\mu_2 = 2429813 \times 10^{-4}$ per day (see Appendix).

The study of Lin *et. al.*, focused on the spread of the disease among camels as the primary host of the virus, and it is essential to know the nature of transmission among camels at a lower rate compared to humans. Where the infection rate by camel to camels show that $\beta_1 = 0.15$ [34]. Also, δ_1 and δ_2 represent the rates at which infected camels become recovered [34].

Another study conducted on a camel's farm in Egypt, where it was found that the percentage of detection MERS-CoV in local camel sick less than those imported (12%

, 21% respectively). The $\gamma = 0.12$ refer to the rate of detecting the sick camels [5]. Since we don't have data of the death camels, we assumed that the death rate due to the infection of (unaware, aware) infected camels are $\xi_1 = 0.33$, $\xi_2 = 0.9$, restrictively. The Table 6.3 provide the values and ranges of the parameters of the camel model (5.2).

Parameters	Baseline value(per day)	Range (per day)	Reference
Λ_c	97.1925	[130, 54]	calculated
μ_2	2429813×10^{-4}	$[0.2429813, 2429813 \times 10^{-7}]$	calculated
β_1	0.15	[0.25, 0.04]	[34]
β_4	0.34	[0.2, 0.46]	assumed
δ_1	0.25	[1/6, 1/2]	[34]
δ_2	0.25	[1/6, 1/2]	[34]
γ	0.12	[1/10, 1/5]	[5]
ξ_1	0.33	[1/5, 1/3]	assumed
ξ_2	0.9	[1/5, 1/3]	assumed

Table 6.3: Parameters of the human model

The Table 6.4 shows the confirmed MERS-CoV cases in Arabian Peninsula and Infected rate of camels per country in the Arabian peninsula [27, 21].

Country	Camel populations by FAOstat 2015	Confirmed MERS-CoV cases	Infected Rate of Camel	Unit
Saudi Arabia	301717	977	$3.238133748 \times 10^{-3}$	$Days^{-1}$
UAE	430372	50	$1.161785618 \times 10^{-4}$	$Days^{-1}$
Qatar	84216	7	$8.311959723 \times 10^{-5}$	$Days^{-1}$
Oman	252660	4	$1.583155228 \times 10^{-4}$	$Days^{-1}$
Kuwait	7718	3	$3.887017362 \times 10^{-4}$	$Days^{-1}$
Bahrain	1055	0	0	$Days^{-1}$
total	1077738	1041	$9.659119378 \times 10^{-4}$	$Days^{-1}$

Table 6.4: Infected rate of camels per country

This chapter concludes how the disease affects the population of camels in the Arabian Peninsula as shown in Table (6.4). The infection rate by MERS-CoV among camels is highest in Saudi Arabia followed by UAE. The Food and Agriculture Organization (FAOstat) shows that the population of camels continuous in increasing so the probability of infection by MERS among camels may increase. Animal models for MERS-CoV infection of humans are needed to elucidate MERS pathogenesis and to develop vaccines and antivirals [27, 21].

Chapter 7: Mathematical Analysis

In this chapter we discuss qualitative properties of the solution, such as positivity and boundedness. Then we define the basic reproduction number \mathcal{R}_0 from the models 5.1-5.2 in page 74. which is an important parameter in mathematical epidemiology. The value of \mathcal{R}_0 determines the stability of the disease free equilibrium (DFE). Also, we analyze the endemic equilibria of the model system 5.1-5.2 in page 74.

7.1 Boundedness and Positivity

In this section, we prove the positivity and the Boundedness for the models of camels and human.

7.1.1 Positivity

Theorem 7.1.1. *suppose that initial conditions are all positive that is $S_p(0) > 0, E_p(0) > 0, I_p(0) > 0, H_p(0) > 0$ and $R_p(0) > 0$. The solution $(S_p(t), E_p(t), I_p(t), H_p(t), R_p(t))$ of the model is positive for all time $t \geq 0$, and uniformly bounded.*

We use the Theorem 7.1.1 from [62] to prove the positivity of solution of the human model system.

Here, we suppose that the differential equations of the human population are equal to the function $f_n(S_p, E_p, I_p, H_p, R_p)$ as given below .

$$\begin{aligned}
\frac{dS_p}{dt} &= \Lambda_p - \mu_1 S_p - \frac{(\beta_2 I_p + \beta_3 E_p + \beta_4 I_c^1 + \beta_5 H_p) S_p}{N_p} + \delta_p R = f_1(S_p, E_p, I_p, H_p, R_p), \\
\frac{dE_p}{dt} &= \frac{(\beta_2 I_p + \beta_3 E_p + \beta_4 I_c^1 + \beta_5 H_p) S_p}{N_p} - \mu_1 E_p - \theta_p E_p = f_2(S_p, E_p, I_p, H_p, R_p), \\
\frac{dI_p}{dt} &= \theta_p E_p - (\mu_1 + \gamma_p + \xi_p^1) I_p = f_3(S_p, E_p, I_p, H_p, R_p), \\
\frac{dH_p}{dt} &= \gamma_p I_c^1 + (\alpha_p + \mu_1 + \xi_p^1) H_p = f_4(S_p, E_p, I_p, H_p, R_p), \\
\frac{dR_p}{dt} &= \alpha_p H_p - (\delta_p + \mu_1) R_p = f_5(S_p, E_p, I_p, H_p, R_p).
\end{aligned} \tag{7.1}$$

Proof. From equations (7.1) and by applying the Theorem 7.1.1 we obtain that $S_p(t) \geq \Lambda_p + \delta_p R > 0$, which is similar to the following equations:

$$\begin{aligned}
f_1(0, E_p, I_p, H_p, R_p) &= \Lambda_p + \delta_p R > 0, \\
f_2(S_p, 0, I_p, H_p, R_p) &= \frac{(\beta_2 I_p + \beta_3 E_p + \beta_4 I_c^1 + \beta_5 H_p) S_p}{N_p} > 0, \\
f_3(S_p, E_p, 0, H_p, R_p) &= \theta_p E_p > 0, \\
f_4(S_p, E_p, I_p, 0, R_p) &= \gamma_p I_c^1 > 0, \\
f_5(S_p, E_p, I_p, H_p, 0) &= \alpha_p H_p > 0.
\end{aligned} \tag{7.2}$$

□

We conclude that the remaining equations show that $(S_p(t), E_p(t), I_p(t), H_p(t), R_p(t))$ they are always positive for all $t > 0$.

The camels model system, We use the same approach which is firstly start with this theorem 7.1.2.

Theorem 7.1.2. *Let the initial condition satisfy that $S_c(0) > 0, I_c^1(0) > 0, I_c^2(0) > 0$. Then, the solution $(S_c(t), I_c^1(t), 0, I_c^2(t))$ of model is positive for all time $t \geq 0$ and uniformly bounded.*

Here, we suppose that the differential equations of the camels population are equal to the function $f_n(S_c, I_c^1, I_c^2)$ as given below.

$$\begin{aligned} \frac{dS_c}{dt} &= \Lambda_c - \mu_2 S_c - \frac{\beta_1 S_c}{N_c} (I_c^1 + I_c^2) + (\delta_1 I_c^1 + \delta_2 I_c^2) = g_1(S_c, I_c^1, I_c^2) \\ \frac{dI_c^1}{dt} &= \frac{\beta_1 S_c}{N_c} (I_c^1 + I_c^2) - (\xi_1 + \gamma + \mu_2) I_c^1 - \delta_1 I_c^1 = g_2(S_c, I_c^1, I_c^2) \\ \frac{dI_c^2}{dt} &= \gamma I_c^1 + (\xi_2 + \mu_2) I_c^2 - \delta_2 I_c^2 = g_3(S_c, I_c^1, I_c^2) \end{aligned} \quad (7.3)$$

Proof. From equations (7.3) and by applying theorem 7.1.2, we obtain that $S_c(t) \geq \Lambda_c + (\delta_1 I_c^1, \delta_2 I_c^2) > 0$ which is similar to the following equations:

$$g_1(0, I_c^1, I_c^2) = \Lambda_c + (\delta_1 I_c^1, \delta_2 I_c^2) > 0,$$

$$g_2(s_c, 0, I_c^2) = \frac{\beta_1 S_c}{N_c}(I_c^2) > 0, \quad (7.4)$$

$$g_3(S_c, I_c^1, 0) = \lambda I_c^1 > 0.$$

□

Hence, we conclude that the remaining equations shows that $(S_c(t), I_c^1(t), I_c^2(t))$ are always positive for all $t > 0$.

7.1.2 Boundedness

Now, the second step shows the boundedness of the solution which depend on the previous result that shows the positivity of the solution.

The total human population denoted as N_p .

$$N_p = S_p + E_p + I_p + H_p + R_p. \quad (7.5)$$

By adding the five equations of the human model and using (7.5), we get the rate of change of the total living population $N_p(t)$ as:

$$\frac{dN_p}{dt} = \Lambda_p - \mu_1(S_p + E_p + I_p + H_p + R_p) = \Lambda_p - \mu_1 N_p.$$

Thus, we get that the rate of change of the total living population $N_p(t)$

$$\frac{dN_p}{dt} = \Lambda_p - \mu_1 N,$$

which lead to

$$\limsup_{t \rightarrow \infty} N_p(t) < \frac{\Lambda_p}{\mu_1}.$$

That means $N_p(t)$ is positive and uniformly bounded.

Also, since $N_p(t) > 0$ and each one of S_p, E_p, I_p, H_p and R_p is positive, it follows that they all are uniformly bounded.

We call N_c the total camels population, where

$$N_c = S_c + I_c^1 + I_c^2 \tag{7.6}$$

By using the previous approach, we add the three equations of the camels model with (7.6), we get the rate of change of the total living population $N_c(t)$.

$$\frac{dN_c}{dt} = \Lambda_c - \mu_2(S_c + I_c^1 + I_c^2) = \Lambda_c - \mu_2 N,$$

thus, we get that the rate of change of the living population $N_c(t)$,

$$\frac{dN_c}{dt} = \Lambda_c - \mu_2 N,$$

which lead to

$$\limsup_{t \rightarrow \infty} N_c(t) < \frac{\Lambda_c}{\mu_2}.$$

That means $N_c(t)$ is positive and uniformly bounded. Also, since $N_c(t) > 0$ and each one of S_c, I_c^1 and I_c^2 is positive, it follows that they all are uniformly bounded.

7.2 The Basic Reproduction Number

It is obvious to see that the system (7.7) has the disease free equilibria E_0 , where

$$E_0 = \left(\frac{\Lambda_p}{\mu_1}, 0, 0, 0, 0, \frac{\Lambda_c}{\mu_2}, 0, 0 \right).$$

To calculate the basic reproduction number, we use the Next Generation Method [64], as follows:

$$\frac{dx_i}{dt} = \mathcal{F}_i(x, y) - \mathcal{V}_i(x, y), i = 1, \dots, n$$

$$\frac{dy_j}{dt} = g_j(x, y), j = 1, \dots, m$$

where

$$x = \begin{pmatrix} E_p \\ I_p \\ H_p \\ I_c^1 \\ I_c^2 \end{pmatrix}, y = \begin{pmatrix} S_p \\ R_p \\ S_c \end{pmatrix}$$

Indeed, \mathcal{F}_i the rate of secondary infections increases the i -th disease compartment and \mathcal{V}_i viewed the rate of disease progression [64]. In matrix form, the dynamical system (7.7) is written as :

$$\mathcal{F}_i = \begin{pmatrix} \frac{(\beta_2 I_p + \beta_3 E_p + \beta_5 H_p + \beta_4 I_c^1) S_p}{N_p} \\ 0 \\ 0 \\ \frac{\beta_1 S_c}{N_c} (I_c^1 + I_c^2) \\ 0 \end{pmatrix}, \quad \mathcal{V}_i = \begin{pmatrix} (\mu_1 + \theta_p) E_p \\ -\theta_p E_p + (\mu_1 + \gamma_p + \xi_p^1) I_p \\ -\gamma_p I_p + (\alpha_p + \mu_2 + \xi_p^1) H_p \\ (\xi^1 + \gamma + \mu_2 + \delta_1) I_c^1 \\ -\gamma I_p^1 + (\xi^2 + \mu_2 + \delta_2) \end{pmatrix}.$$

The linearization of the disease compartment x is $x' = (F - V)x$ with $F = \frac{dF}{dx_i}(E_0)$, $V = \frac{dV}{dx_i}(E_0)$, we get:

$$F = \begin{bmatrix} \beta_3 & \beta_2 & \beta_5 & \beta_4 & 0 \\ 0 & 0 & 0 & 0 & 0 \\ 0 & 0 & 0 & 0 & 0 \\ 0 & 0 & 0 & \beta_1 & \beta_1 \\ 0 & 0 & 0 & 0 & 0 \end{bmatrix}.$$

and

$$V = \begin{bmatrix} (\mu_1 + \theta_p) & 0 & 0 & 0 & 0 \\ -\theta_p & (\mu_1 + \gamma_p + \xi_p^1) & 0 & 0 & 0 \\ 0 & -\gamma_p & (\alpha_p + \mu_1 + \xi_p^1) & 0 & 0 \\ 0 & 0 & 0 & (\xi_1 + \gamma + \mu_2 + \delta_1) & 0 \\ 0 & 0 & 0 & -\gamma & (\xi_2 + \mu_2 + \delta_2) \end{bmatrix}.$$

let

$$A = (\mu_1 + \theta_p), \quad B = \mu_1 + \gamma_p + \xi_p^1, \quad C = \alpha_p + \mu_1 + \xi_p^1$$

$$E = \xi_1 + \gamma + \mu_2 + \delta_1, \quad F = \xi_2 + \mu_2 + \delta_2$$

and the next generation matrix is

$$K = F * V^{-1}$$

where

$$V^{-1} = \begin{bmatrix} \frac{1}{A} & 0 & 0 & 0 & 0 \\ \frac{\theta_p}{AB} & \frac{1}{B} & 0 & 0 & 0 \\ \frac{\theta_p \gamma_p}{ABC} & \frac{\gamma_p}{CB} & \frac{1}{c} & 0 & 0 \\ 0 & 0 & 0 & \frac{1}{E} & 0 \\ 0 & 0 & 0 & \frac{\gamma}{EF} & \frac{1}{F} \end{bmatrix}.$$

Hence,

$$K = \begin{bmatrix} \frac{\beta_3}{A} + \frac{\beta_2 \theta_p}{AB} + \frac{\beta_5 \theta_p \gamma_p}{ABC} & \frac{\beta_2}{B} + \frac{\beta_5 \gamma_p}{CB} & \frac{\beta_5}{C} & \frac{\beta_4}{E} + \frac{\beta_1 \gamma}{EF} & 0 & 0 \\ 0 & 0 & 0 & 0 & 0 & 0 \\ 0 & 0 & 0 & 0 & \frac{\beta_1}{E} + \frac{\beta_1 \gamma}{EF} & \frac{\beta_1}{F} \\ 0 & 0 & 0 & 0 & 0 & 0 \end{bmatrix}.$$

By taking spectral radius of K we find R_0

$$\mathcal{R}_0 = \rho(K) = \max(\mathcal{R}_{01}, \mathcal{R}_{02}),$$

where

$$\mathcal{R}_{01} = \frac{\beta_3}{(\mu_1 + \theta_p)} + \frac{\beta_2 \theta_p}{(\mu_1 + \theta_p)(\mu_1 + \gamma_p + \xi_p^1)} + \frac{\beta_5 \theta_p \gamma_p}{(\mu_1 + \theta_p)(\mu_1 + \gamma_p + \xi_p^1)(\alpha_p + \mu_1 + \xi_p^1)},$$

and

$$\mathcal{R}_{02} = \frac{\beta_1}{(\xi_1 + \gamma + \mu_2 + \delta_1)} + \frac{\beta_1 \gamma}{(\xi_1 + \gamma + \mu_2 + \delta_1)(\xi_2 + \mu_2 + \delta_2)}.$$

Proposition 7.2.1. *The basic reproduction number \mathcal{R}_0 of the System 7.7 is define by the maximum of \mathcal{R}_{01} and \mathcal{R}_{02} .*

It is easy to see that (7.7) has a unique disease free equilibrium E_0 defined by

$$E_0 = \left(\frac{\Lambda_p}{\mu_1}, 0, 0, 0, 0, \frac{\Lambda_c}{\mu_2}, 0, 0 \right).$$

Hence, using the result of [64], we have the following result:

Proposition 7.2.2. *The disease free equilibrium E_0 is locally asymptotically stable if and only if $\mathcal{R}_0 < 1$ and it is unstable if $\mathcal{R}_0 > 1$.*

7.3 Endemic Equilibria

In this section we try to find the possible endemic equilibria of studied model.

$$\begin{aligned} \frac{dS_p}{dt} &= \Lambda_p - \mu_1 S_p - \frac{(\beta_2 I_p + \beta_3 E_p + \beta_4 I_c^1 + \beta_5 H_p) S_p}{N_p} + \delta_p R_p, \\ \frac{dE_p}{dt} &= \frac{(\beta_2 I_p + \beta_3 E_p + \beta_4 I_c^1 + \beta_5 H_p) S_p}{N_p} - (\mu_1 + \theta_p) E_p, \\ \frac{dI_p}{dt} &= \theta_p E_p - (\mu_1 + \gamma_p + \xi_p^1) I_p, \\ \frac{dH_p}{dt} &= \gamma_p I_p - (\alpha_p + \mu_1 + \xi_p^2) H_p, \\ \frac{dR_p}{dt} &= \alpha_p H_p - (\delta_p + \mu_1) R_p, \\ \frac{dS_c}{dt} &= \Lambda_c - \mu_2 S_c - \frac{\beta_1 S_c}{N_c} (I_c^1 + I_c^2) + (\delta_1 I_c^1 + \delta_2 I_c^2), \\ \frac{dI_c^1}{dt} &= \frac{\beta_1 S_c}{N_c} (I_c^1 + I_c^2) - (\xi_1 + \gamma + \mu_2 + \delta_1) I_c^1, \\ \frac{dI_c^2}{dt} &= \gamma I_c^1 - (\xi_2 + \mu_2 + \delta_2) I_c^2, \end{aligned} \tag{7.7}$$

we assume that $I_c^1 \neq 0$ and $I_c^2 \neq 0$. Then

$$\Lambda_c - \mu_2 S_c + (\delta_1 I_c^1 + \delta_2 I_c^2) = (\xi_1 + \gamma + \mu_2) I_c^1 + \delta_1 I_c^1.$$

thus, we have S_c, N_c, I_c^2 as function of I_c^1

$$I_c^2 = \kappa I_c^1$$

$$S_c = \frac{\Lambda_c}{\mu_2} + \Psi I_c^1 \quad (7.8)$$

$$N_c = \frac{\Lambda_c}{\mu_2} + \Phi I_c^1,$$

with

$$\kappa = \frac{\gamma}{\xi_2 + \mu_2 + \delta_2},$$

$$\Psi = \frac{1}{\mu_2} \left[\frac{\delta_2 \gamma}{\xi_2 + \mu_2 + \delta_2} - (\xi_1 + \gamma + \mu_2) \right] < 0,$$

and

$$\Phi = \Psi + \kappa + 1.$$

By plugging S_c, N_c, I_c^2 in equation $\frac{dI_c^1}{dt}$, we have :

$$0 = \frac{\beta_1 \left(\frac{\Lambda_c}{\mu_2} + \Psi I_c^1 \right)}{\left(\frac{\Lambda_c}{\mu_2} + \Phi I_c^1 \right)} (\kappa I_c^1 + I_c^1) - (\xi_1 + \gamma + \mu_2) I_c^1 - \delta_1 I_c^1. \quad (7.9)$$

Since $I_c^1 \neq 0$, then

$$\frac{\beta_1 \left(\frac{\Lambda_c}{\mu_2} + \Psi I_c^1 \right)}{\left(\frac{\Lambda_c}{\mu_2} + \Phi I_c^1 \right)} (\kappa + 1) - (\xi_1 + \gamma + \mu_2) - \delta_1 = 0$$

therefore,

$$\beta_1 \left(\frac{\Lambda_c}{\mu_2} + \Psi I_c^1 \right) (\kappa + 1) = (\xi_1 + \gamma + \mu_2 + \delta_1) \left(\frac{\Lambda_c}{\mu_2} + \Phi I_c^1 \right)$$

$$\frac{\beta_1}{(\xi_1 + \gamma + \mu_2 + \delta_1)} (\kappa + 1) \left(\frac{\Lambda_c}{\mu_2} + \Psi I_c^1 \right) = \frac{\Lambda_c}{\mu_2} + \Phi I_c^1$$

$$\mathcal{R}_{02} \left(\frac{\Lambda_c}{\mu_2} + \Psi I_c^1 \right) = \frac{\Lambda_c}{\mu_2} + \Phi I_c^1$$

$$\frac{\Lambda_c}{\mu_2} (\mathcal{R}_{02} - 1) = (\Phi - \mathcal{R}_{02} \Psi) I_c^1$$

Thus,

$$I_c^1 = \frac{\frac{\Lambda_c}{\mu_2} (\mathcal{R}_{02} - 1)}{\Phi - \Psi \mathcal{R}_{02}}. \quad (7.10)$$

After simplifying $\Phi - \Psi \mathcal{R}_{02}$ (see Appendix) we found that

$$I_c^1 = \frac{\frac{\Lambda_c}{\mu_2} [\mathcal{R}_{02} - 1]}{\Psi [1 - \mathcal{R}_{02}] + \kappa + 1} \quad (7.11)$$

$I_c^1 > 0$ if and only if :

- $\mathcal{R}_{02} > 1$ and $\psi[1 - \mathcal{R}_{02}] + \kappa + 1 > 0$

then, we have

$$\kappa + 1 > \psi[\mathcal{R}_{02} - 1]$$

$$\frac{\kappa+1}{\Psi} > [\mathcal{R}_{02} - 1]$$

hence,

$$I_c^1 > 0 \text{ if } 1 < \mathcal{R}_{02} < \frac{\kappa+1}{\Psi} + 1$$

- $\mathcal{R}_{02} < 1$ and $\psi[1 - \mathcal{R}_{02}] + \kappa + 1 < 0$ which is impossible.

Proposition 7.3.1. *The endemic equilibrium $I_c^1 > 0$ if and only if $1 < \mathcal{R}_{02} < \frac{\kappa+1}{\Psi} + 1$*

The third equilibrium point found when $I_p, E_p, H_p, R_p \neq 0$.

We have

$$\Lambda_p - \mu_1 S_p + \delta_p R_p = \Upsilon$$

$$\Upsilon = (\mu_1 + \theta_p) E_p$$

thus, we have S_p, N_p, E_p, H_p, R_p as functions of I_p

$$\begin{aligned}
E_p &= \frac{\mu_1 + \gamma_p + \xi_p^1}{\theta_p} I_p, \\
\Upsilon &= \frac{(\mu_1 + \gamma_p + \xi_p^1)(\mu_1 + \theta_p)}{\theta_p} I_p, \\
H_p &= \frac{\gamma_p}{\alpha_p + \mu_1 + \xi_p^2} I_p, \\
R_p &= \left(\frac{\alpha_p}{\delta_p + \mu_1} \right) \left(\frac{\gamma_p}{\alpha_p + \mu_1 + \xi_p^2} \right) I_p, \\
S_p &= \frac{\Lambda_p}{\mu_1} + \kappa_1 I_p, \\
N_p &= \frac{\Lambda_p}{\mu_1} + \kappa_2 I_p,
\end{aligned} \tag{7.12}$$

with

$$\kappa_1 = \frac{1}{\mu_1} \left[\frac{\alpha_p \delta_p \gamma_p}{(\delta_p + \mu_1)(\alpha_p + \mu_1 + \xi_p^2)} - \frac{(\mu_1 + \theta_p)(\mu_1 + \gamma_p + \xi_p^1)}{\theta_p} \right] \tag{7.13}$$

$$\kappa_2 = \frac{(\mu_1 + \theta_p)(\mu_1 + \gamma_p + \xi_p^1)}{\theta_p} \left[\frac{\theta_p \alpha_p \delta_p \gamma_p}{(\mu_1 + \theta_p)(\mu_1 + \gamma_p + \xi_p^1)(\delta_p + \mu_1)(\alpha_p + \mu_1 + \xi_p^2)} - 1 \right] \tag{7.14}$$

since:

$$\frac{\theta_p}{\mu_1 + \theta_p} < 1, \frac{\gamma_p}{\mu_1 + \gamma_p + \xi_p^1} < 1, \frac{\delta_p}{\delta_p + \mu_1} < 1, \frac{\alpha_p}{\alpha_p + \mu_1 + \xi_p^2} < 1$$

Then, it is easy to show that $\kappa_1 < 0$

$$\kappa_2 = \kappa_1 + \left(\frac{\mu_1 + \gamma_p + \xi_p^1}{\theta_p}\right) + 1 + \left(\frac{\gamma_p}{\alpha_p + \mu_1 + \xi_p^2}\right) + \left(\frac{\alpha_p}{\delta_p + \mu_1}\right)\left(\frac{\gamma_p}{\alpha_p + \mu_1 + \xi_p^2}\right) \quad (7.15)$$

Now, we investigate the sign of κ_2 . We have

$$\kappa_2 = \kappa_1 + \left(\frac{\mu_1 + \gamma_p + \xi_p^1}{\theta_p}\right) + 1 + \left(\frac{\gamma_p}{\alpha_p + \mu_1 + \xi_p^2}\right) + \left(\frac{\alpha_p}{\delta_p + \mu_1}\right)\left(\frac{\gamma_p}{\alpha_p + \mu_1 + \xi_p^2}\right) \quad (7.16)$$

By simplifying κ_2 , Then we have:

$$\begin{aligned} \kappa_2 &= \frac{\gamma_p}{(\alpha_p + \mu_1 + \xi_p^1)} \left[1 + \frac{\alpha_p}{\delta_p + \mu_1} \left(\frac{\delta_p}{\mu_1} + 1\right)\right] + \frac{(\mu_1 + \gamma_p + \xi_p^1)}{\theta_p} \left[1 - \frac{\mu_1 + \theta_p}{\mu_1}\right] + 1 \\ &= \frac{\gamma_p}{(\alpha_p + \mu_1 + \xi_p^1)} \left[1 + \frac{\alpha_p}{\mu_1}\right] - \frac{(\mu_1 + \gamma_p + \xi_p^1)}{\mu_1} + 1 \\ &= \frac{\gamma_p(\alpha_p + \mu_1)}{\mu_1(\alpha_p + \mu_1 + \xi_p^1)} - \frac{(\mu_1 + \gamma_p + \xi_p^1)}{\mu_1} + 1 \\ &= \frac{1}{\mu_1} \left[\frac{\gamma_p(\alpha_p + \mu_1)}{\alpha_p + \mu_1 + \xi_p^1} - \mu_1 - (\gamma_p + \xi_p^1) + \mu_1 \right] \\ &= \frac{1}{\mu_1} \left[\frac{\gamma_p(\alpha_p + \mu_1)}{\alpha_p + \mu_1 + \xi_p^1} - (\gamma_p + \xi_p^1) \right] < 0 \end{aligned}$$

From the equation E_p at the equilibria, we have :

$$0 = \frac{S_p(\beta_2 I_p + \beta_3 E_p + \beta_4 I_c^1 + \beta_5 H_p)}{N_p} - (\mu_1 + \theta_p)E$$

therefore

$$\left(\frac{\Lambda_p}{\mu_1} + \kappa_1 I_p\right)(\beta_2 I_p + \beta_3 \kappa_5 I_p + \beta_4 I_c^1 + \beta_5 \kappa_4 I_p) = \left(\frac{\Lambda_p}{\mu_1} + \kappa_2 I_p\right)(\mu_1 + \theta_p)(\kappa_5 I_p)$$

we define the κ 's, where

$$\kappa_3 = \left(\frac{\alpha_p}{\delta_p + \mu_1}\right)\left(\frac{\gamma_p}{\alpha_p + \mu_1 + \xi_p^2}\right)$$

$$\kappa_4 = \left(\frac{\gamma_p}{\alpha_p + \mu_1 + \xi_p^2}\right)$$

$$\kappa_5 = \left(\frac{\mu_1 + \gamma_p + \xi_p^1}{\theta_p}\right)$$

therefore $\kappa_i < 0$ when $i = 1, 2$ and $\kappa_i > 0$ when $i = 3, 4, 5$.

Then we find quadratic equation as a function of the variable I_p .

as

$$P(I_p) = AI_p^2 + BI_p + C \tag{7.17}$$

where

$$A = -\kappa_2 \kappa_5 (\mu_1 + \theta_p) + \kappa_1 (\beta_2 + \beta_3 \kappa_5 + \beta_5 \kappa_4),$$

$$B = \kappa_1 \beta_4 I_c^1 + \frac{\Lambda_p}{\mu_1} [\beta_2 + (\beta_3 - (\theta_p + \mu_1)) \kappa_5 + \beta_5 \kappa_4], \tag{7.18}$$

$$C = \frac{\Lambda_p}{\mu_1} \beta_4 I_c^1.$$

Since $I_c^1 > 0$, then $C > 0$.

By substituting κ_4 and κ_5 in \mathcal{R}_{01} , then

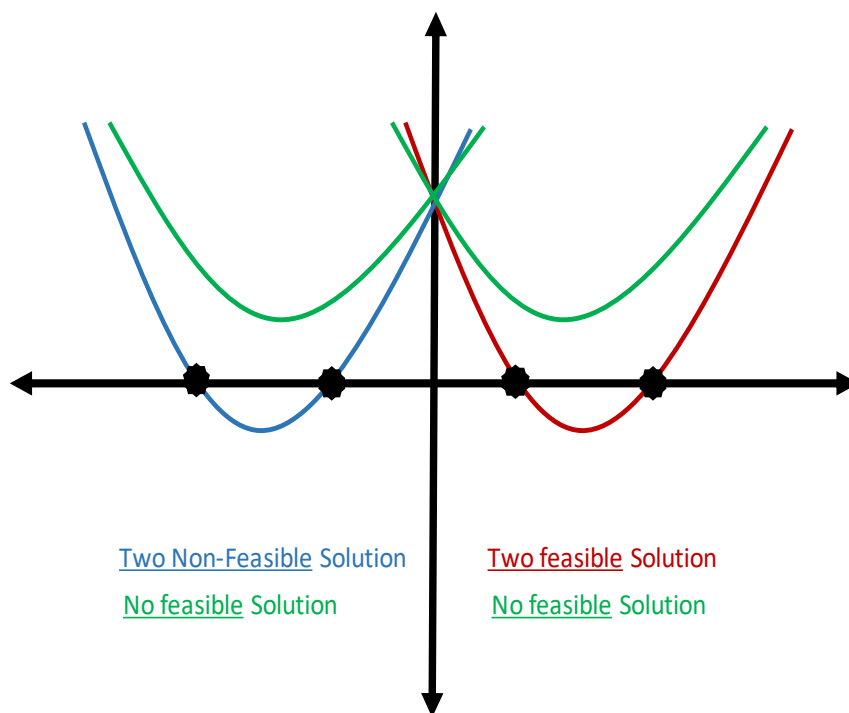
$$\mathcal{R}_{01} = \frac{\theta_p}{(\mu_1 + \theta_p)\kappa_5} \left[\frac{\beta_3}{\kappa_5} + \beta_2 + \beta_5 \kappa_4 \right],$$

by re-arranging the form of A we get

$$A = (\theta_p + \mu_1)\kappa_5(\mathcal{R}_{01} - \kappa_2) \quad (7.19)$$

Since $\kappa_2 < 0$, then $A > 0$ and we conclude the following result.

Proposition 7.3.2. *There is either two feasible endemic equilibrium or none.*



7.4 Jacobian Method-Routh-Hurwitz Criteria

7.4.1 Block Matrix

The Jacobian matrix can be written as

$$J = \begin{bmatrix} A & B \\ C & D \end{bmatrix}$$

The sub-matrices of the Jacobian matrix J are shown below.

$$B = \begin{bmatrix} \delta_p & 0 & -S_p \beta_4 \frac{(N_p - I_c^1)}{(N_p)^2} & 0 \\ 0 & 0 & S_p \beta_4 \frac{(N_p - I_c^1)}{(N_p)^2} & 0 \\ 0 & 0 & 0 & 0 \\ 0 & 0 & 0 & 0 \end{bmatrix}, \quad C = \begin{bmatrix} 0 & 0 & 0 & \alpha_p \\ 0 & 0 & 0 & 0 \\ 0 & 0 & 0 & 0 \\ 0 & 0 & 0 & 0 \end{bmatrix}, \text{ and}$$

also, the matrices A and B shown below

$$A = \begin{bmatrix} -\mu_1 - (\beta_2 I_p^1 + \beta_3 E_p + \beta_4 I_c^1 + \beta_5 H_p) \frac{(N_p - S_p)}{(N_p)^2} & -S_p \beta_3 \frac{(N_p - E_p)}{(N_p)^2} & -S_p \beta_2 \frac{(N_p - I_p)}{(N_p)^2} & -S_p \beta_5 \frac{(N_p - H_p)}{(N_p)^2} \\ (\beta_2 I_p^1 + \beta_3 E_p + \beta_4 I_c^1 + \beta_5 H_p) \frac{(N_p - S_p)}{(N_p)^2} & S_p \beta_3 \frac{(N_p - E_p)}{(N_p)^2} - (\mu_1 + \theta_p) & S_p \beta_2 \frac{(N_p - I_p)}{(N_p)^2} & S_p \beta_5 \frac{(N_p - H_p)}{(N_p)^2} \\ 0 & \theta_p & \gamma_p & 0 \\ 0 & 0 & -(\mu_1 + \gamma_p + \xi_p^1) & -(\alpha_p + \mu_1 + \xi_p^2) \end{bmatrix},$$

$$D = \begin{bmatrix} -(\delta_p + \mu_1) & 0 & 0 & 0 \\ 0 & -\mu_2 - \beta_1 \frac{(I_c^1 + I_c^2)(N_c - S_c)}{(N_c)^2} & -S_c \beta_1 \frac{(N_c - I_c^1)}{(N_c)^2} + \delta_1 & -S_c \beta_1 \frac{(N_c - I_c^2)}{(N_c)^2} + \delta_2 \\ 0 \beta_1 \frac{(I_c^1 + I_c^2)(N_c - S_c)}{(N_c)^2} & S_c \beta_1 \frac{(N_c - I_c^1)}{(N_c)^2} - (\xi_1 + \gamma + \mu_2 + \delta_1) & S_c \beta_1 \frac{(N_c - I_c^2)}{(N_c)^2} & \gamma \\ 0 & 0 & \gamma & -(\xi_2 + \mu_2 + \delta_2) \end{bmatrix}.$$

Define $s_p = \frac{S_p}{N_p}, e_p = \frac{E_p}{N_p}, i_p = \frac{I_p}{N_p}, h_p = \frac{H_p}{N_p}, s_c = \frac{S_c}{N_c}, i_c^1 = \frac{I_c^1}{N_c}, i_c^2 = \frac{I_c^2}{N_c},$

and by (7.7) we assume that $\frac{dS_p}{dt} = 0$ then I get

$$\Lambda_p - \mu_1 S_p + \delta_p R_p = \frac{(\beta_2 I_p + \beta_3 E_p + \beta_4 I_c^1 + \beta_5 H_p) S_p}{N_p}.$$

let $(\beta_2 I_p + \beta_3 E_p + \beta_4 I_c^1 + \beta_5 H_p) = \heartsuit$ then,

$$\heartsuit = \frac{N_p(\Lambda_p - \mu_1 S_p + \delta_p R_p)}{S_p}$$

here we want to reduce the Jacobian matrix J, then by taking the first term of sub-matrix

A and multiplied with \heartsuit

$$\text{then } \heartsuit \times \frac{N_p - S_p}{N_p^2} = \left(\frac{N_p}{-S_p} - 1\right)(\Lambda_p - \mu_1 S_p + \delta_p R_p)$$

Also for $\frac{dS_c}{dt} = 0$, I get that :

$$\Lambda_c - \mu_2 S_c + (\delta_1 I_c^1 + \delta_2 I_c^2) = \frac{\beta_1 S_c}{N_c} (I_c^1 + I_c^2)$$

$$\text{let } \star = \left(\frac{\Lambda_c - \mu_2 S_c + (\delta_1 I_c^1 + \delta_2 I_c^2) N_c}{S_p}\right)$$

$$\text{then } \frac{N_c - S_c}{N_c^2} \times \star = \left(\frac{N_c}{S_c} - 1\right)(\Lambda_c - \mu_2 S_c + (\delta_1 I_c^1 + \delta_2 I_c^2))$$

then, the Jacobian matrix J after reduced shows below

$$B = \begin{bmatrix} \delta_p & 0 & -s_p \beta_4 \left(1 - \frac{I_c^1}{N_p}\right) & 0 \\ 0 & 0 & s_p \beta_4 \left(1 - \frac{I_c^1}{N_p}\right) & 0 \\ 0 & 0 & 0 & 0 \\ 0 & 0 & 0 & 0 \end{bmatrix}, \quad C = \begin{bmatrix} 0 & 0 & 0 & \alpha_p \\ 0 & 0 & 0 & 0 \\ 0 & 0 & 0 & 0 \\ 0 & 0 & 0 & 0 \end{bmatrix}$$

also, the matrices A and B shown below

$$A = \begin{bmatrix} -\mu_1 - (\Lambda_p - \mu_1 S_p + \delta_p R_p) \left(\frac{N_p}{S_p} - 1 \right) & -s_p \beta_3 (1 - e_p) & -s_p \beta_2 (1 - i_p) & -s_p \beta_5 (1 - h_p) \\ (\Lambda_p - \mu_1 S_p + \delta_p R_p) \left(\frac{N_p}{S_p} - 1 \right) & s_p \beta_3 (1 - e_p) - (\mu_1 + \theta_p) & s_p \beta_2 (1 - i_p) & s_p \beta_5 (1 - h_p) \\ 0 & \theta_p & -(\mu_1 + \gamma_p + \xi_p^1) & 0 \\ 0 & 0 & \gamma_p & -(\alpha_p + \mu_1 + \xi_p^2) \end{bmatrix}$$

$$D = \begin{bmatrix} -(\delta_p + \mu_1) & 0 & 0 & 0 \\ 0 & -\mu_2 - (\Lambda_c - \mu_2 S_c + (\delta_1 I_c^1 + \delta_2 I_c^2)) \left(\frac{N_c}{S_c} - 1 \right) & -s_c \beta_1 (1 - i_c^1) + \delta_1 & -s_c \beta_1 (1 - i_c^2) + \delta_2 \\ 0 & (\Lambda_c - \mu_2 S_c + (\delta_1 I_c^1 + \delta_2 I_c^2)) \left(\frac{N_c}{S_c} - 1 \right) & s_c \beta_1 (1 - i_c^1) - (\xi_1 + \gamma + \mu_2 + \delta_1) & s_c \beta_1 (1 - i_c^2) \\ 0 & 0 & \gamma & -(\xi_2 + \mu_2 + \delta_2) \end{bmatrix}$$

with

$$\begin{aligned} a &= -\mu_1 - (\beta_2 i_p^1 + \beta_3 e_p + \beta_4 \frac{l_c^1}{N_p} + \beta_5 h_p)(1 - s_p) \\ a &= -\mu_1 - (\Lambda_p - \mu_1 S_p + \delta_p R_p) \left(\frac{N_p}{S_p} - 1 \right) \end{aligned} \quad (7.20)$$

$$b = -s_p \beta_3 (1 - e_p) \quad (7.21)$$

$$c = -s_p \beta_2 (1 - i_p) \quad (7.22)$$

$$d = -s_p \beta_5 (1 - h_p) \quad (7.23)$$

$$\begin{aligned} e &= \mu_1 - (\beta_2 i_p^1 + \beta_3 e_p + \beta_4 \frac{l_c^1}{N_p} + \beta_5 h_p)(1 - s_p) \\ e &= (\Lambda_p - \mu_1 S_p + \delta_p R_p) \left(\frac{N_p}{S_p} - 1 \right) \end{aligned} \quad (7.24)$$

$$f = s_p \beta_3 (1 - e_p) - (\mu_1 + \theta_p) \quad (7.25)$$

$$g = s_p \beta_2 (1 - i_p) \quad (7.26)$$

$$h = s_p \beta_5 (1 - h_p) \quad (7.27)$$

$$z = \gamma_p \quad (7.28)$$

$$i = -(\alpha_p + \mu_1 + \xi_p^2) \quad (7.29)$$

$$j = \alpha_p \quad (7.30)$$

$$k = -(\delta_p + \mu_1) \quad (7.31)$$

$$l = \delta_p \quad (7.32)$$

$$m = -s_p \beta_4 \left(1 - \frac{l_c^1}{N_p} \right) \quad (7.33)$$

$$n = s_p \beta_4 \left(1 - \frac{l_c^1}{N_p} \right) \quad (7.34)$$

$$y = \theta_p \quad (7.35)$$

$$p = -(\delta_p + \mu_1) \quad (7.36)$$

$$q = -\mu_2 - \beta_1(i_c^1 + i_c^2)(1 - s_c) \quad (7.37)$$

$$q = -\mu_2 - \left(\frac{N_c}{S_c} - 1\right)(\Lambda_c - \mu_2 S_c + (\delta_1 I_c^1 + \delta_2 I_c^2))$$

$$s = -s_c \beta_1(1 - i_c^1) + \delta_1 \quad (7.38)$$

$$v = -s_c \beta_1(1 - i_c^2) + \delta_2 \quad (7.39)$$

$$r = \beta_1(i_c^1 + i_c^2)(1 - s_c) \quad (7.40)$$

$$r = \left(\frac{N_c}{S_c} - 1\right)(\Lambda_c - \mu_2 S_c + (\delta_1 I_c^1 + \delta_2 I_c^2))$$

$$t = s_c \beta_1(1 - i_c^1) - (\xi_1 + \gamma + \mu_2 + \delta_1) \quad (7.41)$$

$$w = s_c \beta_1(1 - i_c^2) \quad (7.42)$$

$$u = \gamma \quad (7.43)$$

$$x = -(\xi_2 + \mu_2 + \delta_2) \quad (7.44)$$

the matrix(7.4.1) with the coefficients signs:

$$J = \begin{bmatrix} - & - & - & - & + & 0 & - & 0 \\ ? & ? & + & + & 0 & 0 & + & 0 \\ 0 & + & - & 0 & 0 & 0 & 0 & 0 \\ 0 & 0 & + & - & 0 & 0 & 0 & 0 \\ 0 & 0 & 0 & + & - & 0 & 0 & 0 \\ 0 & 0 & 0 & 0 & 0 & - & ? & ? \\ 0 & 0 & 0 & 0 & 0 & + & - & + \\ 0 & 0 & 0 & 0 & 0 & 0 & + & - \end{bmatrix}.$$

The eigenvalues of the matrix(7.4.1) are the solution of the equation

$$\det(J - \lambda I) = \det \begin{vmatrix} A - \lambda I & B \\ C & D - \lambda I \end{vmatrix} = 0. \quad (7.45)$$

Note that

$$\begin{aligned} \det(J - \lambda I) &= \det(A - \lambda I) \det(D - \lambda I - C(A - \lambda I)^{-1}B) \\ &= \det(A - \lambda I - B(D - \lambda I)^{-1}C) \det(D - \lambda I) \end{aligned}$$

where

$$(D - \lambda I)^{-1} = \begin{pmatrix} \frac{1}{p-\lambda} & 0 & 0 & 0 \\ 0 & \frac{x(t-\lambda)-wu}{\clubsuit} & \frac{vu-sx}{\spadesuit} & \frac{\lambda v-vt+sw}{\spadesuit} \\ 0 & -\frac{rx}{\clubsuit} & \frac{x(q-\lambda)}{\clubsuit} & \frac{vr-w(q-\lambda)t}{\clubsuit} \\ 0 & \frac{ru}{\clubsuit} & -\frac{u(q-\lambda)}{\clubsuit} & -\frac{sr-(q-\lambda)(t-\lambda)}{\clubsuit} \end{pmatrix}$$

and

$$\begin{aligned} \clubsuit &= u(vr - w(q - \lambda)) - x(sr - (q - \lambda)(t - \lambda)) \\ \spadesuit &= u(-w(-\lambda + q) + vr) - x(-(-\lambda + q)(-\lambda + t) + sr) \end{aligned}$$

Then we have

$$A - \lambda I - B(D - \lambda I)^{-1}C = \begin{bmatrix} a - \lambda & b & c & d - \frac{ly}{p-\lambda} \\ e & f - \lambda & g & h \\ 0 & z & i - \lambda & 0 \\ 0 & 0 & j & k - \lambda \end{bmatrix}$$

and

$$\det(A - \lambda I - B(D - \lambda I)^{-1}C) = \begin{vmatrix} a - \lambda & b & c & d - \frac{ly}{p - \lambda} \\ e & f - \lambda & g & h \\ 0 & z & i - \lambda & 0 \\ 0 & 0 & j & k - \lambda \end{vmatrix}$$

$$= jz[(a - \lambda)h - e(d - \frac{ly}{p - \lambda})] + (k - \lambda)[(a - \lambda)[(i - \lambda)(f - \lambda) - gz] + ecz - eb(i - \lambda)].$$

Then the determination is

$$= -\lambda^5 + a_1\lambda^4 + a_2\lambda^3 + a_3\lambda^2 + a_4\lambda + a_5 = 0.$$

Here

$$\begin{aligned}
 a_1 &= (a + p + f + k + i) \\
 a_2 &= (pa + pf + pk + af + ak + kf + pi + ai + ki + fi - gz - eb) \\
 a_3 &= (pa.f + pak + pk.f + ak.f + pai + pki + pfi + aki + a.fi + k.fi + jzh - ekb - ebp + ezc - agz - gzk - gzp - ieb) \\
 a_4 &= (pak.f + pak + pa.f + pk.f + ak.f + ajzh + jzph + ekzc + epzc - agzk - agzp - gzkp - ekb - ebp - ezjd) \\
 a_5 &= (pak.f + ajzph + ekpzc + ezjly - agzky - ekbp - ezjbd)
 \end{aligned}$$

Also

$$\det(D - \lambda I) = \begin{vmatrix} p - \lambda & 0 & 0 & 0 \\ 0 & q - \lambda & s & v \\ 0 & r & t - \lambda & w \\ 0 & 0 & u & x - \lambda \end{vmatrix} = (p - \lambda) \begin{vmatrix} q - \lambda & s & v \\ r & t - \lambda & w \\ 0 & u & x - \lambda \end{vmatrix} \quad (7.46)$$

$$= (p - \lambda)[(q - \lambda)[(t - \lambda)(x - \lambda) - uw] - r[s(x - \lambda) - uv]]$$

Then the determination is

$$= (p - \lambda)[- \lambda^3 + b_1 \lambda^2 - b_2 \lambda - b_3] = 0.$$

Here

$$b_1 = (x + t + q)$$

$$b_2 = (-uw - sr + tx + qx + qt)$$

$$b_3 = (qtx - qwu - srx + vur)$$

Hence, the characteristic polynomial is a product of two 4th degree polynomials

with

$$\det(A - \lambda I - B(D - \lambda I)^{-1}C) = -\lambda^5 + a_1\lambda^4 + a_2\lambda^3 + a_3\lambda^2 + a_4\lambda + a_5$$

and

$$\det(D - \lambda I) = (p - \lambda)[- \lambda^3 - b_1\lambda^2 - b_2\lambda - b_3].$$

Chapter 8: Numerical Simulations

To visualize the dynamics of MERS infection in the UAE population, we run simulations of the MERS model using **R** software [54] and the open source packages [18, 60]. Using parameter values listed in Table (8.1) with initial conditions given in Table (8.2).

8.1 Time Series Simulation

This section shows the simulation of different values of basic reproduction number \mathcal{R}_0 , to clarify the results of our model and analytical results. First, we will simulate the case $\mathcal{R}_0 < 1$. Then, we will simulate the case $\mathcal{R}_0 > 1$ based on the values of the basic reproduction numbers for the subgroups of \mathcal{R}_{01} and \mathcal{R}_{02} , including the

$$\mathcal{R}_0 = \rho(K) = \max(\mathcal{R}_{01}, \mathcal{R}_{02}),$$

with

$$\mathcal{R}_{01} = \frac{\beta_3}{(\mu_1 + \theta_p)} + \frac{\beta_2 \theta_p}{(\mu_1 + \theta_p)(\mu_1 + \gamma_p + \xi_p^1)} + \frac{\beta_5 \theta_p \gamma_p}{(\mu_1 + \theta_p)(\mu_1 + \gamma_p + \xi_p^1)(\alpha_p + \mu_1 + \xi_p^1)},$$

and

$$\mathcal{R}_{02} = \frac{\beta_1}{(\xi_1 + \gamma + \mu_2 + \delta_1)} + \frac{\beta_1 \gamma}{(\xi_1 + \gamma + \mu_2 + \delta_1)(\xi_2 + \mu_2 + \delta_2)}$$

So we chose our parameters in order to study the epidemic equilibria shown below:

- ▶ Case 1: $\mathcal{R}_{01} < 1$ and $\mathcal{R}_{02} < 1$
- ▶ Case 2: $\mathcal{R}_{01} > 1$ and $\mathcal{R}_{02} < 1$
- ▶ Case 3: $\mathcal{R}_{01} < 1$ and $\mathcal{R}_{02} > 1$
- ▶ Case 4: $\mathcal{R}_{01} > 1$ and $\mathcal{R}_{02} > 1$

Some of the parameters were calculated to suit with a description of my model while others were assembled from other papers of MERS-CoV. Where Λ_p is considered as human populations in UAE which is calculated from [16]. Also Λ_c represent camels populations in UAE are calculated from [19]. The simulation below shows the outcomes of our model in the case of $\mathcal{R}_0 < 1$ for the following parameters. The Table 8.1 display the parameters that used in the simulation at case Disease Free Equilibrium.

The parameters value and unit are presented in Table (8.1).

Parameters	Values	unit	References
Λ_p	47.97	<i>Human</i> \times <i>Days</i> ⁻¹	calculated
Λ_c	97.1925	<i>Camel</i> \times <i>Days</i> ⁻¹	calculated
μ_1	3.198399×10^{-6}	<i>Human</i> \times <i>Days</i> ⁻¹	calculated
μ_2	2429813×10^{-4}	<i>Camel</i> \times <i>Days</i> ⁻¹	calculated
β_1	0.15	<i>Days</i> ⁻¹	[34]
β_2	0.7833	<i>Days</i> ⁻¹	[70]
β_3	0.8756	<i>Days</i> ⁻¹	[70]
β_4	0.34	<i>Days</i> ⁻¹	assumed
β_5	0.4568	<i>Days</i> ⁻¹	[70]
δ_p	0.125	<i>Days</i> ⁻¹	[41]
δ_1	0.25	<i>Days</i> ⁻¹	[34]
δ_2	0.48	<i>Days</i> ⁻¹	[34]
α_p	0.2	<i>Days</i> ⁻¹	[41]
θ_p	0.2	<i>Days</i> ⁻¹	[70]
γ_p	0.708	<i>Days</i> ⁻¹	[14]
γ	0.12	<i>Days</i> ⁻¹	[5]
ξ_p^1	3.36×10^{-6}	<i>Days</i> ⁻¹	calculated
ξ_p^2	3.36×10^{-6}	<i>Days</i> ⁻¹	calculated
ξ_1	0.33	<i>Days</i> ⁻¹	assumed
ξ_2	0.9	<i>Days</i> ⁻¹	assumed

Table 8.1: The parameters values and units

Parameters	Value
S_p	300000
E_p	205
I_p	21
R_p	31
H_p	25
S_c	30000
I_c^1	7
I_c^2	0

Table 8.2: Initial conditions

8.2 Simulation of the Disease Equilibrium

8.2.1 Simulation of the Disease Free Equilibrium

To have better understanding of my model in the case of free equilibria, we plot the figures for the one case per each population as we mentioned previously. The case are as follow:

► Case 1: $\mathcal{R}_{01} < 1$ and $\mathcal{R}_{02} < 1$

For simplicity, we will give all the parameters without unit since the same parameters were given in the previous Table with units.

In the case 1, we choose the following parameters:

$$\Lambda_p = 47.97; \Lambda_c = 96.8; \mu_1 = 3.198399e \times 10^{-6}; \mu_2 = 242 \times 10^{-4}; \beta_1 = 0.58; \beta_2 = 0.7833; \beta_3 = 0.36; \beta_4 = 0.34; \beta_5 = 0.4568; \delta_p = 0.125; \delta_1 = 0.17; \delta_2 = 0.25; \alpha_p = 0.2; \theta_p = 0.4; \gamma_p = 0.708; \gamma = 0.36; \xi_p^1 = 3.36 * 10^{-6}; \xi_p^2 = 3.36 * 10^{-6}; \xi_1 = 0.25; \xi_2 = 0.9;$$

Compartment of humans and camels population when $\mathcal{R}_0 < 1$: the simulation of the model of the case 1 when $\mathcal{R}_0 < 1$ shows that the susceptible human population goes down in the begin of the time course, but gradually converges to the equilibrium point $\frac{\Lambda_p}{\mu_1}$. So, the population of susceptible human decreased sharply from 3,500,000 and stood at 506713.4 then it rise slowly to settle between 1000000. Also, the exposed population get established and rise sharply after 17 days (time) and peak around 793082. The infected population also increases and peaks around 426939.5 and time series simulation show

that the disease pick at value 111.9821 infected people within 20 days. The infected population at final stage reach to the value 0.04357758. The recovered and hospitalized population appear with super high in increasing, where theses two population take a more time before to reach a peak. For more illustration see Figure (8.1).

The simulation of the infected camel compartment does not get to established for the (Aware infectious camels and Unaware infectious camels) population while the susceptible camels population is grow. So, compared to the human dynamic there is no peak occurs in camels population before the human peak.

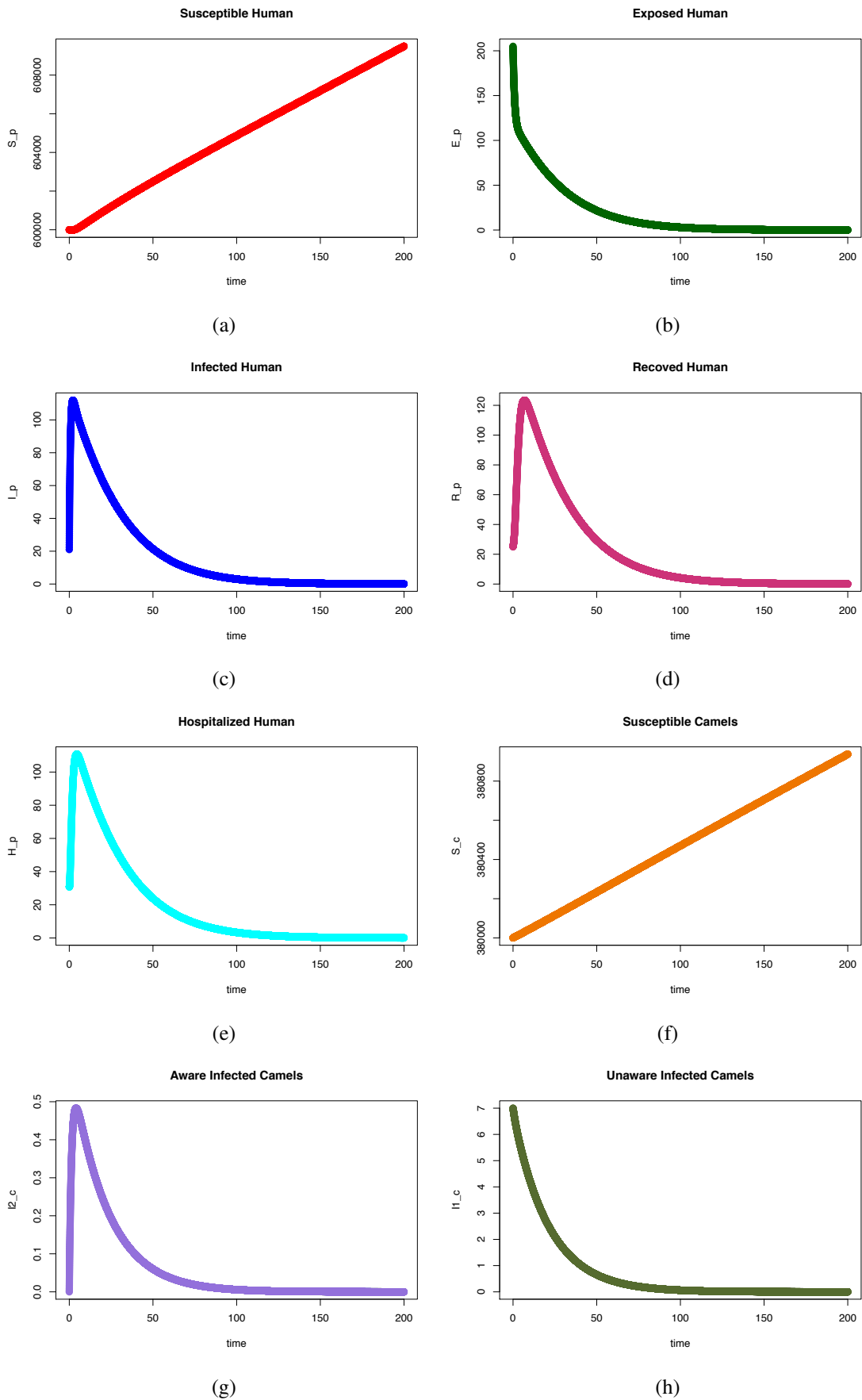


Figure 8.1: Case 1: disease free equilibrium (when $\mathcal{R}_0 < 1$)

we conclude that the Case 1 appears with slight infections to human while there was a fewer burden to camels.

8.2.2 Simulation of the Endemic Equilibrium

To have better understanding of our model in the case of endemic equilibria, we plot each Figure of the three cases per each population . The cases are as follow:

- ▶ Case 2: $\mathcal{R}_{01} > 1$ and $\mathcal{R}_{02} < 1$
- ▶ Case 3: $\mathcal{R}_{01} < 1$ and $\mathcal{R}_{02} > 1$
- ▶ Case 4: $\mathcal{R}_{01} > 1$ and $\mathcal{R}_{02} > 1$

For simplicity, I will give all the parameters without unit since the same parameters were given in the previous Table with units.

In the case 2, I choose the following parameters: $\Lambda_p = 47.97; \Lambda_c = 96.8; \mu_1 = 3.198399e \times 10^{-6}; \mu_2 = 242 \times 10^{-4}; \beta_1 = 0.76; \beta_2 = 0.1; \beta_3 = 0.09; \beta_4 = 0.34; \beta_5 = 0.08; \delta_p = 0.125; \delta_1 = 0.14/2; \delta_2 = 0.25; \alpha_p = 0.2; \theta_p = 0.2; \gamma_p = 0.708; \gamma = 0.12/2; \xi_p^1 = 3.36 * 10^{-6}; \xi_p^2 = 3.36 * 10^{-6}; \xi_1 = 0.13/2; \xi_2 = 0.9/2;$

For the case 3, I used these parameters : $\Lambda_p = 47.97; \Lambda_c = 96.8; \mu_1 = 3.198399e \times 10^{-6}; \mu_2 = 242 \times 10^{-4}; \beta_1 = 0.76; \beta_2 = 0.1; \beta_3 = 0.09; \beta_4 = 0.34; \beta_5 = 0.08; \delta_p = 0.125; \delta_1 = 0.14; \delta_2 = 0.25; \alpha_p = 0.2; \theta_p = 0.2; \gamma_p = 0.9912; \gamma = 0.12; \xi_p^1 = 3.36 * 10^{-6}; \xi_p^2 = 3.36 * 10^{-6}; \xi_1 = 0.13; \xi_2 = 0.9;$

Finally, For the case 4 I have: $\Lambda_p = 47.97; \Lambda_c = 96.8; \mu_1 = 3.198399e \times 10^{-6}; \mu_2 = 242 \times 10^{-4}; \beta_1 = 0.55; \beta_2 = 0.5833; \beta_3 = 0.43; \beta_4 = 0.34; \beta_5 = 0.3568; \delta_p = 0.125; \delta_1 = 0.14; \delta_2 = 0.25; \alpha_p = 0.2; \theta_p = 0.4; \gamma_p = 0.708; \gamma = 0.14; \xi_p^1 = 3.36 * 10^{-6}; \xi_p^2 = 3.36 * 10^{-6}; \xi_1 = 0.1; \xi_2 = 0.9;$

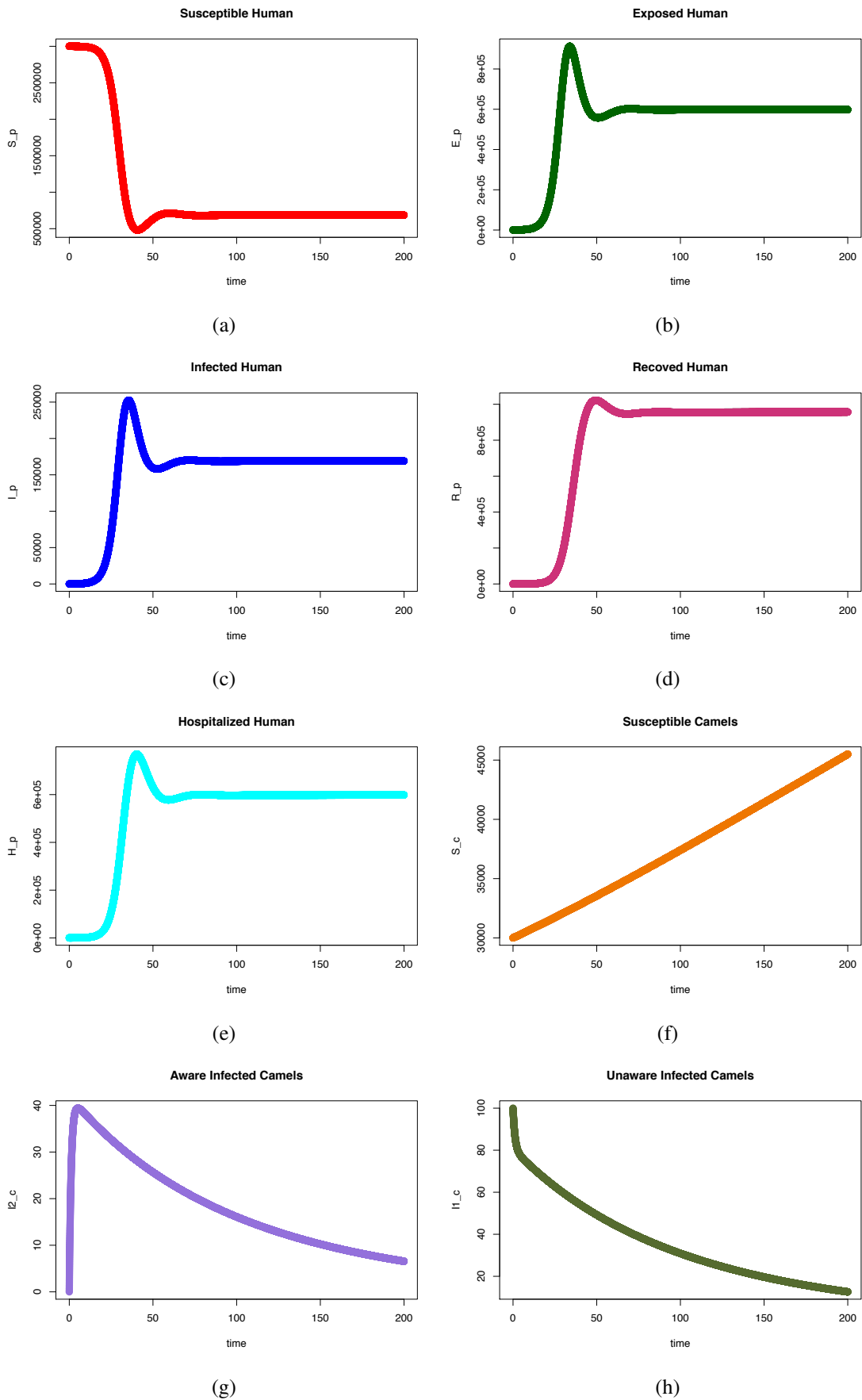


Figure 8.2: Case 2: disease endemic equilibrium (when $\mathcal{R}_0 > 1$)

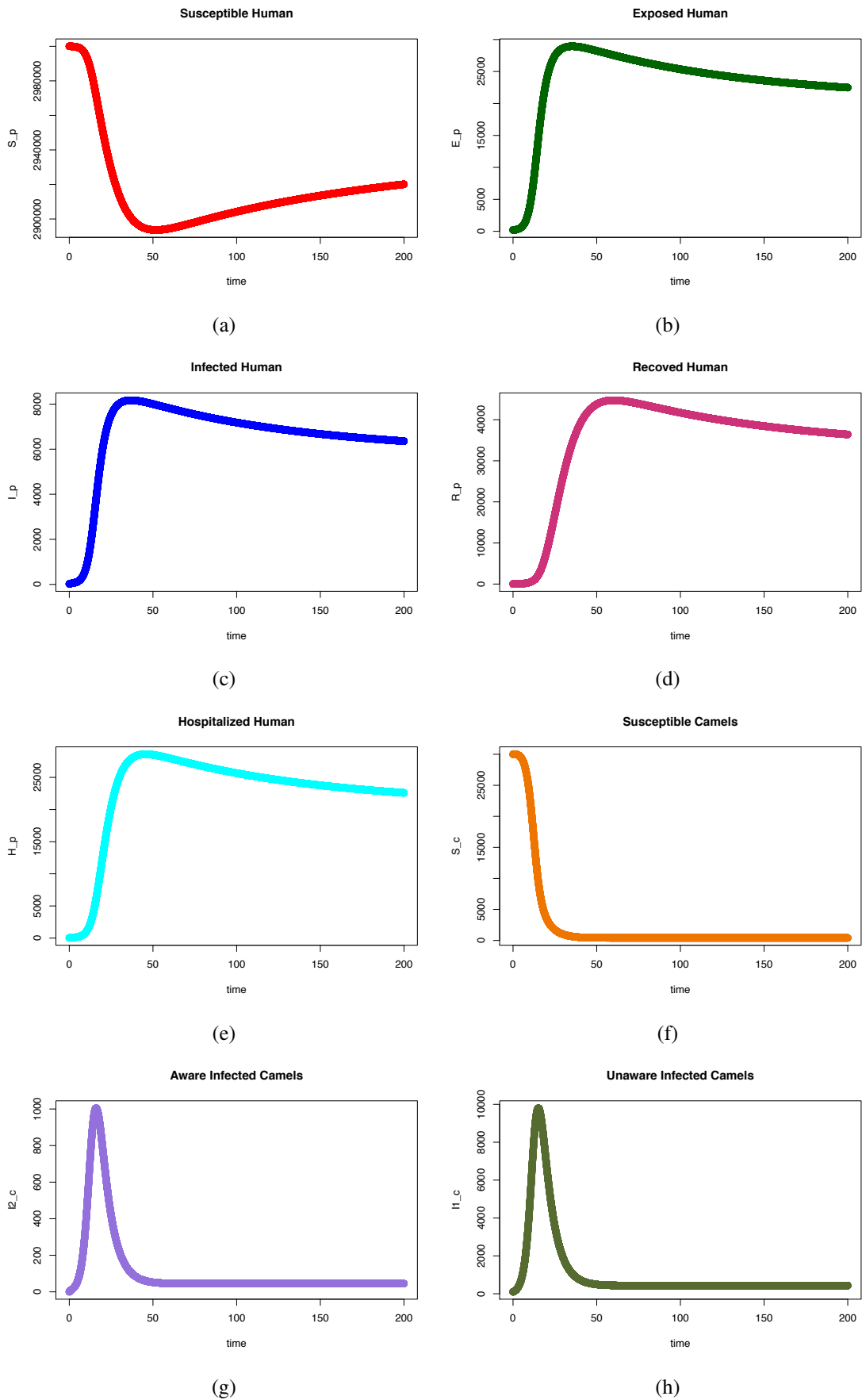


Figure 8.3: Case 3: disease endemic equilibrium (when $\mathcal{R}_0 > 1$)

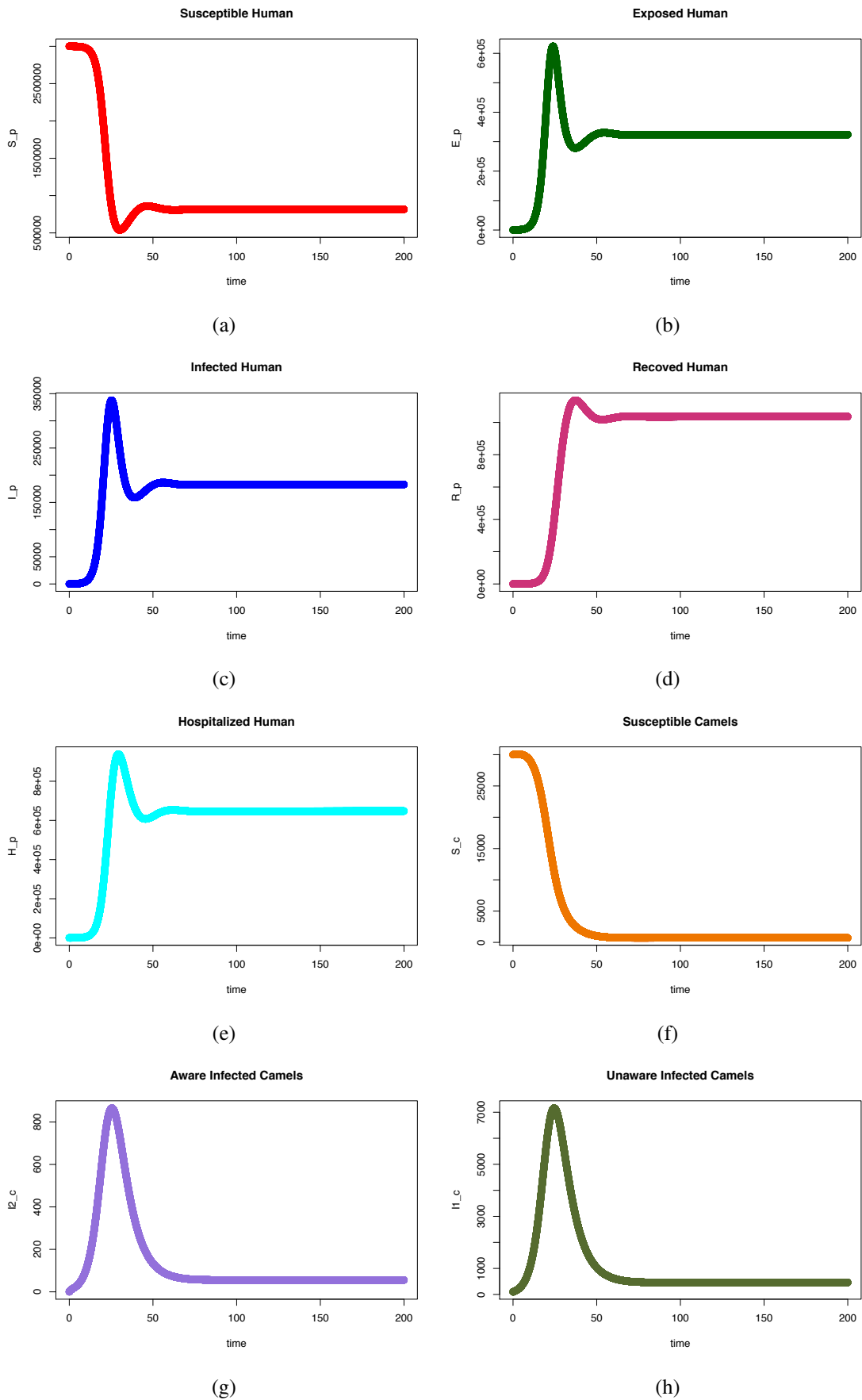


Figure 8.4: Case 4: disease endemic equilibrium (when $\mathcal{R}_0 > 1$)

By analyzing the figures corresponding to the cases, the Case 2 when $\mathcal{R}_{01} > 1$ shows that the susceptible human population (S_p) decreases sharply from 3000000 to 500000 within 40 days then it increasing slowly and settle at 685110. Also, in Case 4 when $\mathcal{R}_{01} > 1$ the S_p was decline more sharply compared to case 2 (see cases in Figure(8.2) and (8.4)). While S_p in Case 4 appear with a slight change whereas it mostly stabilized around 482006.4, that actually because $\mathcal{R}_{01} < 1$. The population of E_p, R_p, H_p presented with the same pattern in Cases 2 and 4, which is increasing rapidly and the increase in Case 4 was earlier than case 3 with similar scale time. The same population in Case 3 shows a little growth on the scale time compared to Case 1 and 3. When $\mathcal{R}_{01} > 1$, the Case 2 and Case 4 shows a high infection in human population where the peak of the infection reached to 252529.7, 337893.9 respectively, while Case 3 shows the less infection and peak at value 8170.837 infected case. That means Case 1 and Case 3 are more endemic equilibria when the disease is endemic in the human population. In fact when $\mathcal{R}_{02} < 1$ the endemic equilibria lower in the human population compared to when $\mathcal{R}_{02} > 1$. That shows the protecting the human population from possible camel infection is beneficial to the overall infection in the UAE.

The analysis of the time series of Case 2 shows that the susceptible population of camels (S_c) displayed an increasing trend when the time increased. Conversely, I_c^1 and I_c^2 is decreasing because $\mathcal{R}_{02} > 1$ which means the disease in camels die out. The Case 3 is opposite to the previous case, where that the decrease in S_c is very sharply during 40 days at the same time the increase of I_c^1 was rapid which reach peak beyond 9798.482 cases of an infected camel. The number of infected camel converged to 431.3864. The I_c^2 was rise slowly at that time, and it reaches close 1000 case of an infected camels. The disease after 50 days shows a scenario of persists disease in a low number of in cases of infected camels. The last case mostly was similar to case 3, but with less rate of infectious between camels whereas the value of the peak was 7157.172 of infected cases and this number converted to 460.5257.

8.3 Sensitivity Analysis

Here we show the index estimation of \mathcal{R}_0 with respect to the parameters and we do the uncertainty analysis

8.3.1 For Infected Population (I_p)

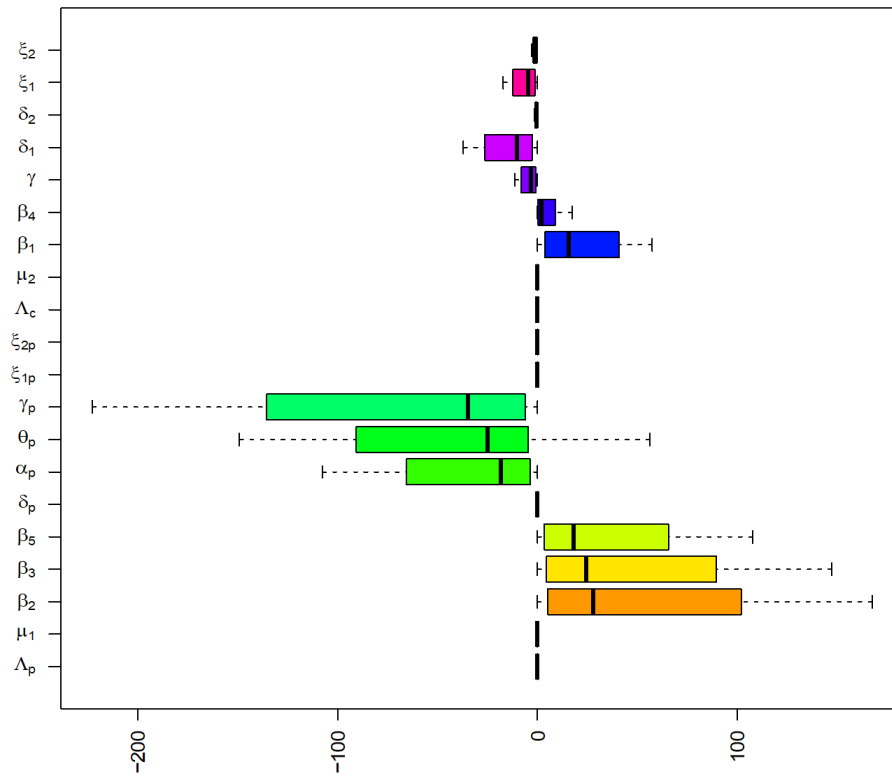
We looking at the sensitivity analysis of all parameters of our model with respect to the variable of infected humans, we find certain parameters have more impact on human infection population than others. This impact could be either positive or negative.

1. Case 1: $\mathcal{R}_{01} < 1$ and $\mathcal{R}_{02} < 1$

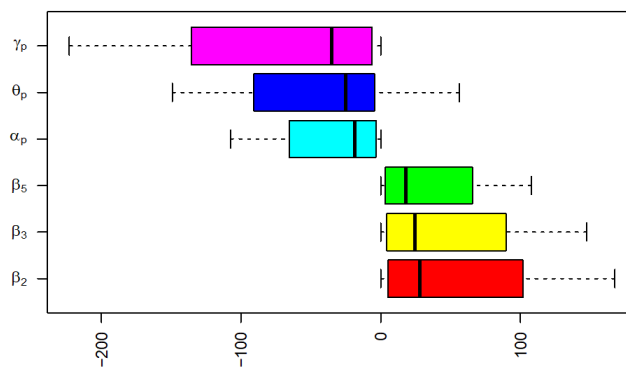
In Figure (8.5), we see that parameters $\Lambda_p, \mu_1, \theta_p, \xi_p^1, \xi_p^2, \Lambda_c, \mu_2$ have almost no effect on I_p . The variables $\beta_1, \beta_4, \gamma, \delta_1, \delta_2, \xi_1, \xi_2$ have slight effect on I_p . More precisely, $\gamma, \delta_1, \delta_2, \xi_1, \xi_2$ have the same negative sign which means the increase of the parameter will result in a decrease of I_p . On the other hand, β_1, β_4 are affecting positively I_p . That is the increase of these variables will slight increase I_p . The remaining variables are of significance to I_p ; particularly $\alpha_p, \theta_p, \gamma_p$. These variables have a high impact on I_p , and their effects are described as follows: the parameters have the opposite sign to I_p . It is normal because the increase in the recovery rate of hospitalized humans, the long period of incubation for an exposed individual until becoming infected, and the increase in the rate of hospitalization of infected humans, means we will not have an infected population.

The parameters that have positive effect on I_p are $\beta_2, \beta_3, \beta_5$ the infection rates of infected individuals, infection rate of exposed individual and infection rate of hospitalized human, respectively. It make sense that increasing the values of these parameters will result in more infectious individual.

The parameters sensitivity with respect to I_p



The parameters with high sensitivity with respect to I_p



The parameters with low sensitivity with respect to I_p

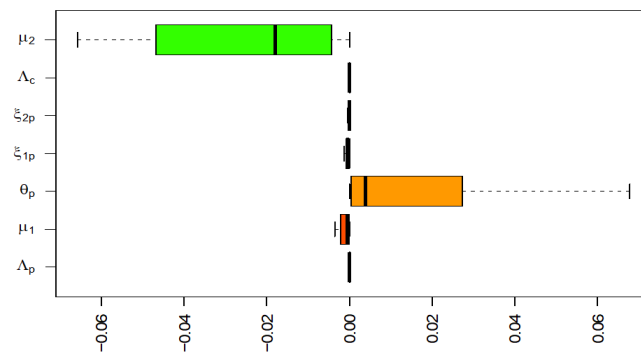


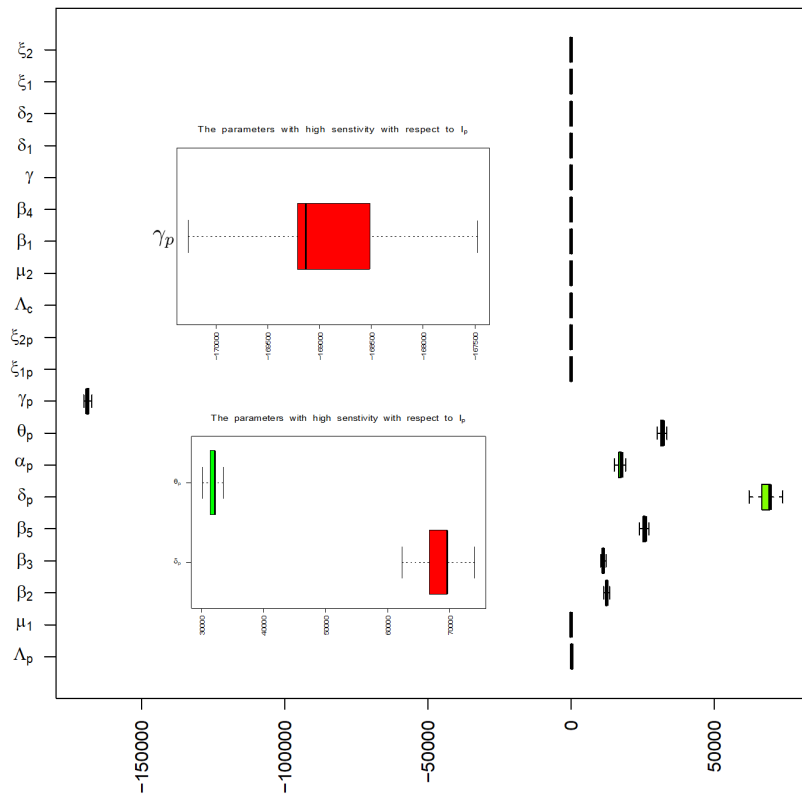
Figure 8.5: Parameters sensitivity to I_p in case 1

2. **Case 2:** $\mathcal{R}_{01} > 1$ and $\mathcal{R}_{02} < 1$

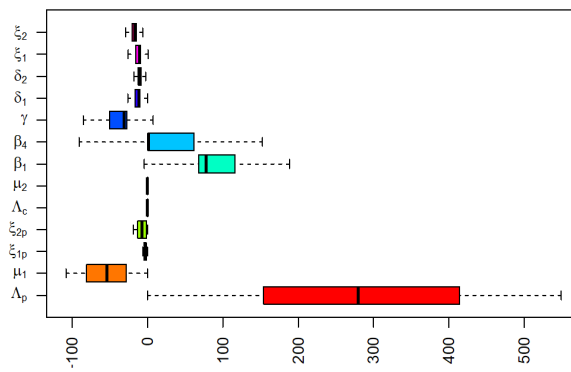
The Figure (8.6) encompassed parameters $\Lambda_p, \mu_1, \xi_p^1, \xi_p^2, \Lambda_c, \mu_2, \beta_1, \beta_4, \gamma, \delta_1, \delta_2, \xi_1, \xi_2$ which have almost low effect on I_p . The variables $\Lambda_p, \mu_1, \beta_1, \beta_4, \gamma$, have slight effect on I_p , while the other remaining parameters have no effect on I_p . Regarding to other parameters as $\beta_2, \beta_3, \beta_5, \alpha_p$ which have a medium effect on I_p with positive sign which means the increase of the parameter will result a increase of I_p . The remain parameters also are significant for I_p ; especially $\delta_p, \theta_p, \gamma_p$. The variable γ_p has a high negative effect on I_p . Contrarily, θ_p and δ_p are affecting I_p in positive way. That means the increase of these variables will sharply increase I_p .

The Figure (8.6) shows the variation of the parameters such as δ_p, θ_p and α_p by 10000, while the variation of the other parameters by lower than that. The sensitivity analysis which is shown in this case refer to the parameters of human such as $\beta_2, \beta_3, \beta_5$ with more sensitive in I_p than camel parameters such as β_1, β_4 . All previous parameters have a positive effect on I_p . γ_p is also of the human parameters but with significant negative effect on I_p and its means more recovered people hospitalizes leads to less infected in human population. Both δ_p and θ_p positively effecting I_p , which explain the more rate of detecting people who are infected will increase the number of sick people.

The parameters sensitivity with respect to I_p



The parameters with low sensitivity with respect to I_p



The parameters with meduim sensitivity with respect to I_p

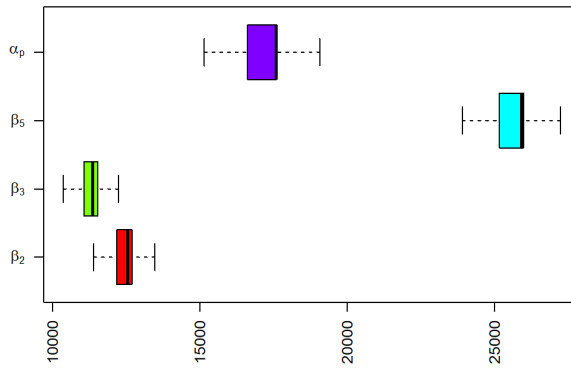


Figure 8.6: Parameters sensitivity to I_p in case 2

3. Case 3: $\mathcal{R}_{01} < 1$ and $\mathcal{R}_{02} > 1$

The parameters $\Lambda_p, \mu_1, \xi_p^1, \xi_p^2, \mu_2, \beta_1, \gamma, \delta_2, \xi_2$ almost have a low effect on I_p . Besides, the parameters $\beta_1, \gamma, \delta_p, \xi_2$ have slight effect on I_p , while the remain variables have no effect on I_p . Differently, the $\delta_p, \Lambda_c, \beta_4, \delta_1, \xi_1$ have an average effect on I_p . Whilst the first three variables have a positive sign which means the increase of the parameter will result a increase of I_p . The last two parameters have a negative effect on I_p . The remain parameters raised major effect to I_p ; particularly $\alpha_p, \theta_p, \gamma_p$ have the opposite sign to I_p . The effects of theses parameters are described as follows: the increase in the recovery rate of hospitalized humans, the long period of incubation for an exposed individual until they become infected the increase in the rate of hospitalization individual of infected humans, means we will not have an infected population. In this case, the parameters with high significant effect on I_p are similar to parameters in case 1 when $\mathcal{R}_{01} < 1$, but Figure (8.7) indicates that, the rate of hospitalization individual of infected humans are less than case 1. That follow as the increasing of infectious between camels when $\mathcal{R}_{02} > 1$. The parameters that have a positive influential on I_p are $\beta_2, \beta_3, \beta_5$. The first three parameters are the infection rates of infected individual(which is shows a low rate), infection rate of exposed individual and infection rate of hospitalized human. And the increase in the value of these parameters will result more infection.

This case shows that the infection is dominated on camels. By looking at the camel parameters with highest effect on I_p such as β_1 and β_4 where β_1 which is describe the infection rate among camels and it show lower infection to human compared to β_4 which is show the infection among human. The surprise result is that β_1 doesn't affect I_p . The disease persists in the camels population but the transmission of the disease among the human is the most dominate. The sensitivity analysis of our parameters when $\mathcal{R}_{02} > 1$ which mean the disease persists in the camel population shows that the parameter of transmission of the disease among human lower sensitive to I_p and that indicates the crucial wish out the human transmission, not the camel transmission.

The parameters sensitivity with respect to I_p

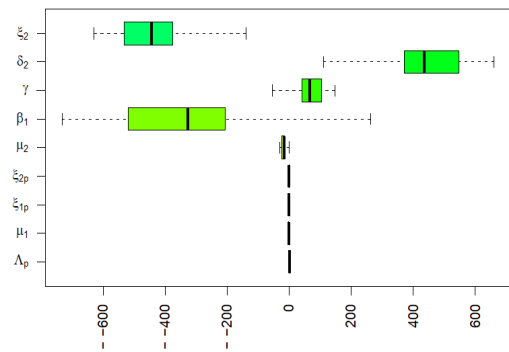
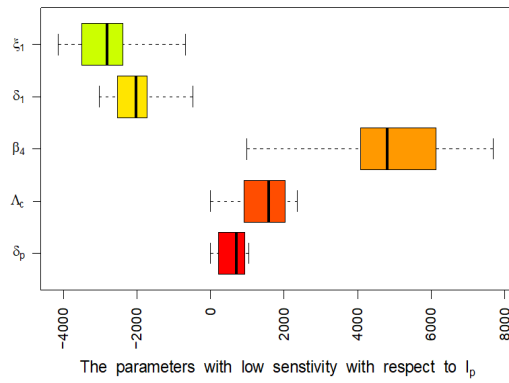
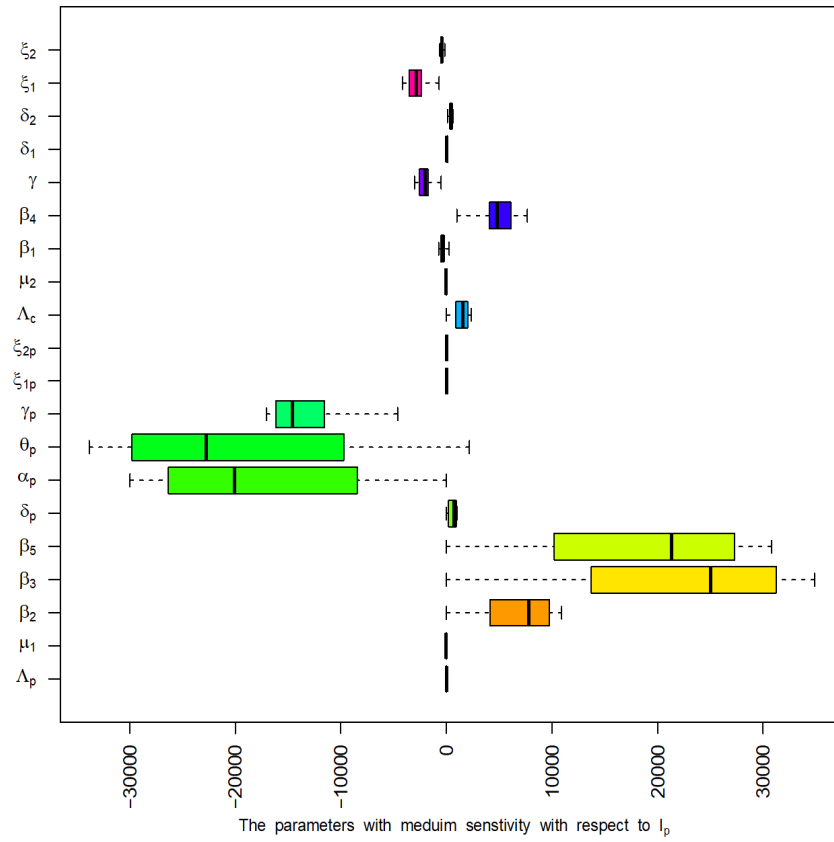


Figure 8.7: Parameters sensitivity to I_p in case 3

4. **Case 4:** $\mathcal{R}_{01} > 1$ and $\mathcal{R}_{02} > 1$

In Figure (8.8), we see that parameters, $\xi_p^1, \xi_p^2, \Lambda_c, \mu_2, \gamma, \delta_1, \delta_2, \xi_1, \xi_2$ have almost low effect on I_p . More precisely, the $\Lambda_p, \mu_1, \beta_1, \beta_4$ have an average effect on I_p . The $\Lambda_p, \beta_1, \beta_4$ have positive sign which means the increase of the parameter will result a increase of I_p while μ_1 has a negative sign which the increase of this parameter will result a decrease of I_p . The remain of the variables are significance to I_p ; particularly $\beta_2, \beta_3, \beta_5, \delta_p, \theta_p, \gamma_p$. The variable γ_p has a high negative effect on I_p . On the other hand, the remain are affecting I_p in positive way. That means the increase of these variables will sharply increase in I_p .

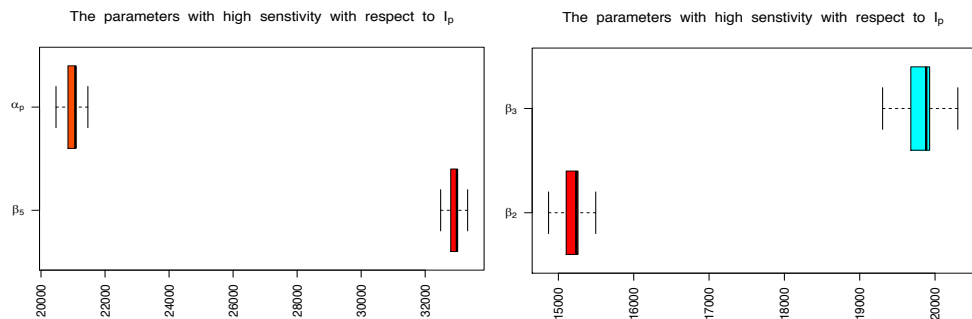
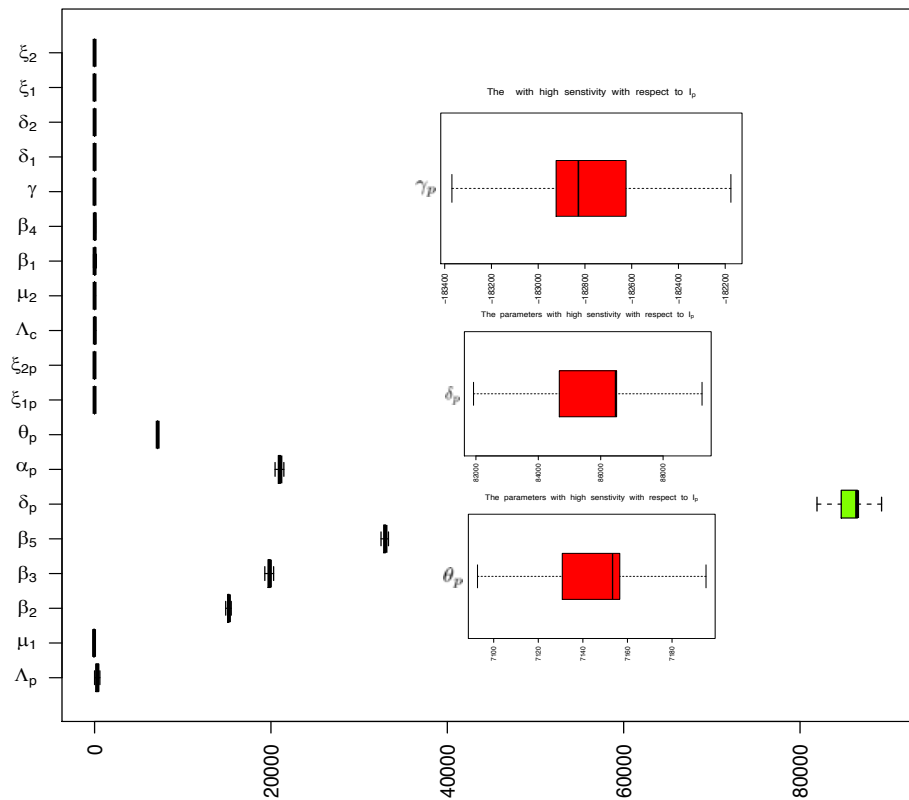
The Figure (8.8) shows the variation of the parameters such as δ_p, θ_p and α_p by 20000, while the variation of the other parameters by lower than that. The sensitivity analysis which is shown in this case refer to the parameters of human such as $\beta_2, \beta_3, \beta_5$ with more sensitive in I_p than camel parameters such as β_1, β_4 . All previous parameters have a positive effect on I_p . In this case only γ_p effect I_p negativity, while the remain parameters has positive effect. The in the value of γ_p means more recovered people hospitalizes leads to less infected in human population. Both δ_p and θ_p positively effecting I_p , which explain the more rate of detecting people who are infected will increase the number of sick people. Also, we should also note the effect of increasing the birth rate of human Λ_p in the spread of the disease, as any increase in the number of human will cause in the future increased the likelihood of the spread of the epidemic.

This case shows that the infection persists among the population of camels and humans, but it is clearly the infection dominance on the human is highest. By looking to the camel parameters with highest effect on I_p such as β_1 and β_4 where β_1 which is describe the infection rate among camels and it show higher infection to human compared to β_4 which is show the infection among human. So in this case β_1 will affect in I_p positively and contributes to the spread of the epidemic among humans, but with small percentage. The disease persists in the camels population but the transmission of the disease among the human is the most dominate. The sensitivity analysis of our parameters when $\mathcal{R}_{02} > 1$ which mean the disease persists in the camel population shows

that the parameter of transmission of the disease among human lower sensitive to I_p and that indicates the crucial wish out the human transmission, not the camel transmission.

The Cases 2 and 4 are similar when $\mathcal{R}_{01} > 1$ to some extent.

The parameters sensitivity with respect to I_p



The parameters with low sensitivity with respect to I_p

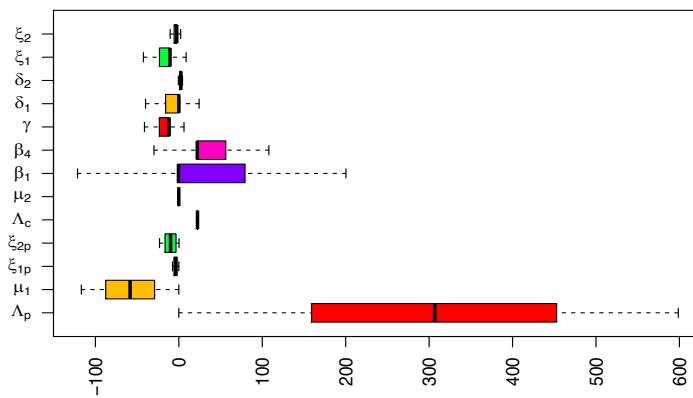


Figure 8.8: Parameters sensitivity to I_p in case 4

8.3.2 For Hospitalized Population (H_p)

The sensitivity analysis of hospitalized population was performed in the same style as for the infected humans population. Figure (8.9) show a general look for the human sensitivity of parameter with respect to infectious human population. The Figure shows the different effects of parameters on H_p that may be positive or negative.

1. Case 1: $\mathcal{R}_{01} < 1$ and $\mathcal{R}_{02} < 1$

Parameters $\Lambda_p, \mu_1, \delta_p, \xi_p^1, \xi_p^2, \Lambda_c, \mu_2$ have no significant sensitive to the H_p . Furthermore, parameters β_1, β_4 have an average positive effect on H_p and $\gamma, \delta_1, \delta_2, \xi_1, \xi_2$ have an average negative effect on H_p . These parameters which has an average effect on H_p have a slight ability to change the H_p size. This differs for the rest of the parameters where an increase or decrease will effect the infected H_p . The three parameters $\beta_2, \beta_3, \beta_5$ are positively sensitive to H_p in descending order where an increase in one of them would rise number of infection in H_p . The remain of the parameters are of significance to H_p ; particularly $\alpha_p, \theta_p, \gamma_p$. These variables have a high impact on H_p , and its effects are described as follows: the variables have the opposite sign to H_p . This is normal because the increase the recovery rate of hospitalized humans, the long period of incubation for an exposed individual until they become infected and the increase in the rate of hospitalization individuals of an infected human, which means we will not have more infection in H_p . So, as we take $\mathcal{R}_{01} < 1$ and $\mathcal{R}_{02} < 1$ then there is no infection so ever until that time. This is practically the case when the diseases doesn't increase and the persist in the human. The Figure (8.9) shows the variation of the parameters such as δ_p, θ_p and α_p by 100, while the variation of the other parameters by lower than that. What happen is the recovery rate, the rate of hospitalization and the rate of detection actually negatively infect H_p .

The parameters sensitivity with respect to H_p

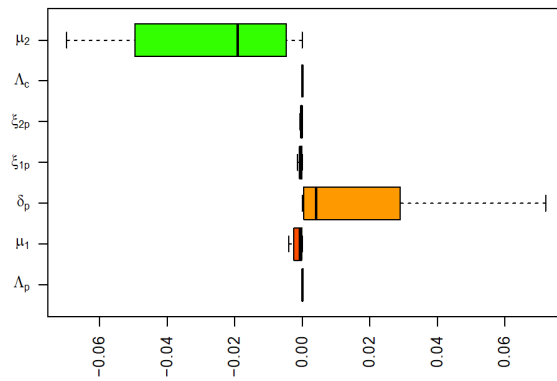
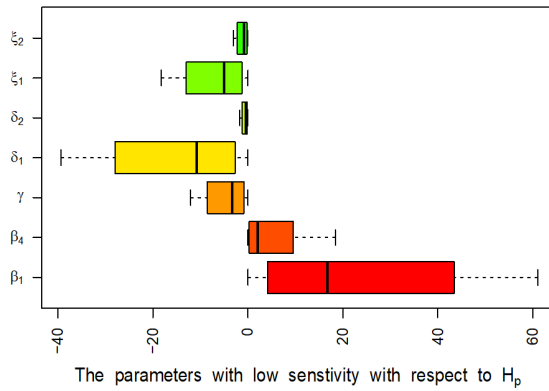
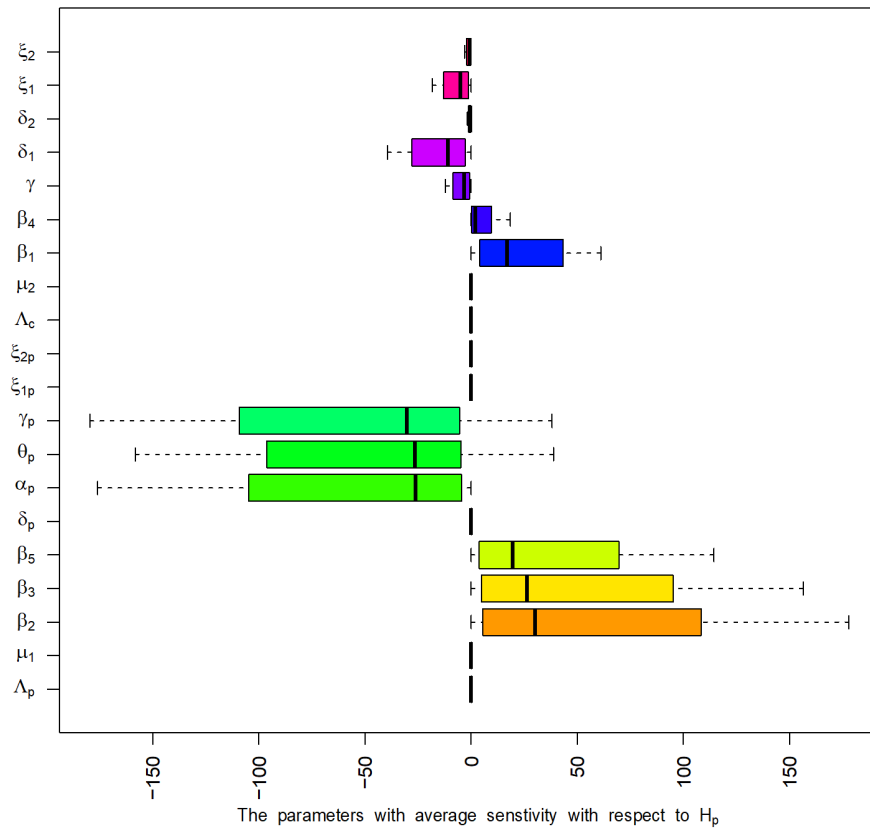


Figure 8.9: Parameters sensitivity to H_p in case 1

2. **Case 2:** $\mathcal{R}_{01} > 1$ and $\mathcal{R}_{02} < 1$

The second case of analysis indicates a high infection in hospitalization population as shown in Figures (8.10). Whereas, most of parameters contribute an effect on H_p but with different measures. The first Figure (8.10) illustrated that the sensitivity of parameters are varies in sign where they may have positive or negative effect on H_p . Parameters $\Lambda_p, \mu_1, \gamma_p, \beta_1, \beta_4, \gamma$ have a low simple sensitive to the H_p . Where the parameter $\xi_p^1, \xi_p^2, \Lambda_c, \mu_2, \delta_1, \delta_2, \xi_1, \xi_2$ are not sensitive at all to H_p . Furthermore, parameters β_2, β_3 have an average positive effect on H_p which are have a slight ability to change the H_p size. This differs for the rest of the parameters where an increase or decrease will effect the infected H_p . The three parameters $\beta_5, \delta, \theta_p$ are positively sensitive to H_p in descending order where an increase in one of them would rise the number of infected population in H_p . The remain of the parameter is significance to H_p ; particularly α_p which has a high negatively effects H_p .

If the persistence of the δ_p increased ,that means we will have more individuals who lose their immunity then more people will getting sick. The remain parameters particularly have the same rate except the Λ_p , offcours is gonna effect everybody else. β_2 and β_3 are medium sensitive in H_p .

The parameters sensitivity with respect to H_p

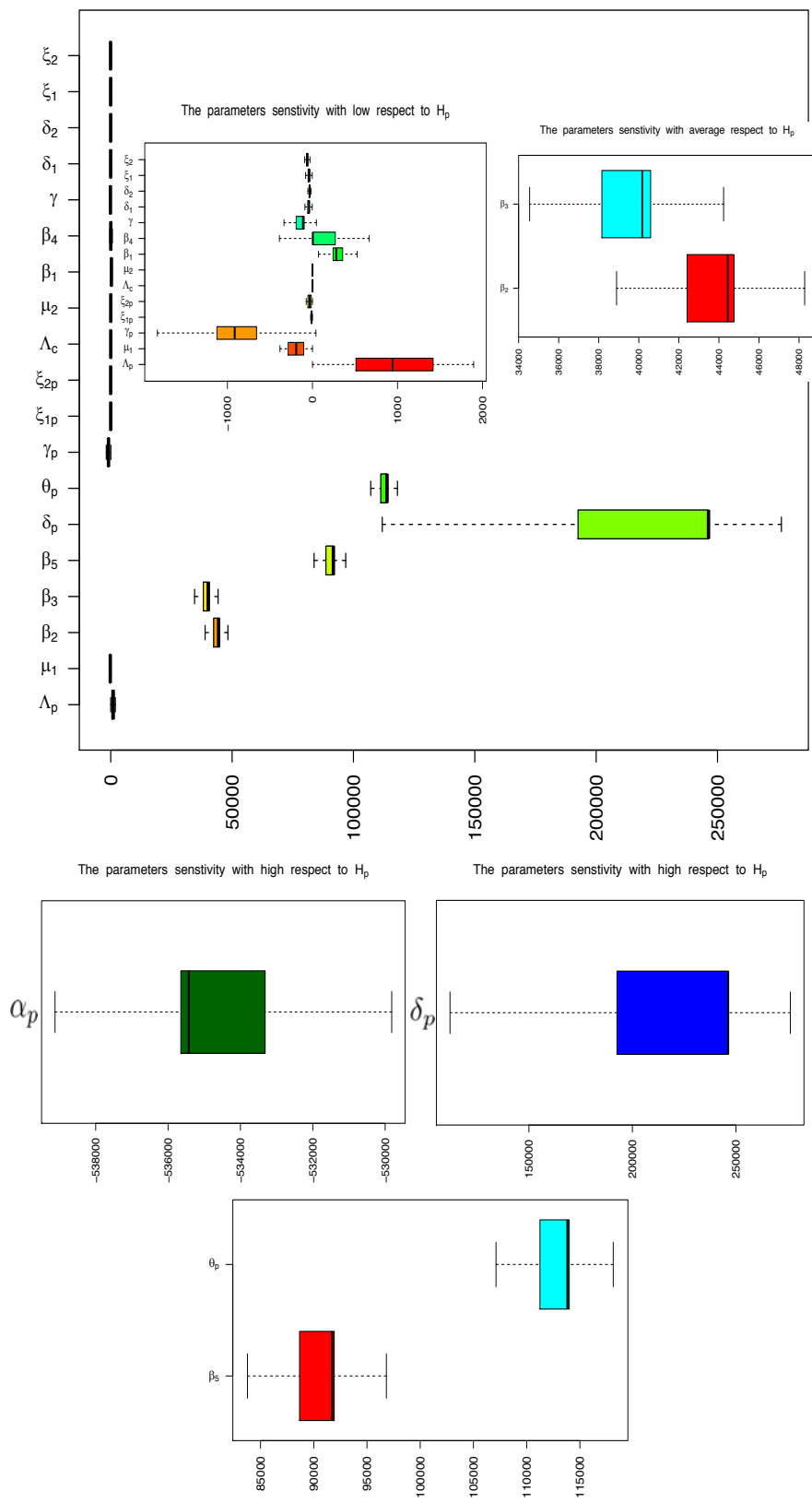


Figure 8.10: Parameters sensitivity to H_p in case 2

3. Case 3: $\mathcal{R}_{01} < 1$ and $\mathcal{R}_{02} > 1$

This case shows that the sensitivity analysis of all parameters has either a positive or negative impact on H_p . In Figure (8.11), I see that variables $\Lambda_p, \mu_1, \xi_p^1, \xi_p^2, \mu_2, \beta_1, \gamma, \delta_2, \xi_2$ have almost low effect on H_p . The variables $\beta_1, \gamma, \delta_p, \xi_2$ have slight effect on H_p , while the remain variables have no effect on H_p . On the other hand, the $\delta_p, \Lambda_c, \beta_4, \delta_1, \xi_1$ have an average effect on H_p . Where the first three variables have a positive sign which means the increase of the parameter will result a increase of H_p . The last two variables have a negative effect on H_p . The remain of the variables are of significance to H_p ; particularly $\alpha_p, \theta_p, \gamma_p$. These variables have a high impact on H_p and its have opposite sign to effects H_p . In this case the remain variable have high significant impact on H_p when $\mathcal{R}_{01} < 1$. The three parameters $\beta_2, \beta_3, \beta_5$ are positively sensitive to H_p in descending order where an increase in one of them would rise the number of infected H_p population. The remain of the parameters are also significant to H_p ; particularly $\alpha_p, \theta_p, \gamma_p$. These variables have a high impact on H_p , and they have a opposite sign to H_p .

The camel parameters in this case show the same effect as case 1, accepted the more transmission between human can be responsible around the infection. This case shows the same situation as when $\mathcal{R}_0 < 1$ accept the variation is highest in this case.

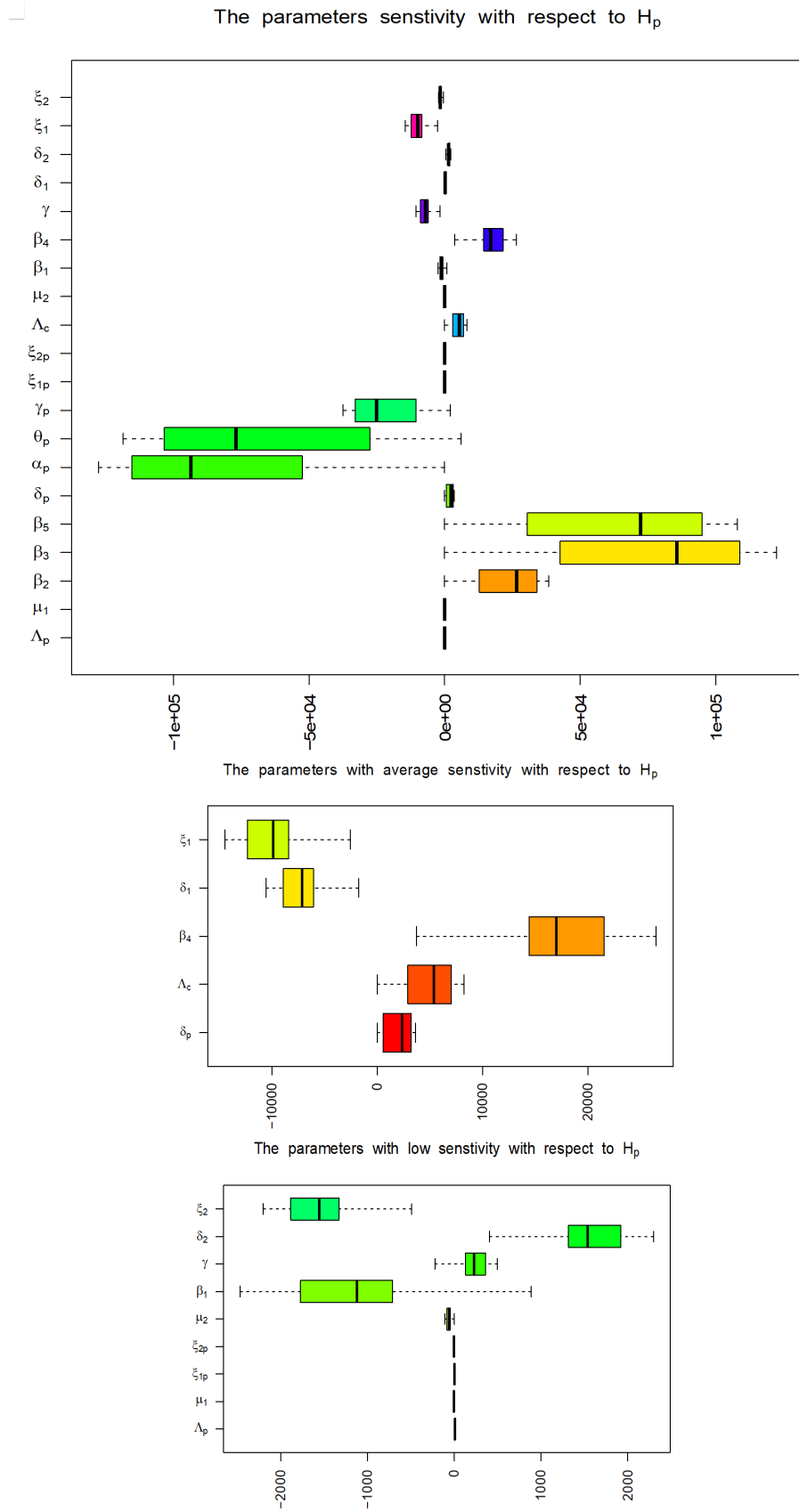
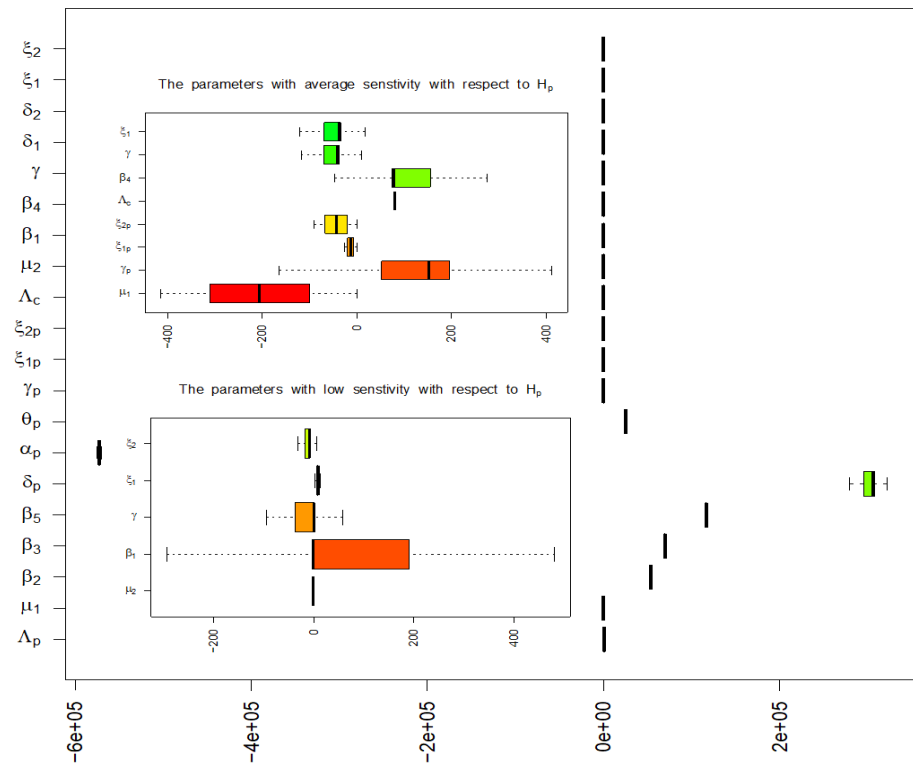


Figure 8.11: Parameters sensitivity to H_p in case 3

4. Case 4 : $\mathcal{R}_{01} > 1$ and $\mathcal{R}_{02} > 1$

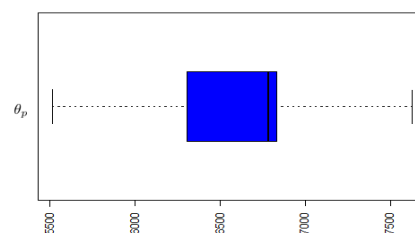
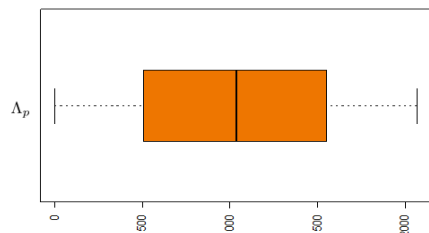
The fourth case of analysis indicates a high infection in hospitalization population as shown in Figures (8.12). The most of parameters are contribute an effect on H_p but with different measures. The first Figure (8.12) illustrated that the sensitivity of parameters are varies in sign where they may have positive or negative effect on H_p . Parameters $\Lambda_p, \mu_1, \gamma_p, \beta_1, \beta_4, \gamma$ have a low simple sensitive to the H_p . Where the parameter $\xi_p^1, \xi_p^2, \Lambda_c, \mu_2, \delta_1, \delta_2, \xi_1, \xi_2$ are not sensitive at all to H_p . Furthermore, parameters β_2, β_3 have an average positive effect on H_p which are have a slight ability to change the H_p size. This differs for the rest of the parameters where an increase or decrease will effect the infected H_p . The three parameters $\beta_5, \delta, \theta_p$ are positively sensitive to H_p in descending order where an increase in one of them would rise the number of infected population in H_p . The remain of the parameter is significance to H_p ; particularly α_p which has a high negatively effects H_p .

The parameters sensitivity with respect to H_p



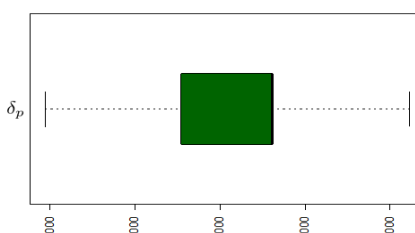
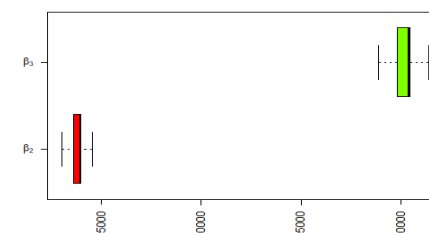
The parameters with high sensitivity with high respect to H_p

The parameters with high sensitivity with high respect to H_p



The parameters with high sensitivity with high respect to H_p

The parameters with high sensitivity with high respect to H_p



The parameters with high sensitivity with high respect to H_p

The parameters with high sensitivity with high respect to H_p

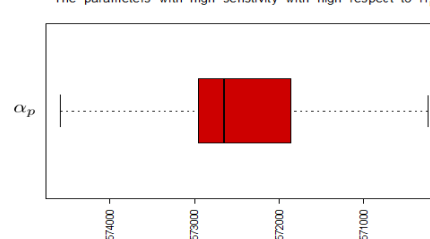
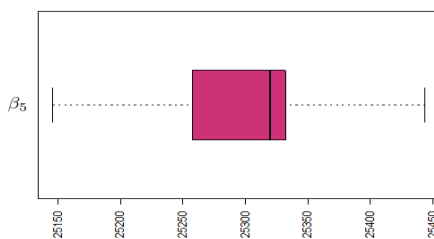


Figure 8.12: Parameters sensitivity to H_p in case 4

8.3.3 For Unaware Infected Camel Population (I_c^1)

The sensitivity analysis of unaware infected camels was performed in the same style as for the infected humans population. Figure (8.13) show a general look for the camel sensitivity of parameters with respect to infectious camel population. The previous figure shows the different effects of parameter on I_c^1 that may be positive or negative.

1. Case 1: $\mathcal{R}_{01} < 1$ and $\mathcal{R}_{02} < 1$

The parameters of the camel populations in this case as you see in Figure (8.13) are slightly effective on I_c^1 . The I_c^1 may increase as a result of increasing β_1 which has a slight positive effect on I_c^1 . Other parameters such as γ , δ_1 , δ_2 , ξ_1 , ξ_2 , have a little effect on I_c^1 which they contribute to reducing I_c^1 whenever they increase since it shows a high negative effect on I_c^1 . The remain parameters Λ_p , μ_1 , β_2 , β_3 , β_5 , δ_p , α_p , θ_p , γ_p , ξ_p^1 , ξ_p^2 , Λ_c , μ_2 , β_4 doesn't show any effect on I_c^1 as shown in Figure (8.13).

This case shows that humans have nothing to do with camels when there is no infection $\mathcal{R}_0 < 1$. In this case, it is clear that there is no infection in camel population where the infection based on the value of β_1 which show slight effect on I_c^1 . ξ_1 and γ have a high role in camels sensitivity, where detecting more infected camels and rising the died in infected camels will decrease the rate of disease spread between camels then between camels to humans.

The important thing that we must highlight that the human does not cause infection to the camel in this disease and that illustrated by Figures (8.13-8.14) of camels sensitivity.

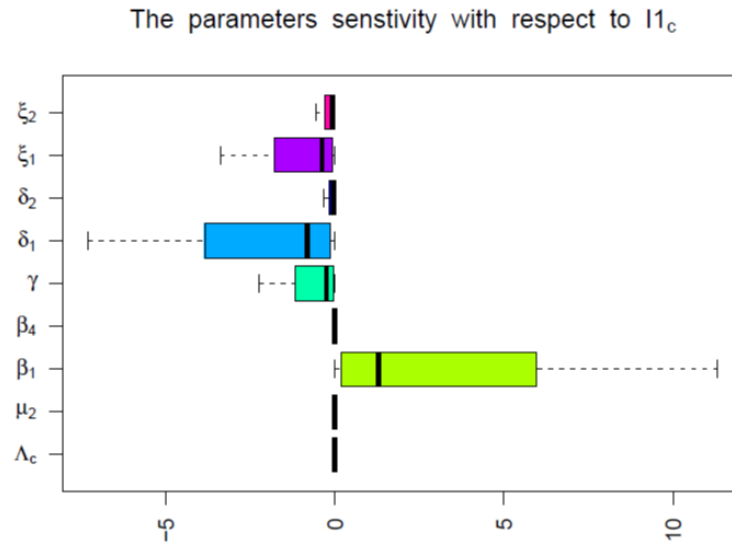


Figure 8.13: Parameters sensitivity to I_c^1 in case 1

2. Case 2: $\mathcal{R}_{01} > 1$ and $\mathcal{R}_{02} < 1$

The parameters of the camel populations in this case as you see in Figure (8.14) are highly effective on I_c^1 . The I_c^1 may increase as a result of increasing β_1 which has a high positive effect on I_c^1 . As for other parameters such as γ, ξ_2 , that contribute to the reduction of the height I_c^1 since it shows a high negative effect on I_c^1 . The parameters $\delta_1, \delta_2, \xi_1$, appears with an medium negative effect on I_c^1 . The remain parameters $\Lambda_p, \mu_1, \beta_2, \beta_3, \beta_5, \delta_p, \alpha_p, \theta_p, \gamma_p, \xi_p^1, \xi_p^2, \Lambda_c, \mu_2, \beta_4$ doesn't show any effect on I_c^1 as shown in Figure (8.14).

In this case the disease persists in the camel population where the value of β_1 increases double the value compared to case 1. Also, ξ_1 and γ have a high role in camels sensitivity. In this case the detecting infected camels has a high rate compared to the deaths of infected camels. These parameters will increase the rate of disease spread between camels then between camels to humans. The parameters of medium effective such as $\delta_1, \delta_2, \xi_1$, which are describe the recovery rate of camel and death rate of infected camel contribute to reduced I_c^1 .

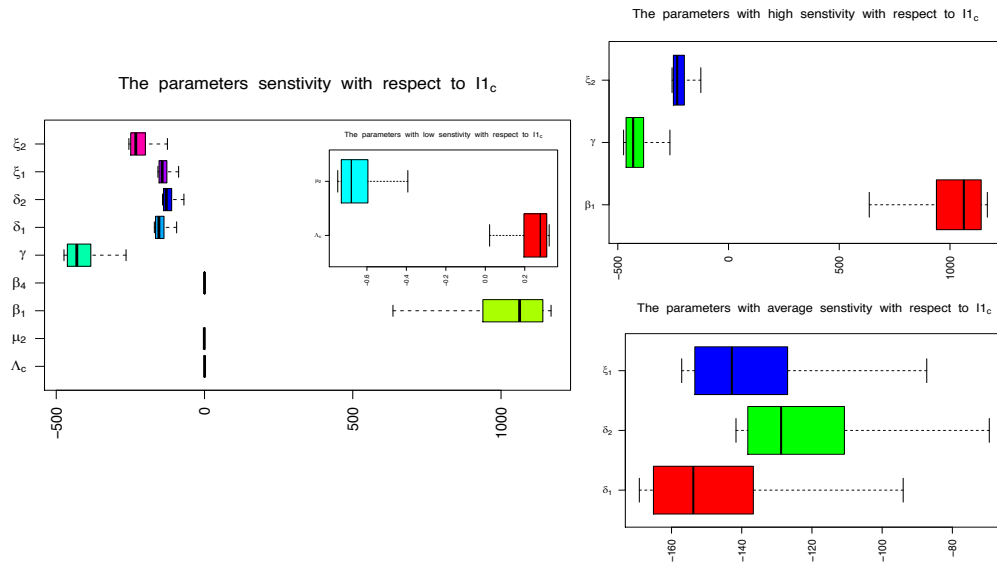


Figure 8.14: Parameters sensitivity to I_c^1 in case 2

3. Case 3: $\mathcal{R}_{01} < 1$ and $\mathcal{R}_{02} > 1$

This case shows how the parameters as γ , ξ_1 and ξ_2 control I_c^1 . The previous parameters shows a high negative effect on I_c^1 which is lead to decrease the number of infected camels. However, the parameters β_1 , δ_1 and δ_2 shows medium effect on I_c^1 while other parameters doesn't effect I_c^1 at all.

In this case, it is clear that there is an infection in camel population where the infection based on the value of β_1 which show slight effect on I_c^1 . ξ_1 and γ have a high role in camels sensitivity, where detecting more infected camels and rising the died in infected camels will decrease the rate of disease spread between camels then between camels to humans.

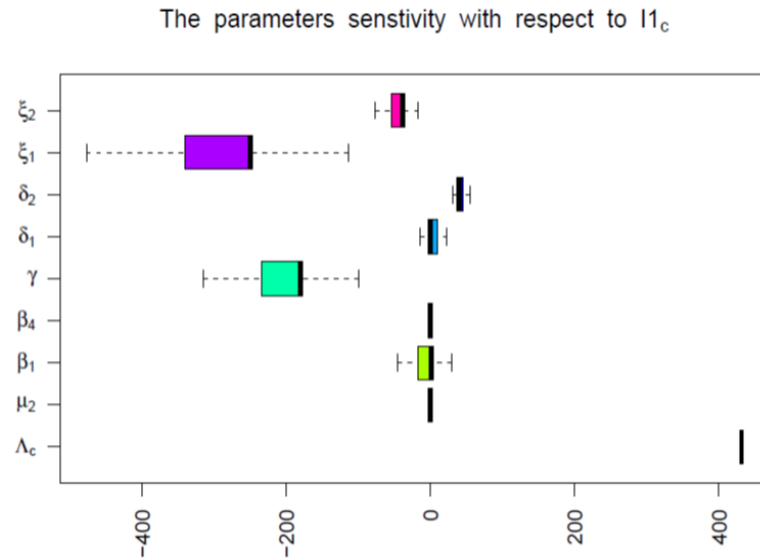


Figure 8.15: Parameters sensitivity to I_c^1 in case 3

4. Case 4: $\mathcal{R}_{01} > 1$ and $\mathcal{R}_{02} > 1$

It is clear that, in this case I_c^1 is greatly effected by the parameters with high positive effect such as Λ_c . Also, the parameters as δ_1 and δ_2 has a slight and average impact on I_c^1 . The other parameters such as β_1 , γ , ξ_1 , ξ_2 , that contribute to the reduction of the height I_c^1 since it shows a high negative effect on I_c^1 . The remain parameters Λ_p , μ_1 , β_2 , β_3 , β_5 , δ_p , α_p , θ_p , γ_p , ξ_p^1 , ξ_p^2 , Λ_c , μ_2 , β_4 dont show any effect on I_c^1 as shown in Figure (8.16).

The case 4 shows the scenario when the disease persists among camel population. It is surprising in this case is that β_1 negatively affect I_c^1 . The detecting rate of sick camel has also a negative effect in I_c^1 .

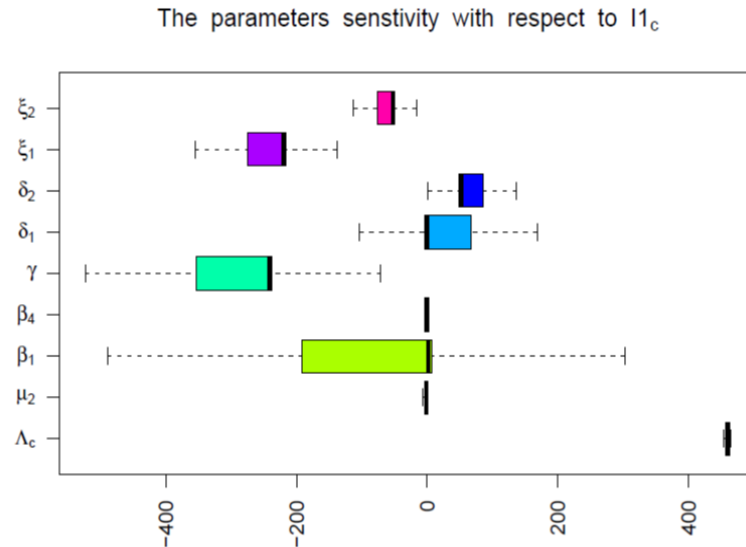


Figure 8.16: Parameters sensitivity to I_c^1 in case 4

8.3.4 For Aware Infected Camel Population (I_c^2)

The sensitivity analysis of aware infected camels was performed in the same style as for the infected humans population. Figure (8.17) show a general look for the camel sensitivity of parameter with respect to infectious camels population. The figure shows the different effects of parameters on I_c^2 that may be positive or negative.

1. Case 1: $\mathcal{R}_{01} < 1$ and $\mathcal{R}_{02} < 1$

It is noticeable that the variable I_c^2 have been impacted with parameters a slight negative impact as result of increase in the value of γ , δ_1 , δ_2 , ξ_1 , ξ_2 would decrease I_c^2 . The parameter β_1 has a slight positive impact on I_c^2 and increasing of this value will increase the rate of I_c^2 on camels population. Parameters Λ_p , μ_1 , β_2 , β_3 , β_5 , δ_p , α_p , θ_p , γ_p , ξ_{1p} , ξ_{2p} , Λ_c , μ_2 , β_4 have no impact on I_c^2 .

The pattern of the sensitivity analysis for Case 1 of unaware infected camels is similar to the pattern of Case 1 for infected aware camels, but the effect of the parameters, in this case, is decidedly smaller.

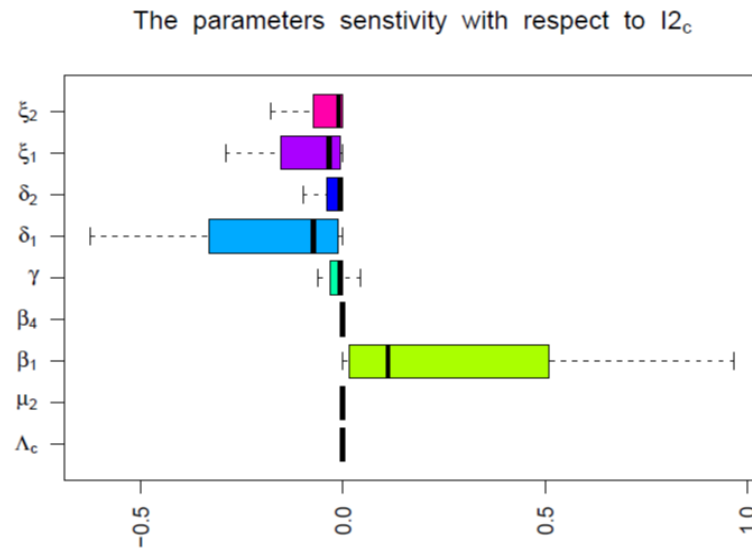


Figure 8.17: Parameters sensitivity to I_c^2 in case 1

2. Case 2: $\mathcal{R}_{01} > 1$ and $\mathcal{R}_{02} < 1$

Figure (8.18) in case 2 shows a general look of the camel sensitivity by parameters with respect to I_c^2 . The first Figure (8.18) shows that the parameters β_1, γ, ξ_1 , has the highest impact on I_c^2 . The parameter β_1 has a positive effect on I_c^2 and usually increasing in the value of this parameters would increase I_c^2 . besides, the parameters γ, ξ_1 has the negative effect on I_c^2 which is contribute to decrease I_c^2 . The remains parameters $\Lambda_p, \mu_1, \beta_2, \beta_3, \beta_5, \delta_p, \alpha_p, \theta_p, \gamma_p, \xi_{1p}, \xi_{2p}, \Lambda_c, \mu_2, \beta_4$ almost have no effect on I_c^2 . This case also shows a similar pattern of sensitivity analysis to case 2 of I_c^1 , but the effect of the parameters in this case was smaller.

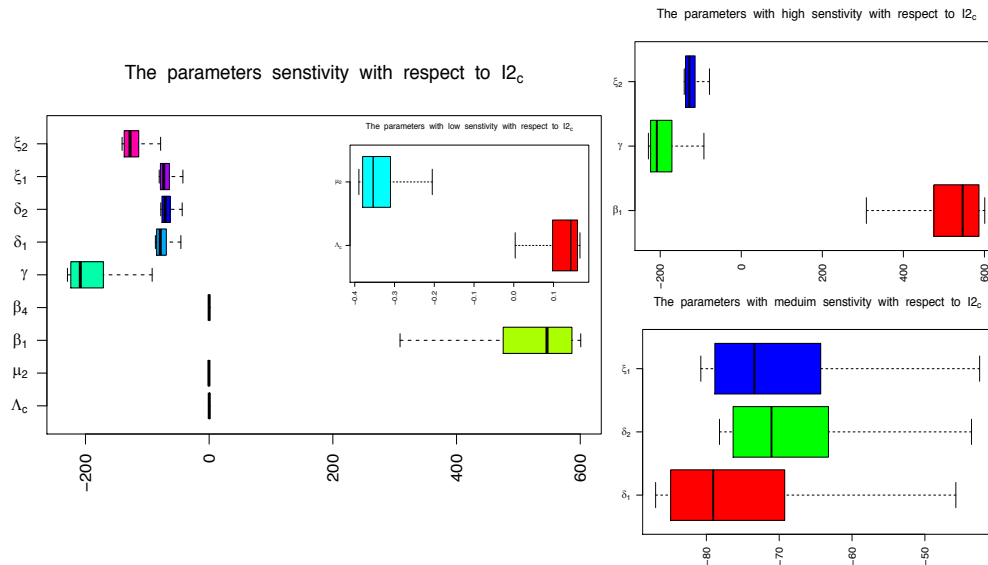


Figure 8.18: Parameters sensitivity to I_c^2 in case 2

3. Case 3: $\mathcal{R}_{01} < 1$ and $\mathcal{R}_{02} > 1$

This case shows a slight effect of parameters on I_c^2 which is shown in Figures (8.19). The highly sensitive of the parameters on I_c^2 result from the impact of $\Lambda_c, \gamma, \xi_1, \xi_2$. The first two parameters Λ_c, γ contribute in the increase of I_c^2 because this parameter has a positive effect. The last two parameters ξ_1, ξ_2 have a negative effect on I_c^2 , whereas increasing this parameter lead to decrease I_c^2 . The remain parameter such as $\Lambda_p, \mu_1, \beta_2, \beta_3, \beta_5, \delta_p, \alpha_p, \theta_p, \gamma_p, \xi_{1p}, \xi_{2p}, \mu_2, \beta_4$ almost have no effect on I_c^2 but the parameter $\beta_1, \delta_1, \delta_2$ are obvious with very slight effect on I_c^2 .

The parameters sensitivity of the I_c^2 in case 3 when \mathcal{R}_0 has the same pattern of case 3 of the unaware infected camels, but the scale of the parameters here are small. The γ shows the positive effect which means increase the rate of detecting a sick camels will increase the rate of infection in camels and this is contrary to what happened in other cases.

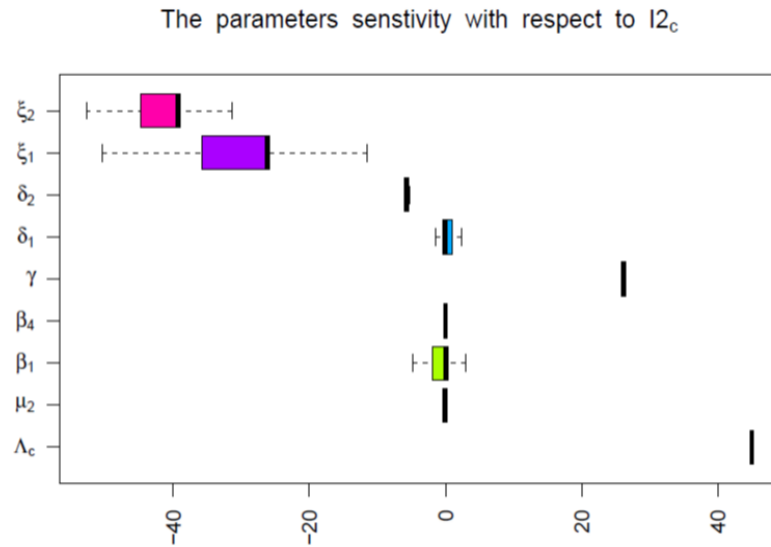


Figure 8.19: Parameters sensitivity to I_c^2 in case 3

4. Case 4: $\mathcal{R}_{01} > 1$ and $\mathcal{R}_{02} > 1$

This case shows a higher effect of parameters on I_c^2 compared to previous case. Figure (8.20) shows the highly camel sensitivity in case 4 resulted from the impact of $\Lambda_c, \beta_1, \gamma, \delta_1, \delta_2, \xi_1, \xi_2$. The first two parameters $\Lambda_c, \gamma, \delta_1$ effect I_c^2 positively which is increase this parameter will also increase I_c^2 . While the parameter $\beta_1, \xi_1, \xi_2, \delta_2$ shows negative effect on I_c^2 . The remain parameter such as $\Lambda_p, \mu_1, \beta_2, \beta_3, \beta_5, \delta_p, \alpha_p, \theta_p, \gamma_p, \xi_{1p}, \xi_{2p}, \mu_2, \beta_4$ almost have no effect on I_c^2 .

This case shows that when detecting more infected camels that means we will have more death cases between camels, this is often because the population of camels does not have the vaccine also the rate of recovery from the disease is usually few.

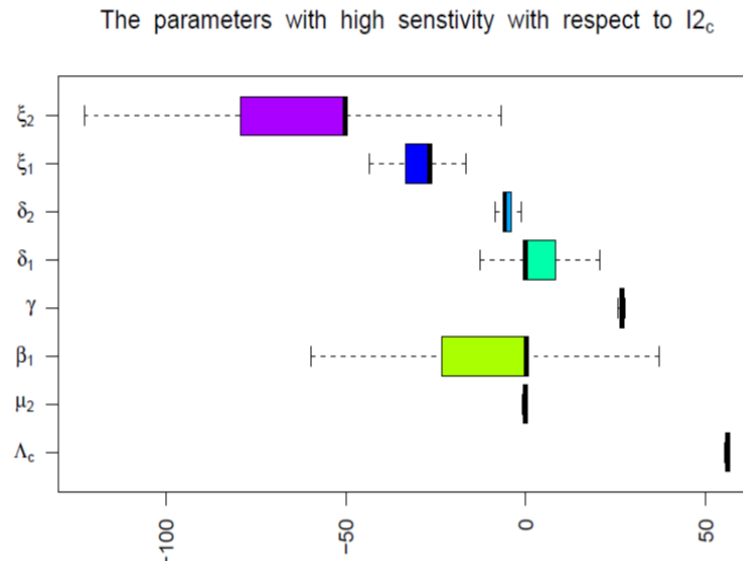


Figure 8.20: Parameters sensitivity to I_c^2 in case 4

8.4 Discussion

The sensitivity analysis of Cases 1 and 3 shows the same pattern when $\mathcal{R}_{01} < 1$ where the parameters such as γ_p , θ_p , α_p affect negatively on I_p . The parameters of human infection rate such as $\beta_2, \beta_3, \beta_5$ show the positive sensitivity to I_p . Case 1 shows the parameters when there is no disease. However, Case 3, shows the parameter when disease persists and the main path of transmission of diseases to human population is via direct infection from camels. The variation of parameters in Case 3 is higher than Case 1, where it increases to more than 30000 times compared to Case 1.

The same thing for the camel population, Case 1 The sensitivity analysis of Cases 1 and 3 shows the same pattern. In Case 2 when the disease persists among camel population the parameters such as γ , ξ_1 increased as result of an increase in the rate of infection among camels population.

As well as, Cases 2 and 4 taking a same approach when they show a similar pattern. The variation of the parameters in Cases 2 and 4 show a slight difference between them approximately. The parameters such as δ_p , θ_p , α_p , β_2 , β_3 , β_5 , all of them effect positively on I_p when $\mathcal{R}_{01} > 1$. However, the only parameter with the negative effect these two Cases are γ_p , which is the rate of hospitalization of an infected human.

Chapter 9: Conclusion

As the MERS-CoV cases are still reported in the Middle East, there are concerns that this disease will eventually become pandemic the region. The fact there is a long list of unanswered questions, about the origin of the virus, the transmission pathways from bat to camels, camels to camels, camel to human and human to human, leave researchers in a big dilemma in understanding the dynamic of the disease and explaining the possible impact of the disease on the public health if an outbreak happen.

The similarity between the MERS-CoV and SARS, as the two viruses are from the same category of Coronaviruses which can be helpful to use the same approaches where it was successful in controlling the SARS, and may be useful control the MERS-CoV. In fact, the zoonotic aspect of the MERS-CoV contribute to the complexity of understanding the dynamic of the disease and hence developing the right controlling strategy of the diseases. Moreover, sociocultural factor that accompanied the progress of the disease had contribute to the difficulties ,that authorities are facing and could facing more, in contain the MERS-CoV.

For example, this complexity is augmented by the fact that there is the event Hajj, every year, that could cause a large transmission among the pilgrims from around the world. In addition, there are cases of super-spreaders, which makes the scenarios of spreading the disease in a big gathering, like Hajj, very concerning.

The UAE had reported cases of MERS-CoV, which makes it among the countries that is concerned by the possible transmission of this disease it is population. Add to that, the Arabic culture, that dominate the life style in country, makes the possible infection from the camels directly . Although the government of the UAE had make an expectational efforts to protect the population from this disease . There is a need of more efforts to understand the depth of the dynamic of this virus and pathways of it transmission.

In this thesis, we aimed to study a mathematical model of the MERS-CoV in the UAE. This model took in consideration not only the human transmission but also the transmission among the camels. To our knowledge, this is the first approach that combined these two populations in one model.

The human population is considered to SEIRS model and camels is modelled by an SIS. The choice of such models can be explained as follows:

The SEIRS reflect the similarity between the SARS and MERS-CoV. In fact, we included in this model the hospitalized people as they are responsible of recent transmission in health care facilities in KSA. Moreover, there are cases of recovery from the infection, which was also carried out in this model. We have also considered the death rate due to the infection as many infected people died because of this infection.

For the camel population, we opted for SIS model because the reports on the camels tolerance of the infection and reoccurrence. The infected population is divided into two aware and unaware because there is a complete ignorance of symptoms of the disease in the camels. Moreover, we assume the human population is infected by the unaware camel population.

Our mathematical analysis showed the possibility of having three transmission scenarios in the human population.

1. No infection : this is the case where the basic reproduction number $\mathcal{R}_0 < 1$
2. Low persistence of infection: this is the case where the infection is high among the camels $\mathcal{R}_{02} > 1$ but the infection among the human is low $\mathcal{R}_{01} < 1$. In this case, the main path of transmission of the disease to the human population is via direct infection from the camel.
3. High persistence of infection: this is the case where the infection is high among human $\mathcal{R}_{01} > 1$. Regardless the level of the infection in the camel population. If the virus can become transmitted from human-to-human then the infection lead to pandemic.

In fact, the time series simulations of these cases shows clearly the existence of these two levels of the infection : The simulation of the low persistence case shows the number of the infected people reach 6000 individual, whoever in the High persistence of infection it reach 175000 individual. This huge increase in the number of the cases (almost 30 times more cases) should give us an idea on the possible burden of the such case on the public health.

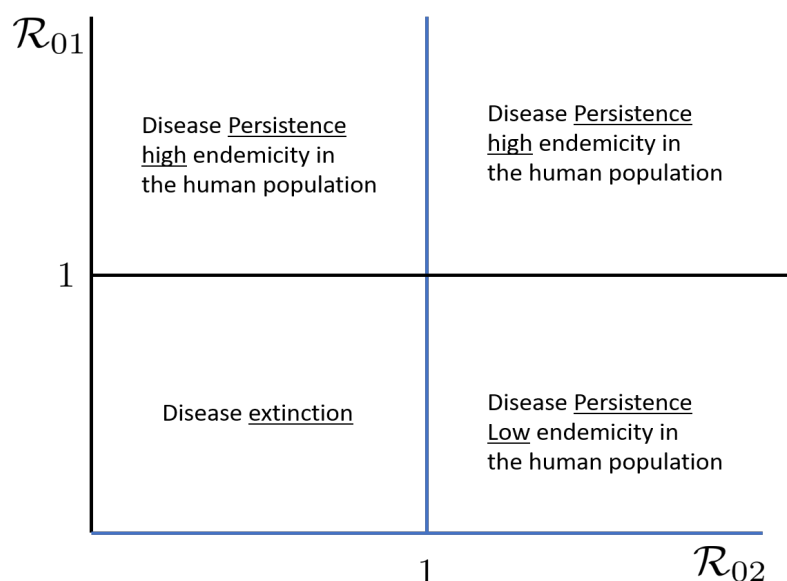


Figure 9.1: Scenarios of MERS transmission among human

The sensitivity analysis of the infected classes with respect to the parameters of the model showed that :

In the case of no infection, the infected population is mildly sensitive negatively to the hospitalization rate γ_p , the recovery rate α_p and the rate of showing symptoms θ_p . Other hand, the infected population is positively sensitive to the three human infection rates: β_2 , β_3 and β_5 .

In the case of the High persistence of infection, the parameters the infected population is highly sensitive to the hospitalization rate, the recovery rate and the rate of showing symptoms. The sensitivity γ_p is negative, However, α_p and θ_p is positive.

In the case of $\mathcal{R}_{01} > 1$, the sensitivity analysis show that there are patterns of

the sensitivity I_p when the persistence of infection case is similar to the no infection but with higher range of the variations of the parameters.

The variable I_c^2 is not sensitive to the human parameters of transmission of the disease. This is very well expected as the the model somehow discopled. We also noticed that when the disease is extinct, the I_c^2 has a very low sensitivity with respect to all parameters of transmission among the camel population.

When the disease persist in the camel population, we see clear patterns of similar sensitivity of I_c^2 with respect to the parameters of transmission among the camels population, with high range of sensitivity when $\mathcal{R}_{01} > 1$ and $\mathcal{R}_{02} > 1$.

The most dominant parameters in this sensitivity are the infection rate among the camel population β_1 and the death rate among the aware and unaware camels: ξ_1 and ξ_2

As this worked showed the possible scenarios of MERS-CoV the UAE, there are perspectives of this work that need to be pursued :

- The global stability analysis of the each endemic equilibria seems to achieved as $\mathcal{R}_{01} > 1$ or $\mathcal{R}_{02} > 1$. This need to be proving analytically.
- The bifurcation analysis should perform to find the parameter that could lead to a switch of stability from low endemicity to high endemicity.
- The investigation of the possible control measures, such as isolation and quarantine, that could reduce the impact of the disease on the public health and among the animal stocks.
- The investigation of the effect of possible vaccination as the international community are initiating efforts to develop it.

References

- [1] A. M. AJLAN, R. A. AHYAD, L. G. JAMJOOM, A. ALHARTHY, AND T. A. MADANI, *Middle east respiratory syndrome coronavirus (mers-cov) infection: chest ct findings*, American Journal of Roentgenology, 203 (2014), pp. 782–787.
- [2] N. AL-ASUOAD, S. ALASWAD, L. RONG, AND M. SHILLOR, *Mathematical model and simulations of mers outbreak: Predictions and implications for control measures*, BIOMATH, 5 (2016), p. 1612141.
- [3] N. AL SHEHHI, F. AZIZ, F. AL HOSANI, B. ADEN, AND I. BLAIR, *Human brucellosis in the emirate of abu dhabi, united arab emirates, 2010-2015*, BMC infectious diseases, 16 (2016), p. 558.
- [4] J. A. AL-TAWFIQ AND Z. A. MEMISH, *Alkhurma hemorrhagic fever virus*, Microbes and infection, 19 (2017), pp. 305–310.
- [5] M. A. ALI, M. M. SHEHATA, M. R. GOMAA, A. KANDEIL, R. EL-SHESHENY, A. S. KAYED, A. N. EL-TAWEEL, M. ATEA, N. HASSAN, O. BAGATO, ET AL., *Systematic, active surveillance for middle east respiratory syndrome coronavirus in camels in egypt*, Emerging microbes & infections, 6 (2017), p. e1.
- [6] A. G. ALZAHIRANI, H. M. AL SHAIBAN, M. A. AL MAZROA, O. AL-HAYANI, A. MACNEIL, P. E. ROLLIN, AND Z. A. MEMISH, *Alkhurma hemorrhagic fever in humans, najran, saudi arabia*, Emerging infectious diseases, 16 (2010), p. 1882.
- [7] A. ASSIRI, J. A. AL-TAWFIQ, A. A. AL-RABEEAH, F. A. AL-RABIAH, S. AL-HAJJAR, A. AL-BARRAK, H. FLEMBAN, W. N. AL-NASSIR, H. H. BALKHY, R. F. AL-HAKEEM, ET AL., *Epidemiological, demographic, and clinical characteristics of 47 cases of middle east respiratory syndrome coronavirus disease from saudi arabia: a descriptive study*, The Lancet infectious diseases, 13 (2013), pp. 752–761.
- [8] H. H. BALKHY AND Z. A. MEMISH, *Rift valley fever: an uninvited zoonosis in the arabian peninsula*, International journal of antimicrobial agents, 21 (2003), pp. 153–157.
- [9] D. A. BENTE, N. L. FORRESTER, D. M. WATTS, A. J. MCAULEY, C. A. WHITEHOUSE, AND M. BRAY, *Crimean-congo hemorrhagic fever: history, epidemiology, pathogenesis, clinical syndrome and genetic diversity*, Antiviral research, 100 (2013), pp. 159–189.
- [10] S. CAUCHEMEZ, P. NOUVELLET, A. CORI, T. JOMBART, T. GARSKE, H. CLAPHAM, S. MOORE, H. L. MILLS, H. SALJE, C. COLLINS, ET AL., *Unraveling the drivers of mers-cov transmission*, Proceedings of the National Academy of Sciences, (2016), p. 201519235.
- [11] F. CHAMCHOD, R. S. CANTRELL, C. COSNER, A. N. HASSAN, J. C. BEIER, AND S. RUAN, *A modeling approach to investigate epizootic outbreaks and enzootic maintenance of rift valley fever virus*, Bulletin of mathematical biology, 76 (2014), pp. 2052–2072.

- [12] J. F. CHAN, S. K. LAU, K. K. TO, V. C. CHENG, P. C. WOO, AND K.-Y. YUEN, *Middle east respiratory syndrome coronavirus: another zoonotic betacoronavirus causing sars-like disease*, *Clinical microbiology reviews*, 28 (2015), pp. 465–522.
- [13] J. CHEN, J. HUANG, J. C. BEIER, R. S. CANTRELL, C. COSNER, D. O. FULLER, G. ZHANG, AND S. RUAN, *Modeling and control of local outbreaks of west nile virus in the united states*, *Discrete & Continuous Dynamical Systems-B*, 21 (2016), pp. 2423–2449.
- [14] G. CHOWELL, S. BLUMBERG, L. SIMONSEN, M. A. MILLER, AND C. VIBOUD, *Synthesizing data and models for the spread of mers-cov, 2013: key role of index cases and hospital transmission*, *Epidemics*, 9 (2014), pp. 40–51.
- [15] *Total mers_cov cases per country 2018*. url = <http://coronamap.com/>. Accessed : 2018 – 09 – 8.
- [16] *United arab emirates population clock*. url = https://countrymeters.info/en/United_Arab_Emirates. Accessed : 2018 – 09 – 8.
- [17] G. CRUZ-PACHECO, L. ESTEVA, AND C. VARGAS, *Seasonality and outbreaks in west nile virus infection*, *Bulletin of mathematical biology*, 71 (2009), pp. 1378–1393.
- [18] D. B. DAHL, *xtable: Export tables to LaTeX or HTML*, 2014. R package version 1.7-4.
- [19] S. C. A. DHABI, *Statistical yearbook of abu Dhabi 2017*, SCAD: Abu Dhabi, UAE, (2011).
- [20] I. FONG, *Emerging animal coronaviruses: First sars and now mers*, in *Emerging Zoonoses*, Springer, 2017, pp. 63–80.
- [21] *Live animals data*. url = <http://www.fao.org/faostat/en/data/QA>. Accessed: 2018-09-8.
- [22] A. FRIEDMAN AND A.-A. YAKUBU, *Anthrax epizootic and migration: persistence or extinction*, *Mathematical biosciences*, 241 (2013), pp. 137–144.
- [23] C. GOSSNER, N. DANIELSON, A. GERVELMEYER, F. BERTHE, B. FAYE, K. KAASIK AASLAV, C. ADLHOCH, H. ZELLER, P. PENTTINEN, AND D. COULOMBIER, *Human-dromedary camel interactions and the risk of acquiring zoonotic middle east respiratory syndrome coronavirus infection*, *Zoonoses and public health*, 63 (2016), pp. 1–9.
- [24] W. M.-C. R. GROUP ET AL., *State of knowledge and data gaps of middle east respiratory syndrome coronavirus (mers-cov) in humans*, *PLoS currents*, 5 (2013).
- [25] X.-N. HAN, S. J. DE VLAS, L.-Q. FANG, D. FENG, W.-C. CAO, AND J. D. F. HABBEMA, *Mathematical modelling of sars and other infectious diseases in china: a review*, *Tropical Medicine & International Health*, 14 (2009), pp. 92–100.
- [26] B. M. HEAD, E. RUBINSTEIN, AND A. F. MEYERS, *Alternative pre-approved and novel therapies for the treatment of anthrax*, *BMC infectious diseases*, 16 (2016), p. 621.

- [27] M. HEMIDA, A. ELMOSLEMANY, F. AL-HIZAB, A. ALNAEEM, F. ALMATHEN, B. FAYE, D. CHU, R. PERERA, AND M. PEIRIS, *Dromedary camels and the transmission of middle east respiratory syndrome coronavirus (mers-cov)*, *Transboundary and emerging diseases*, 64 (2017), pp. 344–353.
- [28] J. M. HUMPHREY, N. B. CLETON, C. B. E. M. REUSKEN, M. J. GLESBY, M. P. G. KOOPMANS, AND L. J. ABU-RADDAD, *Urban chikungunya in the middle east and north africa: A systematic review*, *PLOS Neglected Tropical Diseases*, 11 (2017), pp. 1–19.
- [29] K. E. JONES, N. G. PATEL, M. A. LEVY, A. STOREYGARD, D. BALK, J. L. GITTLEMAN, AND P. DASZAK, *Global trends in emerging infectious diseases*, *Nature*, 451 (2008), pp. 990–993.
- [30] G. KAYALI AND M. PEIRIS, *A more detailed picture of the epidemiology of middle east respiratory syndrome coronavirus*, *The Lancet Infectious Diseases*, 15 (2015), pp. 495–497.
- [31] S. KIM, J. LEE, AND E. JUNG, *Mathematical model of transmission dynamics and optimal control strategies for 2009 a/h1n1 influenza in the republic of korea*, *Journal of theoretical biology*, 412 (2017), pp. 74–85.
- [32] P. KRISHNAPRIYA, M. PITCHAIMANI, AND T. M. WITTEN, *Mathematical analysis of an influenza a epidemic model with discrete delay*, *Journal of Computational and Applied Mathematics*, 324 (2017), pp. 155–172.
- [33] W. LI, Z. SHI, M. YU, W. REN, C. SMITH, J. H. EPSTEIN, H. WANG, G. CRAMERI, Z. HU, H. ZHANG, ET AL., *Bats are natural reservoirs of sars-like coronaviruses*, *Science*, 310 (2005), pp. 676–679.
- [34] Q. LIN, A. P. CHIU, S. ZHAO, AND D. HE, *Modeling the spread of middle east respiratory syndrome coronavirus in saudi arabia*, *Statistical methods in medical research*, 27 (2018), pp. 1968–1978.
- [35] S. LIU, S. RUAN, AND X. ZHANG, *Nonlinear dynamics of avian influenza epidemic models*, *Mathematical biosciences*, 283 (2017), pp. 118–135.
- [36] X. LIU AND P. STECHLINSKI, *Application of control strategies to a seasonal model of chikungunya disease*, *Applied Mathematical Modelling*, 39 (2015), pp. 3194–3220.
- [37] P. O. LOLIKA, S. MUSHAYABASA, C. P. BHUNU, C. MODNAK, AND J. WANG, *Modeling and analyzing the effects of seasonality on brucellosis infection*, *Chaos, Solitons & Fractals*, 104 (2017), pp. 338–349.
- [38] C. R. MACINTYRE, *The discrepant epidemiology of middle east respiratory syndrome coronavirus (mers-cov)*, *Environment Systems and Decisions*, 34 (2014), pp. 383–390.
- [39] I. M. MACKAY AND K. E. ARDEN, *Middle east respiratory syndrome: an emerging coronavirus infection tracked by the crowd*, *Virus research*, 202 (2015), pp. 60–88.

- [40] T. MALIK, P. SALCEANU, A. MUBAYI, A. TRIDANE, AND M. IMRAN, *West nile dynamics: virus transmission between domestic and wild bird populations through vectors*, Can. Appl. Math. Quart, 20 (2012), pp. 535–556.
- [41] T. M. MALIK, A. A. ALSALEH, A. B. GUMEL, AND M. A. SAFI, *Optimal strategies for controlling the mers coronavirus during a mass gathering*, Global Journal of Pure and Applied Mathematics, 11 (2015), pp. 4831–4865.
- [42] Z. A. MEMISH AND A. A. AL-RABEEAH, *Public health management of mass gatherings: the saudi arabian experience with mers-cov*, 2013.
- [43] H. A. MOHD, J. A. AL-TAWFIQ, AND Z. A. MEMISH, *Middle east respiratory syndrome coronavirus (mers-cov) origin and animal reservoir*, Virology journal, 13 (2016), p. 87.
- [44] O. MONDIALE DE LA SANTE, W. H. ORGANIZATION, ET AL., *Weekly epidemiological record, 2017*, Weekly Epidemiological Record= Releve epidemiologique hebdomadaire, 92 (2017), pp. 717–728.
- [45] D. MOULAY, M. AZIZ-ALAOUI, AND M. CADIVEL, *The chikungunya disease: modeling, vector and transmission global dynamics*, Mathematical biosciences, 229 (2011), pp. 50–63.
- [46] S. C. MPESHE, H. HAARIO, AND J. M. TCHUENCHE, *A mathematical model of rift valley fever with human host*, Acta Biotheoretica, 59 (2011), pp. 231–250.
- [47] T. NIU, H. D. GAFF, Y. E. PAPELIS, AND D. M. HARTLEY, *An epidemiological model of rift valley fever with spatial dynamics*, Computational and mathematical methods in medicine, 2012 (2012).
- [48] W. H. ORGANIZATION ET AL., *Who mers-cov global summary and assessment of risk*, 2017.
- [49] M. PAL, *Importance of zoonoses in public health*, Indian Journal of Animal Sciences, 75 (2005), pp. 586–591.
- [50] V. G. PANJETI AND L. A. REAL, *Mathematical models for rabies*, Advances in Imaging and Electron Physics, 79 (2011), pp. 377–395.
- [51] G. PAPPAS, P. PAPADIMITRIOU, N. AKRITIDIS, L. CHRISTOU, AND E. V. TSIANOS, *The new global map of human brucellosis*, The Lancet infectious diseases, 6 (2006), pp. 91–99.
- [52] C. POLETTO, V. COLIZZA, AND P.-Y. BOËLLE, *Quantifying spatiotemporal heterogeneity of mers-cov transmission in the middle east region: a combined modelling approach*, Epidemics, 15 (2016), pp. 1–9.
- [53] K. RANJAN, M. PRASAD, AND G. PRASAD, *Bats: Carriers of zoonotic viral and emerging infectious diseases*, Journal of Experimental Biology, 4 (2016), p. 3S.
- [54] RSTUDIO TEAM, *RStudio: Integrated Development Environment for R*, RStudio, Inc., Boston, MA, 2012.
- [55] S. RUAAN, *Modeling the transmission dynamics and control of rabies in china*, Mathematical biosciences, 286 (2017), pp. 65–93.

- [56] S. RUAN, *Spatiotemporal epidemic models for rabies among animals*, Infectious Disease Modelling, 2 (2017), pp. 277–287.
- [57] D. RUIZ-MORENO, I. S. VARGAS, K. E. OLSON, AND L. C. HARRINGTON, *Modeling dynamic introduction of chikungunya virus in the united states*, PLoS Neglected Tropical Diseases, 6 (2012), p. e1918.
- [58] M. SAYED-AHMED, *Incidence history of west nile virus in africa and middle east, with an emphasis on egypt: A review*, J Dairy Vet Anim Res, 3 (2016), p. 00080.
- [59] C. I. SIETTOS AND L. RUSSO, *Mathematical modeling of infectious disease dynamics*, Virulence, 4 (2013), pp. 295–306.
- [60] K. SOETAERT AND T. PETZOLDT, *Inverse modelling, sensitivity and monte carlo analysis in R using package FME*, Journal of Statistical Software, 33 (2010), pp. 1–28.
- [61] *Demographic formulas*. url = <http://adph.org/healthstats/assets/Formulas.pdf>. Accessed: 2018-09-3.
- [62] H. R. THIEME, *Mathematics in population biology*, Princeton University Press, 2003.
- [63] K. TOHMA, M. SAITO, C. S. DEMETRIA, D. L. MANALO, B. P. QUIAMBAO, T. KAMIGAKI, AND H. OSHITANI, *Molecular and mathematical modeling analyses of inter-island transmission of rabies into a previously rabies-free island in the philippines*, Infection, Genetics and Evolution, 38 (2016), pp. 22–28.
- [64] P. VAN DEN DRIESSCHE AND J. WATMOUGH, *Further notes on the basic reproduction number*, Mathematical Epidemiology, (2008), pp. 159–178.
- [65] M. G. WALSH, A. W. DE SMALEN, AND S. M. MOR, *Wetlands, wild bovidae species richness and sheep density delineate risk of rift valley fever outbreaks in the african continent and arabian peninsula*, PLoS neglected tropical diseases, 11 (2017), p. e0005756.
- [66] L. WANG AND G. CRAMERI, *Emerging zoonotic viral diseases*, Rev sci tech Off int Epiz, 33 (2014).
- [67] U. WERNERY, *Zoonoses in the arabian peninsula*, Saudi medical journal, 35 (2014), p. 1455.
- [68] U. WERNERY, T. KETTLE, M. MOUSSA, H. BABIKER, AND J. WHITING, *West nile fever in the united arab emirates*, Wildlife Middle East, 2 (2007), p. 2.
- [69] M. E. WOOLHOUSE, D. T. HAYDON, AND R. ANTIA, *Emerging pathogens: the epidemiology and evolution of species jumps*, Trends in ecology & evolution, 20 (2005), pp. 238–244.
- [70] Z.-Q. XIA, J. ZHANG, Y.-K. XUE, G.-Q. SUN, AND Z. JIN, *Modeling the transmission of middle east respirator syndrome corona virus in the republic of korea*, PloS one, 10 (2015), p. e0144778.
- [71] L. YAKOB AND A. C. CLEMENTS, *A mathematical model of chikungunya dynamics and control: the major epidemic on réunion island*, PloS one, 8 (2013), p. e57448.

- [72] C. YANG, P. O. LOLIKA, S. MUSHAYABASA, AND J. WANG, *Modeling the spatiotemporal variations in brucellosis transmission*, *Nonlinear Analysis: Real World Applications*, 38 (2017), pp. 49–67.
- [73] A. ZUMLA, D. S. HUI, AND S. PERLMAN, *Middle east respiratory syndrome*, *The Lancet*, 386 (2015), pp. 995–1007.

Appendix

In this Appendix, we will introduce some calculation:

Finding Condition of Φ

Proof. we need to prove that $\Phi < 0$ by contradiction try and assume that the statement is false, proceed from there and at some point you will arrive to a contradiction.

when

$$\kappa = \frac{\gamma}{\xi_2 + \mu_2 + \delta_2}, \Psi = \frac{1}{\mu_2} \left[\frac{\delta_2 \gamma}{\xi_2 + \mu_2 + \delta_2} - (\xi_1 + \gamma + \mu_2) \right] < 0,$$

since κ and Ψ are negative.

$$\text{Then } \Psi = \frac{\delta_2}{\mu_2} \kappa - \frac{(\xi_1 + \gamma + \mu_2)}{\mu_2}$$

$$\Phi = \Psi + \kappa + 1, = \frac{\delta_2}{\mu_2} \kappa + \kappa + 1 - \frac{(\xi_1 + \gamma + \mu_2)}{\mu_2}.$$

$$\text{Since } \frac{(\xi_1 + \gamma + \mu_2)}{\mu_2} > 1 \text{ then } 1 - \frac{(\xi_1 + \gamma + \mu_2)}{\mu_2} < 0.$$

Let's assume that assume $\Phi > 0$ then

$$\left(\frac{\delta_2}{\mu_2} + 1 \right) \kappa > \frac{(\xi_1 + \gamma + \mu_2)}{\mu_2} - 1$$

hence

$$(\delta_2 + \mu_2) \kappa > \xi_1 + \gamma$$

which

$$\kappa > \frac{\xi_1 + \gamma}{\delta_2 + \mu_2}$$

Using the the fact that $\frac{\gamma}{\xi_2 + \mu_2 + \delta_2}$, we have

$$\frac{\gamma}{\xi_2 + \mu_2 + \delta_2} > \frac{\xi_1 + \gamma}{\delta_2 + \mu_2}$$

, we deduce that

$$\gamma(\delta_2 + \mu_2) > (\xi_1 + \gamma)(\xi_2 + \mu_2 + \delta_2)$$

$0 > \xi_1(\xi_2 + \mu_2 + \delta_2) + \gamma\xi_2$, which is impossible, then by contradiction $\Phi < 0$

□

Find Condition for $I_c^1 > 0$

We have that

$$\kappa = \frac{\gamma}{\xi_2 + \mu_2 + \delta_2}.$$

Then

$$\Psi = \frac{1}{\mu_2} \left[\frac{\delta_2 \gamma}{\xi_2 + \mu_2 + \delta_2} - (\xi_1 + \gamma + \mu_2) \right]$$

$$\Psi = \frac{1}{\mu_2} [\delta_2 \kappa - (\xi_1 + \gamma + \mu_2)]$$

and

$$\Phi = \frac{\delta_2}{\mu_2} \kappa + \kappa - \frac{(\xi_1 + \gamma + \mu_2)}{\mu_2} + 1$$

$$\Phi = \kappa \left(\frac{\delta_2}{\mu_2} + 1 \right) + 1 - \frac{(\xi_1 + \gamma + \mu_2)}{\mu_2}.$$

Hence

$$\begin{aligned}\mathcal{R}_{02} &= \frac{\beta_1}{(\xi_1 + \gamma + \mu_2 + \delta_1)} \left(1 + \frac{\gamma}{\xi_2 + \mu_2 + \delta_2}\right) \\ \mathcal{R}_{02} &= \frac{\beta_1}{(\xi_1 + \gamma + \mu_2 + \delta_1)} (1 + \kappa)\end{aligned}$$

$$I_c^1 = \frac{\frac{\Lambda_c}{\mu_2} (\mathcal{R}_{02} - 1)}{\Phi - \Psi \mathcal{R}_{02}}.$$

Next, we simplify $\Phi - \Psi \mathcal{R}_{02}$

$$\Phi - \Psi \mathcal{R}_{02} = \kappa \left(\frac{\delta_2}{\mu_2} + 1 \right) + 1 - \frac{\xi_1 + \gamma + \mu_2}{\mu_2} - \frac{\beta_1}{\xi_1 + \gamma + \mu_2 + \delta_1} (1 + \kappa) \left[\frac{1}{\mu_2} [\delta_2 \kappa - (\xi_1 + \gamma + \mu_2)] \right]$$

$$\kappa \left(\frac{\delta_2}{\mu_2} + 1 \right) + 1 - \frac{\xi_1 + \gamma + \mu_2}{\mu_2} - \frac{\beta_1 (1 + \kappa)}{\xi_1 + \gamma + \mu_2 + \delta_1} \left[\frac{\delta_2}{\mu_2} \kappa - \frac{(\xi_1 + \gamma + \mu_2)}{\mu_2} \right]$$

$$\frac{\kappa \delta_2}{\mu_2} \left[1 - \frac{\beta_1 (1 + \kappa)}{\xi_1 + \gamma + \mu_2 + \delta_1} \right] + \kappa + 1 - \frac{(\xi_1 + \gamma + \mu_2)}{\mu_2} \left[1 - \frac{\beta_1 (1 + \kappa)}{\xi_1 + \gamma + \mu_2 + \delta_1} \right]$$

$$\frac{\kappa \delta_2}{\mu_2} [1 - \mathcal{R}_{02}] + \kappa + 1 - \frac{(\xi_1 + \gamma + \mu_2)}{\mu_2} [1 - \mathcal{R}_{02}]$$

$$\frac{\kappa \delta_2}{\mu_2} \left[1 - \frac{(\xi_1 + \gamma + \mu_2)}{\mu_2} \right] [1 - \mathcal{R}_{02}] + \kappa + 1$$

$$\Psi [1 - \mathcal{R}_{02}] + \kappa + 1$$

we need to show that $I_c^2 > 0$, when $I_c^2 = \frac{\frac{\Lambda_c}{\mu_2} [\mathcal{R}_{02} - 1]}{\Psi [1 - \mathcal{R}_{02}] + \kappa + 1}$. The numerator and denominator of I_c^2 should have a similar sign to be > 0 . It is clear that $\frac{\Lambda_c}{\mu_2} [\mathcal{R}_{02} - 1] > 0$ that because $\mathcal{R}_{02} > 1$. Now we should prove that $\Psi [1 - \mathcal{R}_{02}] + \kappa + 1 > 0$.

$I_2^1 > 0$ if and only if

$$\mathcal{R}_{02} > 1 \text{ and } \Psi [1 - \mathcal{R}_{02}] + \kappa + 1 > 0$$

$$\kappa + 1 > \Psi [\mathcal{R}_{02} - 1] \frac{\kappa + 1}{\Psi} > [\mathcal{R}_{02} - 1] \quad 1 < \mathcal{R}_{02} < \frac{\kappa + 1}{\Psi} + 1$$

$\mathcal{R}_{02} < 1$ and $\Psi [1 - \mathcal{R}_{02}] + \kappa + 1 < 0$ which is impossible.

Simplify κ_2 and Finding their Condition

When

$$\kappa_2 = \kappa_1 + \left(\frac{\mu_1 + \gamma_p + \xi_p^1}{\theta_p} \right) + 1 + \left(\frac{\gamma_p}{\alpha_p + \mu_1 + \xi_p^2} \right) + \left(\frac{\alpha_p}{\delta_p + \mu_1} \right) \left(\frac{\gamma_p}{\alpha_p + \mu_1 + \xi_p^2} \right) \quad (1)$$

By simplify κ_2 , Then we have:

$$\begin{aligned}
\kappa_2 &= \frac{\gamma_p}{(\alpha_p + \mu_1 + \xi_p^1)} \left[1 + \frac{\alpha_p}{\delta_p + \mu_1} \left(\frac{\delta_p}{\mu_1} + 1 \right) \right] + \frac{(\mu_1 + \gamma_p + \xi_p^1)}{\theta_p} \left[1 - \frac{\mu_1 + \theta_p}{\mu_1} \right] + 1 \\
&= \frac{\gamma_p}{(\alpha_p + \mu_1 + \xi_p^1)} \left[1 + \frac{\alpha_p}{\mu_1} \right] - \frac{(\mu_1 + \gamma_p + \xi_p^1)}{\mu_1} + 1 \\
&= \frac{\gamma_p(\alpha_p + \mu_1)}{\mu_1(\alpha_p + \mu_1 + \xi_p^1)} - \frac{(\mu_1 + \gamma_p + \xi_p^1)}{\mu_1} + 1 \\
&= \frac{1}{\mu_1} \left[\frac{\gamma_p(\alpha_p + \mu_1)}{\alpha_p + \mu_1 + \xi_p^1} - \mu_1 - (\gamma_p + \xi_p^1) + \mu_1 \right] \\
&= \frac{1}{\mu_1} \left[\frac{\gamma_p(\alpha_p + \mu_1)}{\alpha_p + \mu_1 + \xi_p^1} - (\gamma_p + \xi_p^1) \right]
\end{aligned}$$

The conditions of positivity and negativity of κ_2 :

$$\text{since } \kappa_2 = \frac{1}{\mu_1} \left[\frac{\gamma_p(\alpha_p + \mu_1)}{\alpha_p + \mu_1 + \xi_p^1} - (\gamma_p + \xi_p^1) \right]$$

$$\text{Then } \gamma_p(\alpha_p + \mu_1) > (\gamma_p + \xi_p^1)(\alpha_p + \mu_1 + \xi_p^1)$$

and $0 > \xi_p^1(\alpha_p + \mu_1 + \xi_p^1) + \gamma_p \xi_p^1$, which is Not Possible.

hence $\kappa_2 < 0$

Finding $\kappa_3, \kappa_4, \kappa_5$, and their Condition

$$\kappa_3 = \left(\frac{\alpha_p}{\delta_p + \mu_1} \right) \left(\frac{\gamma_p}{\alpha_p + \mu_1 + \xi_p^2} \right)$$

$$\kappa_4 = \left(\frac{\gamma_p}{\alpha_p + \mu_1 + \xi_p^2} \right)$$

$$\kappa_5 = \left(\frac{\mu_1 + \gamma_p + \xi_p^1}{\theta_p} \right)$$

its easy to see that, $\kappa_i, i = 3, 4, 5 > 0$

$$\begin{aligned}
P(\lambda) = & -\lambda^3 - [\beta_3 + (\mu_1 + \gamma_p + \xi_p^1) + (\alpha_p + \mu_1 + \xi_p^2) + (\mu_1 + \theta_p)]\lambda^2 \\
& + [(\mu_1 + \gamma_p + \xi_p^1)[\beta_3 - (\mu_1 + \theta_p) - (\alpha_p + \mu_1 + \xi_p^2)](\alpha_p + \mu_1 + \xi_p^2)[\beta_3 - (\mu_1 + \theta_p)] + \beta_2\theta_p]\lambda \\
& + (\alpha_p + \mu_1 + \xi_p^2)(\mu_1 + \gamma_p + \xi_p^1)[\beta_3 - (\mu_1 + \theta_p)] + \theta_p[\beta_2(\alpha_p + \mu_1 + \xi_p^2) + \beta_5\gamma_p]
\end{aligned} \tag{2}$$

so, we multiply $P(\lambda)$ by (-1) then I get

$$\begin{aligned}
P(\lambda) = & \lambda^3 + [\beta_3 + (\mu_1 + \gamma_p + \xi_p^1) + (\alpha_p + \mu_1 + \xi_p^2) + (\mu_1 + \theta_p)]\lambda^2 \\
& - [(\mu_1 + \gamma_p + \xi_p^1)[\beta_3 - (\mu_1 + \theta_p) - (\alpha_p + \mu_1 + \xi_p^2)](\alpha_p + \mu_1 + \xi_p^2)[\beta_3 - (\mu_1 + \theta_p)] + \beta_2\theta_p]\lambda \\
& - [(\alpha_p + \mu_1 + \xi_p^2)(\mu_1 + \gamma_p + \xi_p^1)[\beta_3 - (\mu_1 + \theta_p)] + \theta_p[\beta_2(\alpha_p + \mu_1 + \xi_p^2) + \beta_5\gamma_p]]
\end{aligned} \tag{3}$$

$$P(\lambda) = \lambda^3 + a_1\lambda^2 + a_2\lambda + a_3$$

$$J = \begin{bmatrix}
-\mu_1 - (\beta_2 I_p^1 + \beta_3 E_p + \beta_4 I_c^1 + \beta_5 H_p)(s_p) & -S_p \beta_3(e_p) & -S_p \beta_2(i_p) & -S_p \beta_5(h_p) & \delta_p & 0 & -S_p \beta_4(i_c^1) & 0 \\
(\beta_2 I_p^1 + \beta_3 E_p + \beta_4 I_c^1 + \beta_5 H_p)(s_p) & S_p \beta_3(e_p) - (\mu_1 + \theta_p) & S_p \beta_2(i_p) & S_p \beta_5(h_p) & 0 & 0 & S_p \beta_4(i_c^1) & 0 \\
0 & \theta_p & -(\mu_1 + \gamma_p + \xi_p^1) & 0 & 0 & 0 & 0 & 0 \\
0 & 0 & \gamma_p & -(\alpha_p + \mu_1 + \xi_p^2) & 0 & 0 & 0 & 0 \\
0 & 0 & 0 & \alpha_p & -(\delta_p + \mu_1) & 0 & 0 & 0 \\
0 & 0 & 0 & 0 & 0 & -\mu_2 - \beta_1(s_c) & -S_c \beta_1(i_c^1) + \delta_1 & -S_c \beta_1(i_c^2) + \delta_2 \\
0 & 0 & 0 & 0 & 0 & \beta_1(I_c^1 + I_c^2)(s_c) & S_c \beta_1(i_c^1) - (\xi_1 + \gamma + \mu_2 + \delta_1) & S_c \beta_1(i_c^2) \\
0 & 0 & 0 & 0 & 0 & 0 & \gamma & -(\xi_2 + \mu_2 + \delta_2)
\end{bmatrix}$$

by using block matrix, we have

$$J = \begin{bmatrix} A & B \\ C & D \end{bmatrix}$$

where

$$A = \begin{bmatrix} a & b & c & d \\ e & f & g & h \\ 0 & 0 & i & 0 \\ 0 & 0 & j & k \end{bmatrix}, B = \begin{bmatrix} l & 0 & m & 0 \\ 0 & 0 & n & 0 \\ 0 & 0 & 0 & 0 \\ 0 & 0 & 0 & 0 \end{bmatrix}, C = \begin{bmatrix} 0 & 0 & 0 & y \\ 0 & 0 & 0 & 0 \\ 0 & 0 & 0 & 0 \\ 0 & 0 & 0 & 0 \end{bmatrix} \text{ and } D = \begin{bmatrix} p & 0 & 0 & 0 \\ 0 & q & s & v \\ 0 & r & t & w \\ 0 & 0 & u & x \end{bmatrix}$$

The eigenvalues are the solution of the equation

$$\det \begin{vmatrix} A - \lambda I & B \\ C & D - \lambda I \end{vmatrix} = 0 \quad (4)$$

note that

$$\begin{aligned} \det \begin{vmatrix} A - \lambda I & B \\ C & D - \lambda I \end{vmatrix} &= \det(A - \lambda I) \det(D - \lambda I - C(A - \lambda I)^{-1}B) \\ &= \det(A - \lambda I - B(D - \lambda I)^{-1}C) \det(D - \lambda I). \end{aligned}$$

$$(D - \lambda I)^{-1} \times C = \begin{bmatrix} 0 & 0 & 0 & \frac{y}{p-\lambda} \\ 0 & 0 & 0 & 0 \\ 0 & 0 & 0 & 0 \\ 0 & 0 & 0 & 0 \end{bmatrix},$$

$$B \times (D - \lambda I)^{-1} \times C = \begin{bmatrix} 0 & 0 & 0 & \frac{ly}{p-\lambda} \\ 0 & 0 & 0 & 0 \\ 0 & 0 & 0 & 0 \\ 0 & 0 & 0 & 0 \end{bmatrix},$$

$$(A - \lambda I) - B \times (D - \lambda I)^{-1} \times C = \begin{bmatrix} a - \lambda & b & c & \frac{d(p-\lambda) - ly}{p-\lambda} \\ e & f - \lambda & g & h \\ 0 & 0 & ip - \lambda & 0 \\ 0 & 0 & j & kp - \lambda \end{bmatrix}$$

$$\det \begin{vmatrix} A - \lambda I & B \\ C & D - \lambda I \end{vmatrix} = \det(A - \lambda I - B(D - \lambda I)^{-1}C) \det(D - \lambda I).$$

$$\det(A - \lambda I - B(D - \lambda I)^{-1}C) = \begin{vmatrix} a - \lambda & b & c & \frac{d(p-\lambda) - ly}{p-\lambda} \\ e & f - \lambda & g & h \\ 0 & 0 & i - \lambda & 0 \\ 0 & 0 & j & k - \lambda \end{vmatrix} \quad (5)$$

$$= -(\lambda - i)(\lambda - k)((a - \lambda)(\lambda - f) + eb)$$

which is equal

$$= [\lambda^4 + \tilde{a}\lambda^3 + \tilde{b}\lambda^2 + \tilde{c}\lambda + \tilde{d}]$$

let

$$\tilde{a} = (-a - f - k - i),$$

$$\tilde{b} = (af - eb + ak + kf + ai + if + ik),$$

$$\tilde{c} = (-akf + ekb - aif + eib - aik - ikf),$$

$$\tilde{d} = -eikb + aikf.$$

$$\det(D - \lambda I) = \begin{vmatrix} p - \lambda & 0 & 0 & 0 \\ 0 & q - \lambda & s & v \\ 0 & r & t - \lambda & w \\ 0 & 0 & u & x - \lambda \end{vmatrix} \quad (6)$$

$$= (p - \lambda)(u(w(\lambda - q) + vr) - (sr - (\lambda - q)(\lambda - t))(x - \lambda))$$

which is equal

$$= [\lambda^4 + \bar{a}\lambda^3 + \bar{b}\lambda^2 + \bar{c}\lambda + \bar{d}]$$

let

$$\bar{a} = (-p - x - t - q),$$

$$\bar{b} = (-uw + px + pt + pq - sr + tx + qx + qt),$$

$$\bar{c} = (puw + uwq - uvr + psr - ptx - pqx - pqt + srx - qtx),$$

$$\bar{d} = puvr - puwq - psrx + pqt x.$$

Proof.

$$\begin{aligned}
1 &> \left(\frac{\gamma + \xi_2 + \mu_2 + \delta_2}{\xi_2 + \mu_2 + \delta_2}\right) \mathcal{R}_{02} \\
\frac{\xi_2 + \mu_2 + \delta_2}{\gamma + \xi_2 + \mu_2 + \delta_2} &> \xi_2 + \mu_2 + \delta_2 \\
\frac{\xi_2 + \mu_2 + \delta_2}{\gamma + \xi_2 + \mu_2 + \delta_2} &\sim 1 + \frac{\xi_2 + \mu_2 + \delta_2}{\xi_1 + \gamma + \mu_2 + \delta_1} \\
\frac{1}{\gamma + \xi_2 + \mu_2 + \delta_2} &\sim \xi_2 + \mu_2 + \delta_2 + \frac{1}{\xi_1 + \gamma + \mu_2 + \delta_1}
\end{aligned} \tag{7}$$

suppose $x = (\xi_2 + \mu_2 + \delta_2)$ and $c = (\xi_1 + \mu_2 + \delta_1)$

$$\text{then } \frac{1}{\gamma+x} \sim x + \frac{1}{c+\gamma}$$

$$f(x) = x - \frac{1}{\gamma+x} + \frac{1}{c+\gamma} > 0$$

$$f'(x) = 1 + \frac{1}{(\gamma+x)^2} > 0$$

$$x - \frac{1}{\gamma+x} + \frac{1}{c+\gamma} = 0$$

$$x + \frac{1}{c+\gamma} = \frac{1}{\gamma+x}$$

$$x(\gamma+x) + \frac{\gamma+x}{c+\gamma} - 1 = 0$$

$$x^2 + \left(\gamma + \frac{1}{c+\gamma}\right)x + \frac{\gamma}{c+\gamma} - 1 = 0$$

$$\Delta = \left(\gamma - \frac{1}{c+\gamma}\right)^2 - 4\left(\frac{\gamma}{c+\gamma}\right)$$

$$= \left(\gamma - \frac{1}{c+\gamma}\right)^2 > 0$$

$$\Delta = \left(\gamma - \frac{1}{c+\gamma}\right)^2 - 4\left(\frac{\gamma}{c+\gamma}\right)$$

$$x = \frac{-(\gamma + \frac{1}{c+\gamma}) \pm (\gamma - \frac{1}{c+\gamma})^2}{2} \tag{10}$$

$$x = \frac{-(\gamma + \frac{1}{c+\gamma})^2 + (\gamma - \frac{1}{c+\gamma})}{2}$$

$$\text{If } x > \frac{-(\gamma + \frac{1}{c+\gamma}) + \sqrt{(\gamma - \frac{1}{c+\gamma})}}{2}$$

Then $f(x) > 0$

$$2(\xi_2 = \mu_2 + \delta_2) > -(\gamma + \frac{1}{\xi_1 + \mu_2 + \delta_1}) + \gamma - \frac{1}{c+\gamma} \text{ it is true } \gamma > \frac{1}{c+\gamma} \quad (11)$$

$$\frac{\xi_2 + \mu_2 + \delta_2}{\gamma + \xi_2 + \mu_2 + \delta_2} < 1 + \frac{\xi_2 + \mu_2 + \delta_2}{\xi_1 + \gamma + \mu_2 + \delta_2}$$

If Not

$$2(\xi_2 + \mu_2 + \delta_2 + \gamma) > -\frac{1}{\xi_1 + \mu_2 + \delta_1} + \frac{1}{\xi_1 + \mu_2 + \delta_1} \quad (12)$$

$$2(\xi_2 + \mu_2 + \delta_2 + \gamma) > 0$$

□

The Coefficients of the Characteristic Equation Corresponding to Diseases Transmission among Human Matrix

The characteristic equation corresponding to diseases transmission among human matrix J_1 is

$$P(\lambda) = \lambda^3 + a_1\lambda^2 + a_2\lambda + a_3$$

where the coefficients are

$$F_1 = \mu_1 + \theta_p,$$

$$F_2 = \mu_1 + \gamma_p + \xi_p^1,$$

$$F_3 = \alpha_p + \mu_1 + \xi_p^2,$$

$$a_1 = F_1(1 - \mathcal{R}_{01}) + F_2 + F_3$$

$$a_2 = F_2F_1(1 - \mathcal{R}_{01}) - F_3F_1[(1 - \mathcal{R}_{01})] - F_3F_2 - \beta_2\theta_p$$

$$a_3 = F_2F_3F_1(1 - \mathcal{R}_{01}) - \theta_p[\beta_2F_3 + \beta_5\gamma_p]$$

$$\begin{aligned} a_1a_2 = & (F_1)^2F_2(1 - \mathcal{R}_{01})^2 + ((F_1)^2)F_3(1 - \mathcal{R}_{01})^2 - F_1F_2F_3(1 - \mathcal{R}_{01})^2 - \beta_2\theta_pF_1(1 - \mathcal{R}_{01}) \\ & + (F_2 + F_3)[F_2F_1(1 - \mathcal{R}_{01}) + F_3 + F_1(1 - \mathcal{R}_{01}) - F_3F_2 - \beta_2\theta_p] \end{aligned}$$

$$\begin{aligned} a_1a_2 - a_3 = & (F_1)^2(1 - \mathcal{R}_{01})^2[F_3 + F_2] - \beta_2\theta_pF_1(1 - \mathcal{R}_{01}) \\ & + (F_2 + F_3)[F_2F_1(1 - \mathcal{R}_{01})] + F_1F_3(1 - \mathcal{R}_{01}) - F_3F_2 - \beta_2\theta_p + \theta_p[\beta_2F_3 + \beta_5\gamma_p] \end{aligned}$$